



UNIL | Université de Lausanne

Unicentre

CH-1015 Lausanne

<http://serval.unil.ch>

Year : 2013

LASSA VIRUS ENTRY IN ANTIGEN PRESENTING CELLS AND EVALUATION OF A NOVEL NANOPARTICLE VACCINE PLATFORM AGAINST ARENAVIRUSES

Cabecinhas Ana Rita Gonçalves

Cabecinhas Ana Rita Gonçalves, 2013, LASSA VIRUS ENTRY IN ANTIGEN PRESENTING CELLS AND EVALUATION OF A NOVEL NANOPARTICLE VACCINE PLATFORM AGAINST ARENAVIRUSES

Originally published at : Thesis, University of Lausanne

Posted at the University of Lausanne Open Archive.
<http://serval.unil.ch>

Droits d'auteur

L'Université de Lausanne attire expressément l'attention des utilisateurs sur le fait que tous les documents publiés dans l'Archive SERVAL sont protégés par le droit d'auteur, conformément à la loi fédérale sur le droit d'auteur et les droits voisins (LDA). A ce titre, il est indispensable d'obtenir le consentement préalable de l'auteur et/ou de l'éditeur avant toute utilisation d'une oeuvre ou d'une partie d'une oeuvre ne relevant pas d'une utilisation à des fins personnelles au sens de la LDA (art. 19, al. 1 lettre a). A défaut, tout contrevenant s'expose aux sanctions prévues par cette loi. Nous déclinons toute responsabilité en la matière.

Copyright

The University of Lausanne expressly draws the attention of users to the fact that all documents published in the SERVAL Archive are protected by copyright in accordance with federal law on copyright and similar rights (LDA). Accordingly it is indispensable to obtain prior consent from the author and/or publisher before any use of a work or part of a work for purposes other than personal use within the meaning of LDA (art. 19, para. 1 letter a). Failure to do so will expose offenders to the sanctions laid down by this law. We accept no liability in this respect.



UNIL | Université de Lausanne

Faculté de biologie
et de médecine

Institut de Microbiologie

**LASSA VIRUS ENTRY IN ANTIGEN
PRESENTING CELLS AND EVALUATION OF A
NOVEL NANOPARTICLE VACCINE
PLATFORM AGAINST ARENAVIRUSES**

Thèse de doctorat ès sciences de la vie (PhD)

Présentée à la Faculté de biologie et de médecine de l'Université de Lausanne
par

Ana Rita Gonçalves Cabecinhas

Master en Génomique et Biologie Expérimentale de l'Université de Lausanne

Jury

Prof. Sophie Martin, Présidente
Prof. Stefan Kunz, Directeur de thèse
P.D. Dr Denise Nardelli Haefliger, Experte
Prof. Lars Hangartner, Expert

LAUSANNE 2013

Imprimatur

Vu le rapport présenté par le jury d'examen, composé de

<i>Président</i>	Madame Prof. Sophie Martin
<i>Directeur de thèse</i>	Monsieur Prof. Stefan Kunz
<i>Experts</i>	Madame Dr Denise Nardelli-Haefliger
	Monsieur Dr Lars Hangartner

le Conseil de Faculté autorise l'impression de la thèse de

Madame Ana Rita Gonçalves

Master en génomique et biologie expérimentale de l'Université de Lausanne

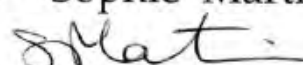
intitulée

**LASSA VIRUS ENTRY IN ANTIGEN PRESENTING CELLS
AND EVALUATION OF A NOVEL NANOPARTICLE
VACCINE PLATFORM AGAINST ARENA VIRUSES**

Lausanne, le 18 octobre 2013

pour ^aLe Doyenne
de la Faculté de Biologie et de Médecine

Prof. Sophie Martin



ACKNOWLEDGEMENTS

To begin with I would like to wholeheartedly thank my supervisor, Prof. Stefan Kunz, first for giving me the opportunity to accomplish my Ph.D. thesis in his group, then for his availability, supervision and his precious advises. I also greatly appreciated his enthusiastic way of unreservedly sharing the wealth of knowledge and experience he possesses and that fundamentally contributed to the accomplishment of this work.

My sincere thanks go to our collaborators from Prof. Melody Swartz's group at the EPFL, who actively contributed to the accomplishment of the vaccine development part of my thesis: Dr Sachiko Hirose and Marcela Rincon-Restrepo.

I would also like to thank Dr Nardelli-Haeffliger, Prof. Lars Hangartner and Prof. Sophie Martin for kindly accepting to be part of my thesis committee and jury, as well as, for their precious advices and feedback.

It is my great pleasure to thank all the previous and actual members of Stefan's group specially Dr Antonella Pasquato, Dr Sylvia Rothenberger, Dr Giulia Pasqual, Dr Emilie Zürcher, Dr Dominique Burri, Dr Marie-Laurence Moraz, Dr Christelle Pythoud and Joël da Palma for their help and support. And for the very nice and funny moments we spent together.

Finally, I would like to warmly thank my close family, specially my Mum and my Partner, for their presence and support in general, but specially during the last 4 years.

TABLE OF CONTENTS

ACKNOWLEDGEMENTS	4
TABLE OF CONTENTS	5
ABBREVIATIONS	7
SUMMARY	9
RÉSUMÉ	11
GENERAL INTRODUCTION	13
ARENAVIRUSES.....	14
<i>Arenaviradae</i> family.....	14
<i>Viral particle structure and genome organisation</i>	15
<i>The arenavirus life-cycle</i>	16
<i>Arenavirus pathogenesis and clinical disease</i>	17
<i>Immune responses to Arenaviruses</i>	20
C-TYPE LECTINS AS CANDIDATE LASV RECEPTORS ON HUMAN DENDRITIC CELLS	21
CURRENT THERAPY AGAINST ARENAVIRUSES.....	22
CURRENT STATUS OF ARENAVIRUSES VACCINE DEVELOPMENT	23
POLYPROPYLENE SULFIDE NANOPARTICLE AS VACCINE PLATFORM.....	24
CURRENT STATUS ON PPS NPS RESEARCH IN THE VACCINATION FIELD	26
THESIS PROJECTS	28
PROJECT-I: LASV ENTRY IN HUMAN ANTIGEN PRESENTING CELLS	29
PROJECT-II: EVALUATION OF A NOVEL NANOPARTICLE VACCINE PLATFORM AGAINST ARENAVIRUSES	29
RESULTS OF PROJECT-I	30
LASV ENTRY IN HUMAN ANTIGEN PRESENTING CELLS	30
ABSTRACT	33
INTRODUCTION.....	34
MATERIALS AND METHODS.....	36
RESULTS	41
DISCUSSION	54
ACKNOWLEDGEMENTS	57
REFERENCES.....	58
RESULTS OF PROJECT-II:	62
EVALUATION OF A NOVEL NANOPARTICLE VACCINE PLATFORM AGAINST ARENAVIRUSES	62
SUMMARY OF PROJECT-II.....	63
INTRODUCTION.....	64
PART I: INDUCTION OF A PROTECTIVE ANTIBODY RESPONSE	66
1.1. <i>Design and production of the vaccine antigen</i>	66
1.2. <i>Conjugation of the vaccine antigen MACVΔGP1 onto PPS NPs</i>	67

1.3. Evaluation of MACVΔGPI NPs in vivo.....	70
1.4. A “Second generation” of MACVΔGPI constructs.....	72
1.5. The receptor-binding MACVGPI loop 10 as antigen.....	76
PART 2: INDUCTION OF A PROTECTIVE T CELL RESPONSE	78
2.1. Conjugation of MHC I LCMV peptides onto PPS NPs.....	78
2.2. Evaluation of NPs bearing CD8 T cell epitope peptides in vivo	79
DISCUSSION AND OUTLOOK	81
1. PROJECT-I	82
1.1. What is the exact role of DC-SIGN in the LASV entry process in MDDC?.....	82
1.2. What is the role of the LASV receptor DG in LASV infection in MDDC?.....	83
1.3. What is the intracellular trafficking route of LASV in MDDC?	86
1.4. Identification of novel LASV entry factors in human DCs.....	87
2. PROJECT-II	90
2.1. Induction of an efficient humoral immune response against MACV GPI	90
2.2. Towards a multivalent vaccine against the major pathogenic NW arenaviruses	93
2.3. The challenge of generating a protective NPs vaccine against LASV.....	94
MATERIALS AND METHODS	98
REFERENCES.....	105
APPENDIX.....	116

ABBREVIATIONS

agRNA	antigenomic RNA
AHF	Argentinean hemorrhagic fever
APCs	antigen-presenting cell(s)
BSL	biosafety level
CDC	center of disease control
CTL	cytotoxic lymphocyte
CME	clathrin mediated endocytosis
DCs	dendritic cell(s)
DC-SIGN	dendritic cell-specific intercellular adhesion molecule-3-grabbing non-integrin
DG	dystroglycan
ECM	extracellular matrix
EE	early endosome
EEA1	early endosome-associated protein 1
ELISA	enzyme-linked immunosorbent assay
ELISpot	enzyme-linked immunospot
EPFL	école polytechnique de Lausanne
ESCRT	endosomal sorting complexes required for transport
GNA	<i>Galanthus nivalis</i> agglutinin
GTOV	guanarito virus
GPC, GP1, GP2	glycoprotein precursor, glycoprotein 1 and 2
GuHCl	guanidinium hydrochloride
HA	hemagglutinin
HEK 293	human embryonic kidney 293 cells
HIV	human immunodeficiency virus
HPLC/MS	high-performance liquid chromatography/mass spectrometry
JUNV	junin virus
hTfR1	human transferrin receptor 1
ICS	intracellular staining
ICTV	international committee on taxonomy
IFN	interferon
IgG	immunoglobulin
IGR	intergenomic region
ILV	intraluminal vesicles
KDa	kilo dalton
Kd	dissociation coefficient
LAMP1	lysosomal-associated membrane protein 1
LASV	lassa virus
LCMV	lymphocytic choriomeningitis virus
LE	late endosome
LN	lymph node
LSEctin	liver and lymph node sinusoidal endothelial cell C-type lectin
MACV	machupo virus
MDDC	monocyte derived dendritic cell
MDM	monocyte derived macrophages
MEA	mercaptoethylamine
MHC	major histocompatibility complex
Mtb	<i>Mycobacterium tuberculosis</i>
MOPV	mopeia virus
MPs	macrophage(s)
MVB	multivesicular body
nAbs	neutralizing antibodies

NHP	non-human primates
NIAID	national institute of allergy and infectious disease
NIH	national institutes of health
NK	natural killer cells
NPs	nanoparticle
NP	nucleoprotein
NW	new world
O/N	over night
ORF	open reading frame
OVA	ovalbumin
OW	old world
PC	pro-protein convertase
PE	phycoerythrin
PEG	polyethyleneglycol
PPG	polypropylene glycol
PPS	polypropylene sulfide
PRRs	pathogen recognition receptors
rLCMV-LASVGP	recombinant lymphocytic choriomeningitis virus carrying the LASV GP
rLCMV-VSVG	recombinant lymphocytic choriomeningitis virus carrying the VSV glycoprotein
Rib	ribavirin
rVSV	recombinant vesicular stomatis virus
RNP	ribonucleoprotein particle
RT	room temperature
RTCs	replication-transcription complexes
RVFV	Rift Valley fever virus
S-4FB	succinimidyl-formylbenzamide
S-HyNIC	succinimidyl-6-hydrazino-nicotinamide
SKI-1/S1P	subtilisin kexin isozyme-1/site 1 protease
TAM	tyro3, axl, mer
TCEP	tris(2-carboxyethyl)phosphine hydrochloride
TCID	tissue culture infectious dose
TfR1	transferrin receptor 1
TLR	toll-like receptor
UUKV	uukuniemi virus
VEEV	venezuelan equine encephalitis virus
(V)HF	(viral) hemorrhagic fever
WGA	wheat germ agglutinin

SUMMARY

Arenaviruses are a large and diverse family of viruses that merit significant attention as causative agents of severe hemorrhagic fevers in humans. Lassa virus (LASV) in Africa and the South American hemorrhagic fever viruses Junin (JUNV), Machupo (MACV), and Guanarito (GTOV) have emerged as important human pathogens and represent serious public health problems in their respective endemic areas.

A hallmark of fatal arenaviruses hemorrhagic fevers is a marked immunosuppression of the infected patients. Antigen presenting cells (APCs) such as macrophages and in particular dendritic cells (DCs) are early and preferred targets of arenaviruses infection. Instead of being recognized and presented as foreign antigens by DCs, arenaviruses subvert the normal mechanisms of pathogen recognition, invade DCs and establish a productive infection. Viral replication perturbs the DCs' ability to present antigens and to activate T and B cells, contributing to the marked virus-induced immunosuppression observed in fatal disease. Considering their crucial role in the development of an anti-viral immune response, the mechanisms by which arenaviruses, and in particular LASV, invade DCs are of particular interest. The C-type lectin DC-specific Intercellular adhesion molecule-3-grabbing nonintegrin (DC-SIGN) was recently identified as a potential entry receptor for LASV. The first project of my thesis focused therefore on the investigation of the role of DC-SIGN in LASV entry into primary human DCs. My data revealed that DC-SIGN serves as an attachment factor for LASV on human DCs and can facilitate capture of free virus and subsequent cell entry. However, in contrast to other emerging viruses, of the phlebovirus family, I found that DC-SIGN does likely not function as an authentic entry receptor for LASV. Moreover, I was able to show that LASV enters DCs via an unusually slow pathway that depends on actin, but is independent of clathrin and dynamin.

Considering the lack of effective treatments and the limited public health infrastructure in endemic regions, the development of protective vaccines against arenaviruses is an urgent need. To address this issue, the second project of my thesis aimed at the development of a novel recombinant arenavirus vaccine based on a nanoparticle (NPs) platform and its evaluation in a small animal model. During the first phase of the project I designed, produced, and characterized suitable vaccine antigens. In the second phase of the project, I generated antigen-conjugated NPs, developed vaccine formulations, and tested the NPs for their ability to elicit anti-viral T cell responses as well as anti-viral antibodies. I demonstrated that the NPs

platform is able to activate both cellular and humoral branches of the adaptive anti-viral immunity, providing proof-of-principle.

In sum, my first project will allow, in a long term perspective, a better understanding of the viral pathogenesis and contribute to the development of novel antiviral strategies. The second project will expectidly offer a new treatment option against arenaviruses.

RÉSUMÉ

Les Arénavirus sont une vaste et diverse famille de virus dont certains membres sont à l'origine de nombreux cas de fièvre hémorragique sévère chez l'homme. Au cours des dernières années, le virus de Lassa (LASV, Afrique) et les arénavirus sud-américains Junin (JUNV), Machupo (MACV) et Guanarito (GTOV) ont émergé en tant qu'importants pathogènes pour l'homme et représentent un problème de santé publique majeur dans leurs zones d'endémie respectives.

Les cas de fièvre hémorragique causés par des arénavirus sont caractérisés par une immunosuppression marquée chez les patients infectés. Les cellules présentatrices de l'antigène, telles que les macrophages et en particulier les cellules dendritiques (DCs), sont des cibles précoces et privilégiées du virus. Au lieu d'être reconnus et présentés comme des corps étrangers par les DCs, les arénavirus peuvent subvertir les voies normales de reconnaissance des agents pathogènes, envahir les DCs et y établir une infection productive. La réplication virale perturbe alors le fonctionnement normal des cellules, les rendant incapables de présenter correctement les antigènes et d'activer les cellules T et B, contribuant ainsi à l'immunosuppression induite par le virus dans les cas mortels de fièvre hémorragique.

Compte tenu de leur rôle majeur dans le développement de la réponse immunitaire antivirale, l'investigation des mécanismes par lesquels les arénavirus, et en particulier le LASV, envahissent les DCs est un enjeu capital. La molécule DC-SIGN a récemment été identifiée comme un récepteur potentiel d'entrée pour le LASV. Mon premier projet de thèse s'est focalisé sur l'étude du rôle de DC-SIGN dans l'entrée du LASV dans les DCs primaires humaines. Les résultats ont révélé que le DC-SIGN fonctionne comme facteur d'attachement à la surface des DCs et peut faciliter la capture des virions libres, aidant ainsi leur pénétration dans la cellule. Cependant, contrairement à ce qui a pu être établi pour d'autres virus émergents de la famille des phlebovirus, DC-SIGN n'assume certainement pas la fonction de véritable récepteur entrée pour le LASV. De plus, j'ai démontré que celui-ci s'introduit dans les DCs via une voie anormalement lente qui dépend de l'actine, mais qui est indépendante de la clathrine et de la dynamine.

Compte tenu de l'absence de traitement efficace contre les arénavirus et l'infrastructure de santé publique limitée dans les régions touchées, le développement de vaccins contre ces virus se révèle nécessaire. Mon second projet de thèse s'est concentré sur le développement d'un vaccin recombinant contre les arénavirus basé sur l'utilisation de nanoparticules (NPs), ainsi

que sur son évaluation dans un modèle murin. Au cours de la première phase du projet, j'ai conçu, produit et caractérisé les antigènes vaccinaux. Dans la deuxième phase du projet, j'ai généré des antigènes liés aux NPs, mis au point des formulations de vaccins et testé les NPs pour leur capacité à induire une réponse cellulaire antivirale ainsi que la production d'anticorps antiviraux. J'ai pu démontrer que les NPs sont capables d'activer les branches humorale et cellulaire de l'immunité adaptative anti-virale.

En résumé, mon premier projet permettra, à long terme, une meilleure compréhension de la pathogénèse virale et contribuera au développement de nouvelles stratégies antivirales. Mon second projet offrira, nous l'espérons, un nouveau traitement contre les arénavirus.

GENERAL INTRODUCTION

ARENAVIRUSES

Arenaviridae family

The *Arenaviridae* is a large and diverse family of viruses composed of the single *Arenavirus* genus (Fig.1), that merit significant attention as important emerging human pathogens and powerful models for experimental virology [6]. The *Arenavirus* genus includes around 30 known virus species, but only 25 are recognized by the International committee on Taxonomy (ICTV) (Fig.1). All known arenavirus species are carried by rodents, except Tacaribe virus, whose suspected host reservoir are fruitbats, and their geographical distribution maps to that of their natural hosts. Arenaviruses are classified into two major groups according to genetic and serologic characteristics, and geographic localization: the 1) Old World (OW) and 2) New World (NW) arenaviruses. The OW arenaviruses are endemic to Africa, whereas the NW arenaviruses are present in the Americas. While OW arenaviruses constitute a single lineage, NW arenaviruses are separated into four clades A/Rec, A, B, and C (Fig.1). [7] [8]

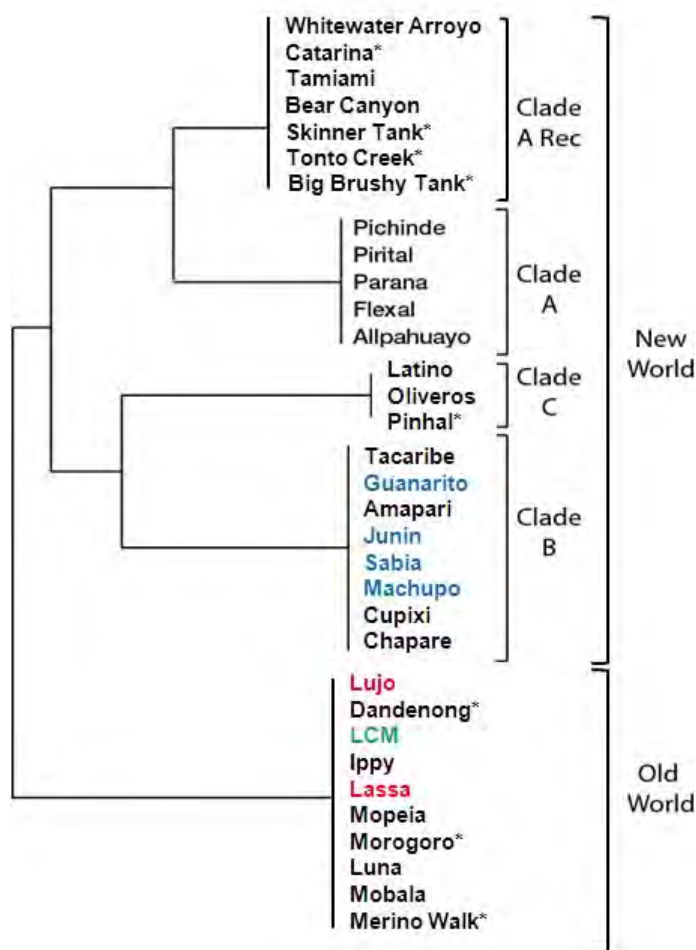


Figure 1. The *Arenaviridae* family. OW arenaviruses are found in Africa with exception of lymphocytic choriomeningitis virus (LCMV), which has a worldwide distribution. The NW arenaviruses clade A/Rec and A through C, are found in North and South America, respectively. The OW and the NW clade C viruses use mainly alpha-dystroglycan as receptor whereas NW Clade B viruses use transferrin receptor 1 (TFR1) as a receptor. NW clade A and A/Rec viruses use unknown receptors. Confirmed human pathogens are colored in blue (+ Chapare), red or green. The schematic cladogram on the left indicates the phylogenetic relationships between the viral clades.

(*) Not yet recognized by ICTV

Picture modified from [2].

Viral particle structure and genome organisation

Arenaviruses are enveloped viruses which contain a bi-segmented negative single-stranded RNA genome (Fig.2A) comprised of a large (L) and a small (S) fragment (Fig.2B) [9]. Each RNA strand allows the synthesis of two different polypeptides in opposite direction. A non-coding hairpin structure serves as intergenic region (IGR) and separates the two open reading frames (ORF) in ambisense orientation (Fig.2B). The viral glycoprotein precursor (GPC), is post-translationally processed by the host pro-protein convertase (PC) subtilisin-kexin-isozyme-1 (SKI-1), also known as site 1 protease (S1P), into the envelope glycoprotein (GP) 1 and the transmembrane GP2 implicated in viral fusion. GPC and the nucleoprotein (NP) are encoded by the S RNA (Fig.2B), whereas the L polymerase and Z matrix protein are encoded by the L RNA (Fig.2B). Viral replication is exclusively cytoplasmic and infectious progeny viruses assemble and bud from the plasma membrane (Fig.3).

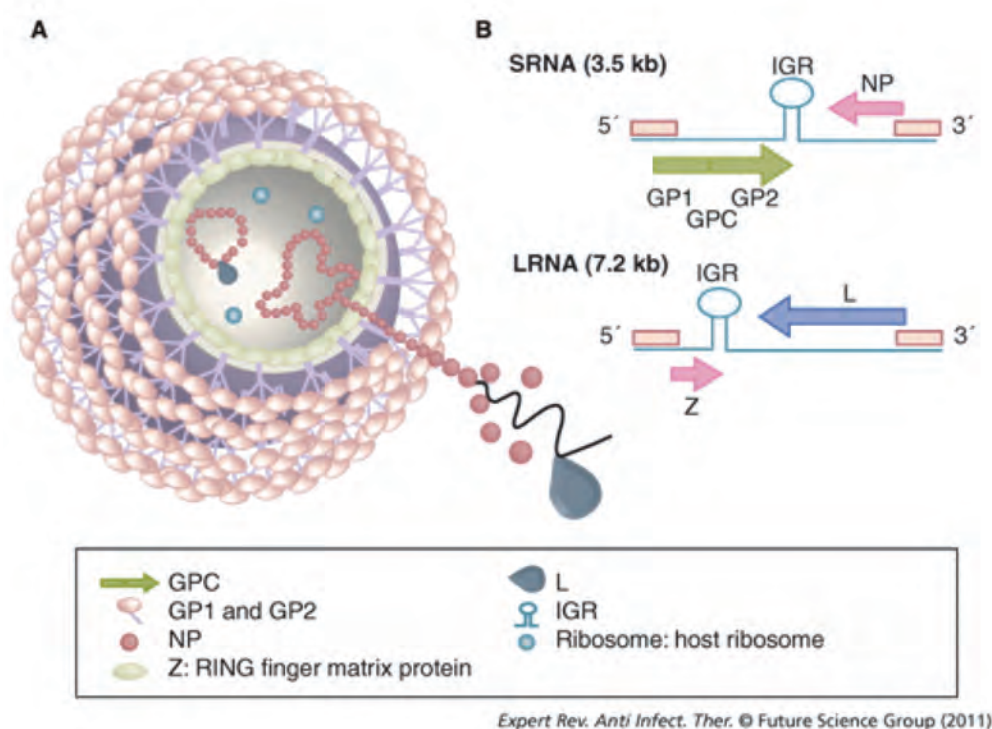


Figure 2. Representation of arenavirus particle and genome. **A)** Schematic representation of the arenavirus particle. The viral genome is completely encapsulated by the viral NP forming the ribonucleoprotein particle (RNP). The L protein, a RNA-dependent RNA polymerase, also associates with RNP and is essential for early viral transcription and replication. In association with the inner leaflet of the viral membrane envelope localizes the matrix protein Z, which interacts with the C-terminal part of the transmembrane GP2 moiety of the mature GP1/GP2 complex. The GP1 protein contains the host receptor binding site and constitutes the distal part of the GP1/GP2 complex, whereas GP2 corresponds to the membrane-proximal part and is necessary for viral fusion. Mature GP1/GP2 complexes presumably form trimers. **B)** Arenavirus coding strategy. Each of the two ssRNA segments, L and S, uses an ambisense coding strategy to direct the synthesis of two polypeptides in opposite orientations and is separated by an IGR predicted to have a stable hairpin structure. The 5' ends of the genomic arenavirus RNA cannot serve as a template for translation and viral protein expression requires prior transcription, as in true negative-strand viruses. GP: Glycoprotein; GPC: Glycoprotein precursor; IGR: Intergenic region; L: RNA-dependent RNA polymerase; NP: Nucleoprotein. [4]

The arenavirus life-cycle

The pathways used by OW and NW arenaviruses for entry into host cells are distinct but both are receptor-dependent [10] (Fig.3). The use of the genetically conserved and ubiquitously expressed cell-surface proteins α -dystroglycan (α -DG) [11] and transferrin receptor 1 (TfR1) [12] as main receptors by the lymphocytic choriomeningitis virus (LCMV), Lassa virus (LASV), clade C NW arenaviruses, and clade B NW arenaviruses respectively, explains their wide host range and cell-type tropism. Recently, members of the Tyro3, Axl, Mer (TAM) receptor tyrosine kinases (Axl and Tyro3) and the C-type lectins Dendritic Cell-Specific Intercellular adhesion molecule-3-Grabbing Non-integrin (DC-SIGN), as well as Liver and lymph node Sinusoidal Endothelial cell C-type lectin (LSECtin) were found as candidate receptors for LASV that can mediate viral entry in absence of α -DG[13].

Attachment of OW arenaviruses to cellular DG promotes virus-receptor internalization into smooth vesicles [14]. This endocytotic process is dependent on membrane cholesterol, but clathrin, dynamin, and caveolin-independent and does not depend on Rab5 or Rab7, indicating that the virus-receptor complex bypasses classical Early Endosome-Associated protein 1 (EEA1) positive endosomes. The virus is delivered to multivesicular bodies (MVB) of the late endosome, where the virus-receptor complex is sorted into intraluminal vesicles (ILV) by the endosomal sorting complexes required for transport (ESCRT) machinery [15]. In contrast to OW and NW clade C arenavirus, NW clade B virus cell entry involves clathrin-mediated endocytosis (CME) and follows a classical Rab5 and Rab7-dependent endosomal entry pathway [16]. As for OW arenaviruses, NW arenavirus fusion requires a pH < 5.5, corresponding to late endosomal fusion.

Viral RNA replication is initiated by the viral RNA-dependent RNA polymerase L upon the release of the viral genome into the infected cells' cytoplasm (Fig.3). The first step of viral replication is the initiation of transcription by the viral L polymerase using promoters on each 5' end of the genomic RNA segments, generating mRNAs coding for NP and L. Transcription termination is mediated by the IGR downstream of the 3' end of each ORF. Modest concentrations of NP early in infection prevent the polymerase from reading through the IGR, thus favoring transcription over replication. With time, NP accumulates, forcing the polymerase to shift to the "replication mode" reading across the IGR to produce the full-length anti-genome (ag) RNAs which will serve as templates for the transcription of GPC and Z mRNAs [17]. Using agRNA as template, L produces large quantities of genomic L and S RNAs late in the infection cycle. Little is known about the molecular organization of the

arenavirus replication-transcription complexes (RTCs). Recent studies visualized arenavirus RTCs as discrete cytosolic clusters associated with NP, viral genomic and agRNA, but being largely devoid of viral mRNA [18]. Assembly and release of arenavirus infectious progeny occurs at the plasma membrane and requires that the viral RNPs associates with membrane domains enriched in mature viral GP and Z, so-called “budding zones”. The assembly of arenavirus particles and the budding process is driven mainly by the Z protein, which acts as a *bona fide* matrix protein and contains late domain motifs (PTAP and PPPY) [19,20,21]. Incorporation of mature GP into nascent virions requires a functional interaction with Z [22], which in turn recruits components of the ESCRT, in particular the ESCRT-I component Tsg101, that is crucial for arenavirus budding [19,20].

Arenaviruses life cycle

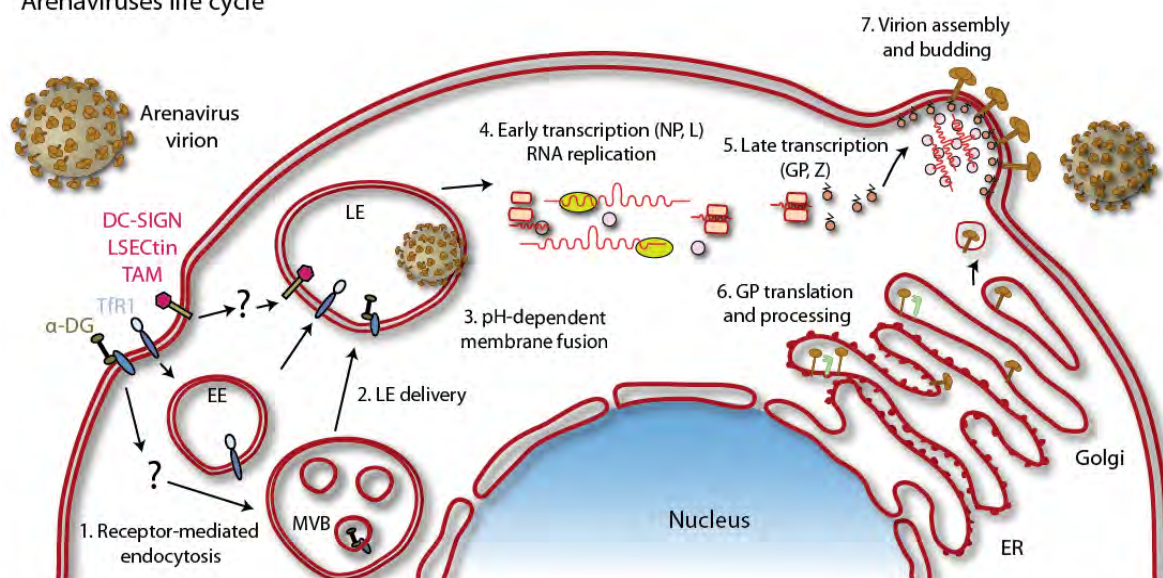


Figure 3. Life cycle of Arenavirus. LASV and JUNV use α -DG and TFR1, respectively, as primary receptors. LASV can also use TAM receptor tyrosine kinases Axl and Tyro3 and C-type lectins (DC-SIGN and LSECtin) as receptors. Please see the text for more details. Early endosome (EE), Multivesicular body (MVB). Late endosome (LE). Uninvestigated or under investigation steps (?). Figure modified from [2].

Arenavirus pathogenesis and clinical disease

Humans are accidental hosts of arenaviruses and contract the virus via close contact with persistently infected rodents, contaminated food and drink, or through skin lesions or aerosols. OW arenaviruses such as LASV and NW arenaviruses as JUNV and MACV viruses are responsible for hemorrhagic fever (HF) syndromes, whose severity can vary from mild febrile disease to lethal hemorrhagic fever [23,24]. Human-to-human transmission is also possible via contaminated blood, body fluids, and organ transplants (particularly in the case of

LCMV). LASV, the most prevalent OW arenavirus associated with human disease, is responsible for 300'000-500'000 infections per year with a mortality rate of 1-2% at the community level, raising to 15-30% among hospitalized patients [25]. This fatality rate can rise to >50% in nosocomial outbreaks, in particular in pregnant women and neonates. The per case mortality of JUNV and MACV, the most common disease-associated NW arenavirus, can reach 30-50% [26].

OW (LASV) and NW (JUNV and MACV) arenaviruses pathogenesis has been extensively covered by excellent recent reviews [4,27,28] thus I will only briefly summarize it in the next paragraphs. After an incubation period of 1-3 weeks, patients infected with arenaviruses develop unspecific “flu-like” symptoms as fever, asthenia and general malaise. A majority of infected patients recover while the others rapidly progress with increasing signs and symptoms of shock associated with hemorrhagic and/or neurological (particularly in JUNV infected patients) manifestations, which may be lethal. Permanent sensorineural deafness with lifelong hearing loss can arise as a Lassa fever complication late in disease's course or in early convalescence. The patients who recover generally do so 2–3 weeks after disease onset and clear the virus from the blood.[4,27]

Antigen-presenting cells (APCs), such as macrophages (MPs) and in particular dendritic cells (DCs) are major targets of OW (LASV and LCMV) and NW (JUNV) arenaviruses early during infection. As APCs, which are key cells for the induction and regulation of immune responses, they are widely spread among body tissues and can, for some subsets, circulate via the blood stream, and are thought to contribute to the spread of the virus in systemic infection. They are likely important sites of viral replication leading to release of viral particles, which then can infect and initiate viral replication in the liver, spleen, kidney, heart, vascular endothelium and adrenal cortex [4,27,28]. LASV-infected DCs are not activated, do not mature and do not produce inflammatory cytokines. MPs are also not activated but can produce small amounts of type I interferons (IFN). This absence of DCs activation and maturation may be linked to the immunosuppression observed in severe Lassa fever cases, as it leads to a major impairment of DCs function and modification of the cytokines/chemokines secretion profile [29]. Indeed, productive infection of human DCs with LASV perturbs their ability to activate T cells [30,31]. In contrast to LASV, the non-pathogenic OW Mopeia virus (MOPV) is able to fully activate DCs and MPs as well as stimulating type I IFN secretion and an efficient T cell response [32]. Type I IFNs are known to be important for control of the initial burst size of the virus, as well as the induction and maintenance of an efficient adaptive

immune response [33]. Thus, the absence of type I IFN secretion by the infected APCs probably plays a key role in the pathogenesis and the immunosuppression observed in severe Lassa fever cases, as suggested by recent studies in non-human primate (NHP) models [34]. The viral entry pathway(s), the viral intracellular trafficking and the exact mechanisms leading to the functional impairment of human DCs in the context of LASV infection are largely unknown and represented a major focus of my thesis work.

Tissue injury and systemic deregulations commonly associated with arenaviruses' infection include characteristic lesions in spleen and liver, immunosuppression, as well as lymphopenia affecting T, B and natural killer (NK) cells. The characteristic "cytokine storm" observed in other viral hemorrhagic fevers (VHFs) characterized by elevated IFN and cytokines levels, hemorrhages, thrombocytopenia, and platelet dysfunction are largely absent in Lassa fever but seem more common in Junin and Machupo HFs. Disseminated intravascular coagulation, an important feature of Ebola and Marburg HFs, is almost never observed in Lassa fever, and rare even in NW arenaviruses HFs. [4,35,36].

The limited bleeding from mucosal surfaces, little cellular damage, and modest infiltration of inflammatory cells observed in histological samples of severe Lassa fever cases do not explain the fatal disease outcome [35]. This is not the case in patients infected with NW arenaviruses, where lethal disease could at least be partially explained by the widespread organ damages and a rather classical hemorrhagic shock syndrome. One might classify NW arenaviruses as more typical hemorrhagic viruses whereas the pathogenesis of LASV seems rather atypical [4,37,38].

In contrast to LASV and the South American HF viruses, LCMV infection in adult immunocompetent humans manifests mainly as aseptic meningitis and encephalitis. However, in immunocompromised individuals, LCMV is a severe pathogen that causes a devastating systemic infection associated with multi-organ failure that shows striking parallels to fatal Lassa fever [39,40].

Viremia is a highly predictive factor for the outcome of human arenavirus infection. Indeed high viral loads ($\geq 1 \times 10^6$ tissue culture infectious dose (TCID) 50/ml) at time of hospitalization correlate with a fatal outcome [26,41]. This suggests that the virus is in tight competition with the immune system. Thus if we provide the immune system an advantage over the virus, as it would be the case by inducing neutralizing antibodies (nAbs), which would act as gatekeepers, we would tip the balance in favor of the immune system.

Immune responses to Arenaviruses

The immune responses to LASV were recently extensively reviewed by Russier [42] and Hayes [43]. Several lines of evidence indicate that acute infection with the OW arenaviruses LASV and LCMV in immunocompetent hosts is mainly controlled by cellular immunity, in particular anti-viral CD8 T cells [44]. Despite the fact that high levels of antibodies (Abs), both IgM and IgG, are also produced early in disease, they are not protective and generally not neutralizing [41]. The individuals, which seroconvert have mainly GPC, NP, and Z protein specific Abs that are either strain-specific or broadly cross-reactive [45]. nAbs are also present but appear late in convalescence and are frequently of low titers. Attempts to use human convalescent plasma for post-exposure prophylaxis in Lassa fever patients had occasionally beneficial effects. However, due to the generally low nAbs amounts, therapy with convalescent plasma seems not a viable option [46]. Notably, in experimental animal studies in guinea pigs and primates infected with LASV, nAbs were efficacious, providing proof-of-concept for a beneficial role of nAbs as a potential immunological correlate of protection [47,48].

In the case of NW arenavirus infections, survivors develop a strong cellular immune response early in infection that controls the infection. nAbs tend to appear at 2-3 weeks of illness [26], but their exact role in clearing the virus is not known [36]. The significant drop of viral loads before appearance of nAbs suggests a major role of T cell responses in the protection against NW arenavirus. However, survivors generally show robust titers of nAbs in convalescence. After vaccination with the currently available anti-JUNV vaccine, Candid-1, virus specific T cell responses, as well as protective antibodies can be detected [49]. The reasons for the remarkable difference in the kinetics and quality of the antibody response between OW and NW arenaviruses are currently unknown.

C-TYPE LECTINS AS CANDIDATE LASV RECEPTORS ON HUMAN DENDRITIC CELLS

As mentioned above, early and preferred targets of LASV are APCs of the patient's immune system, in particular DCs. According to their nature as major sentinels for pathogen detection and antigen presentation, DCs express a set of specialized pathogen recognition receptors (PRRs) and have mechanisms of endocytosis, used for antigen internalization and processing, that are not present in other cells [50,51]. Interestingly, some PRRs present on DCs can function not only in pathogen recognition, but can also be abused by some viruses as receptors to mediate infection, in particular DC-SIGN and the mannose receptor [52,53]. The best-studied example, DC-SIGN, is a type II C-type lectin that contains a carbohydrate recognition domain that binds pathogen-derived carbohydrates in a calcium-dependent manner. DC-SIGN is present on many classes of DCs and is normally involved in endocytosis of antigens and delivery to late endosomes/lysosomes followed by processing and subsequent presentation in the context of the major histocompatibility complex (MHC) II. DC-SIGN can facilitate infection or transmission of a variety of enveloped viruses, such as HIV-1 [54,55], the filoviruses Ebola and Marburg virus [56,57], SARS coronavirus [58], the flaviviruses Dengue virus [59,60] and West Nile virus [61]. Recently, DC-SIGN has been identified as the cell entry receptor for arthropod-borne bunyaviruses of the genus phlebovirus, including Rift Valley fever (RVFV) and Uukuniemi viruses (UUKV) in human DCs [62]. In a recent expression cloning approach, DC-SIGN has been identified as a candidate receptor for LASV. However, its actual role in LASV invasion of human DCs has not yet been addressed. Since early infection of DCs plays likely a crucial role in the virus-induced immunosuppression that underlies the pathogenesis of fatal Lassa fever in man, the characterization of the receptors and endocytotic pathways involved in this process are of great importance. The identification of novel LASV receptors involved in infection of human DCs may allow the targeting of the virus-receptor interaction. Moreover, the identification of the pathway of LASV entry into DCs may reveal essential cellular factors that will then be evaluated for their potential in antiviral therapy in our translational research program aiming at the development of novel therapeutics against LASV.

CURRENT THERAPY AGAINST ARENAVIRUSES

The only licensed drug for treatment of human arenavirus infection is the nucleoside analogue ribavirin (Rib) (1- β -D-ribofuranosyl-1,2,4-triazole-3-carboxamide) [63]. *In vitro* and *in vivo* studies have documented that Rib reduces both morbidity and mortality in humans associated with LASV infection [46], and experimentally in MACV [64] and JUNV [26] infections, if given early in the course of clinical disease. Over the past two decades efforts have been made to discover novel drug candidates to combat arenaviruses and only a short and by no means comprehensive overview can be given here: inhibitors of the inosine 5'-monophosphate dehydrogenase [65], the S-adenosylhomocysteine hydrolase [66], phenothiazines compounds [67], brassinosteroids [68] and myristic acid [69] have been reported to have anti-arenaviral activity. Several zinc-finger-reactive compounds with antiretroviral potential showed activity against arenaviruses [70,71] and evidence has been provided for an involvement of the viral Z protein in their mechanism of action [72]. Studies from our laboratory identified amphipathic DNA polymers as potent inhibitors of arenavirus cell entry [73]. More recently, high throughput screens of small molecules by others and our group identified several potent small molecule inhibitors of arenavirus cell entry [74,75,76] that are currently being evaluated as anti-arenavirus drugs. Many enveloped viruses strictly require cleavage of their envelope glycoprotein precursors by host proteases of PC family. The PC SKI-1/S1P is crucial for productive infection by a number of highly pathogenic arenaviruses, including LASV [77], the South American hemorrhagic fever viruses JUNV, MACV, GTOV, and SABV [78]. Processing of the arenavirus GPC by SKI-1/S1P enables cell-to-cell spread of infection and the production of infectious progeny virus from infected cells [77,78,79,80]. In proof-of-concept studies, targeting GPC maturation with peptide- [81] or protein- [82] based SKI-1/S1P inhibitors was found to efficiently block arenavirus cell-to-cell propagation. Importantly, these investigations showed that inhibition of GPC processing is sufficient to markedly limit infection. Recently, Pfizer Inc. identified a new small molecule inhibitor of SKI-1/S1P, PF-429242, which potently inhibits productive infection and spread of both NW and OW arenaviruses *via* interference with the SKI-1/S1P-mediated GPC priming [83,84]. To the best of my knowledge none of these drug candidates has undergone further evaluation in pre-clinical and clinical trials.

CURRENT STATUS OF ARENAVIRUSES VACCINE DEVELOPMENT

Arenaviruses vaccine research started in the 1980s and initially focused on LASV. Several vaccine approaches were investigated since then: 1) inactivated viruses, 2) virus-like particles, 3) epitope-specific peptides, 4) DNA vaccines, 5) alphavirus vectors (Venezuelan equine encephalitis virus (VEEV)), and 6) recombinant/reassortant viruses (detailed in table 1, reviewed by Lukashevich [85]). Most of these vaccines have been evaluated in small animal model as well as NHP.

Table 1. Non exhaustive summary of LASV vaccination strategies.				
Pathogen	Genes	Vector	Animal model	References
LASV	NP, GPC	peptides	Mouse	[44,86]
	all	purified whole Lassa virus γ -irradiated	Rhesus monkeys	[87]
	NP, GPC	vaccinia virus	Strain 13 guinea pigs, rhesus monkeys	[88,89]
	GPC	VSV	Cynomolgus macaques	[90]
	GPC, GP1, GP2	chimeric yellow fever 17D $\text{\textcircled{R}}$	Mouse, strain 13 guinea pigs	[91,92]
	NP, GPC	Mopeia/Lassa reassortant ML29 clone!	Mouse, strain 13 guinea pigs, rhesus macaques and marmosets, immunocompromized rhesus macaques	[93,94,95]
	GPC, NP	VEEV replicon	Strain 13 guinea pigs	[96]
	NP, GPC, Z	virus-like-particle	Mouse	[97]
	NP	plasmid DNA	Mouse	[98]
	NP	aroA attenuated <i>S. typhimurium</i>	Mouse	[99]

$\text{\textcircled{R}}$ The yellow fever 17D vector is already approved for human use (phaseIII ChimeriVax™-dengue and ChimeriVax-Japanese encephalitis (IMOJEV®) from Sanofi-Pasteur. [100].

!Very promising candidate for clinical application

Initial trials with killed LASV vaccines in NHP failed to elicit a protective immune response [87] and subsequent efforts focused on the development of live vaccines. In one attempt, LASV was attenuated by generating genetic reassortants with the less pathogenic MOPV [93]. This reassortant vaccine, called ML29 showed efficacy in guinea pigs [94] and small NHP [95]. However, despite the attenuation of ML29 in comparison to LASV, the use of this live vaccine faces severe limitations in populations living in endemic regions due to the high prevalence of infection with human immunodeficiency virus HIV-1 and other immunosuppressive conditions. Evaluation of recombinant viral platforms for antigen delivery, including vaccinia virus [88], alphavirus replicons [96], vesicular stomatitis virus [90], and the Yellow Fever virus vaccine strain 17D [92] revealed that expression of LASV

GP was necessary and sufficient to confer protection in different animal models. However, the immunological correlate(s) of protection were not clearly defined. A limitation of recombinant viral platforms are host immunity to the vector backbone and unresolved biosafety issues of replicating agents like recombinant vesicular stomatis virus (VSV) expressing LASV GP. To my knowledge, none of these vaccine platforms has been further developed and so far no human vaccine trials have taken place. The only human vaccine available against arenavirus, and only in Argentina, is Candid-1 [101], which is currently only used in populations at risk, but has not been licensed elsewhere. To my knowledge no other vaccine targets than LASV and JUNV are currently under investigation in the arenavirus vaccine research field.

POLYPROPYLENE SULFIDE NANOPARTICLE AS VACCINE PLATFORM

To be used as viable vaccine options, synthetic alternatives to killed or live attenuated vaccines must fulfill several criteria. This includes delivery of antigen to APCs, especially DCs. Antigen-stimulated DCs have then to be able to present it in context of the MHC I and II and to be activated, thus triggering the subsequent activation of T and B cells. This induction of T and B lymphocytes has, in turn, to lead to the generation of a protective adaptive immune response.

The laboratories of our collaborators Dr. Melody Swartz and Dr. Jeffrey Hubbell at the Ecole Polytechnique Fédérale Lausanne (EPFL), have recently developed Pluronic stabilized polypropylene sulfide (PPS) nanoparticles (NPs) that have promising characteristics as a vaccine platform [5]. These NPs are chemically synthesized via a reverse emulsion polymerization reaction as described in Figure 4. They are composed of a hydrophobic core of cross-linked PPS, which is degradable in oxidative conditions as it is the case within the lysosome, and an hydrophilic Pluronic F-127 surface consisting of a block copolymer of polyethylene glycol (PEG) and polypropylene glycol (PPG) [5,102] (Fig.4). The NPs size can be varied within a range from 20 to 250 nm by adjusting the PEG-Pluronic proportions.

The efficacy and promise of the PPS NPs platform derive from three novel features: 1) their 25-30 nm size, which allows their efficient target to the draining lymph nodes (LN) where the density of immature DCs is high [3,103], 2) a chemical surface that could be engineered to activate the complement system, which can then give an additional adjuvant capacity to the NPs itself for DCs activation and B cell modulation [5] and 3) their easy production and stability in wet storage at room temperature (RT).

Both in draining LN and the spleen, NPs interact with APCs, T and B cells. Myeloid cells are capable of internalizing the NPs by macropinocytosis (Fig.5) and presenting the NPs-conjugated antigens in both MHC I and II [104], whereas the modulation of T and B cells by NPs is exclusively extracellular. Indeed T and B cells do not internalize NPs (Fig.5) [3].

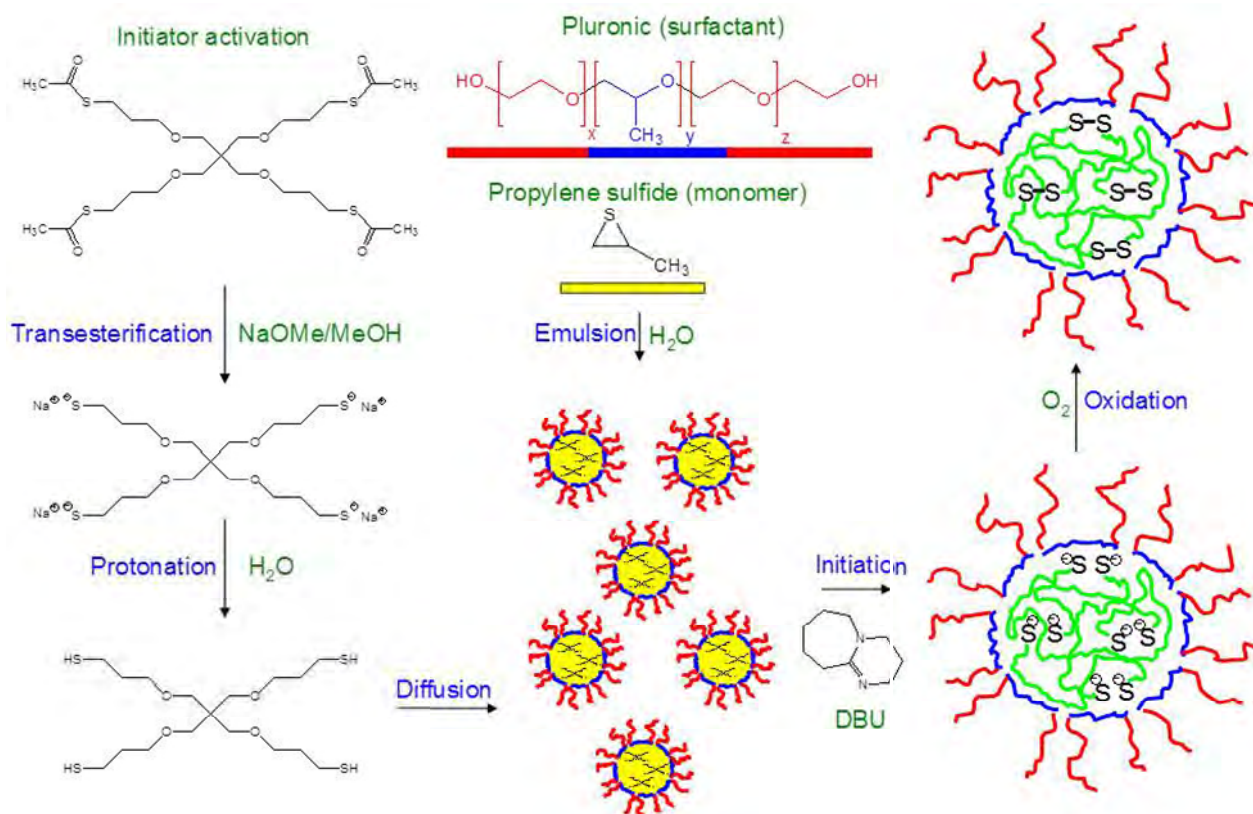


Figure 4. Synthesis of Pluronic covered PPS NPs. PPS NPs are synthesized by reverse emulsion polymerization of PPS. Pluronic F127 is used as a surfactant and a tetra-arm thiol is used as polymerization initiator. The resulting NPs consist of a cross-linked rubbery PPS core stabilized by disulfide bonds and with PEG brushes at the surface. Further functionalization of the Pluronic corona allows the production of biologically-functional NPs. [1] In green: PPS; in blue: PPG-block of Pluronic; in red: PEG-block of Pluronic.

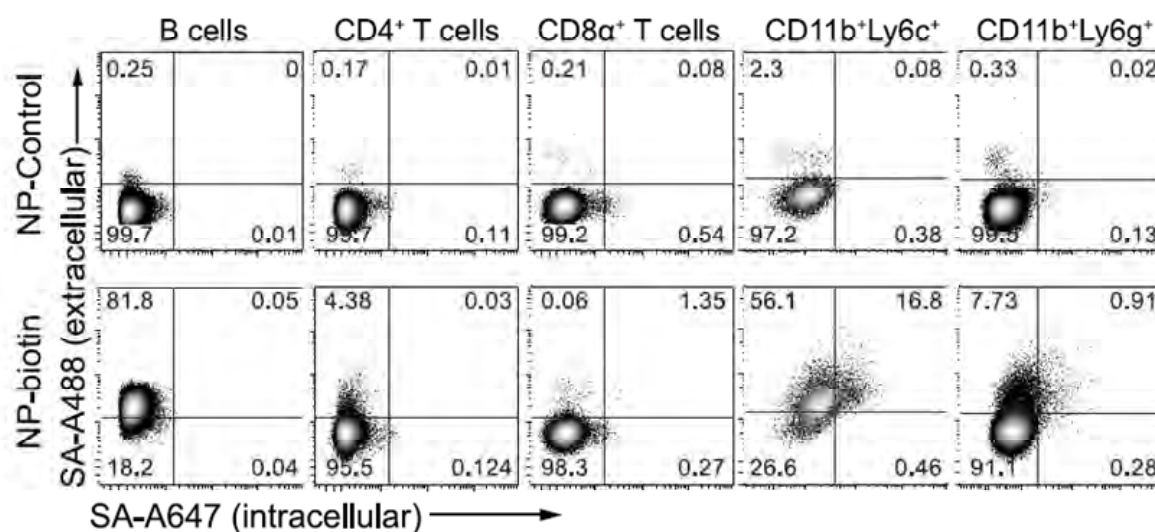


Figure 5. NPs are internalized by monocytes but only associate with lymphocytes. Biotinylated NPs (NP-biotin) association with splenic (B, CD4, and CD8 cells) and bone marrow (CD11b+Ly6c+ and CD11b+Ly6g+) cells after 12 h incubation in vitro. NPs were surface stained with streptavidin-A488 and after permeabilization with streptavidin-A647. Modified from [3].

CURRENT STATUS ON PPS NPS RESEARCH IN THE VACCINATION FIELD

The PPS NPs platform has mainly been evaluated using ovalbumin (OVA) as a model antigen. In this context, NPs exhibited a high potential to trigger both humoral and cellular immunity (Fig.6B and C). This ability was dependent of the NPs size and complement activation (Fig.6A and C) [105,106]. Indeed, in animals lacking C3, the antibodies production was severely impaired (Fig.6B and C) [107,108]. The importance of the antigen conjugation to the NPs was assessed after intradermal, intranasal, and intrapulmonary administration [109] [110]. The presence of toll-like receptors (TLR) agonists, such as CpG [110], was shown to further improve the antibody and T cell responses [109,110]. Antibody isotype-switching, including class switch to IgA [109], could be observed in the bronchoalveolar lavage upon mucosal administration of antigen-conjugated NPs and different adjuvants. Furthermore, the subsequent recruitment of T cells in the pulmonary tissues conferred protection against *Mycobacterium tuberculosis* (Mtb) (Erdman strain) and influenza-ova [111] upon pulmonary delivery of antigen Ag85b, or OVA, respectively [110].

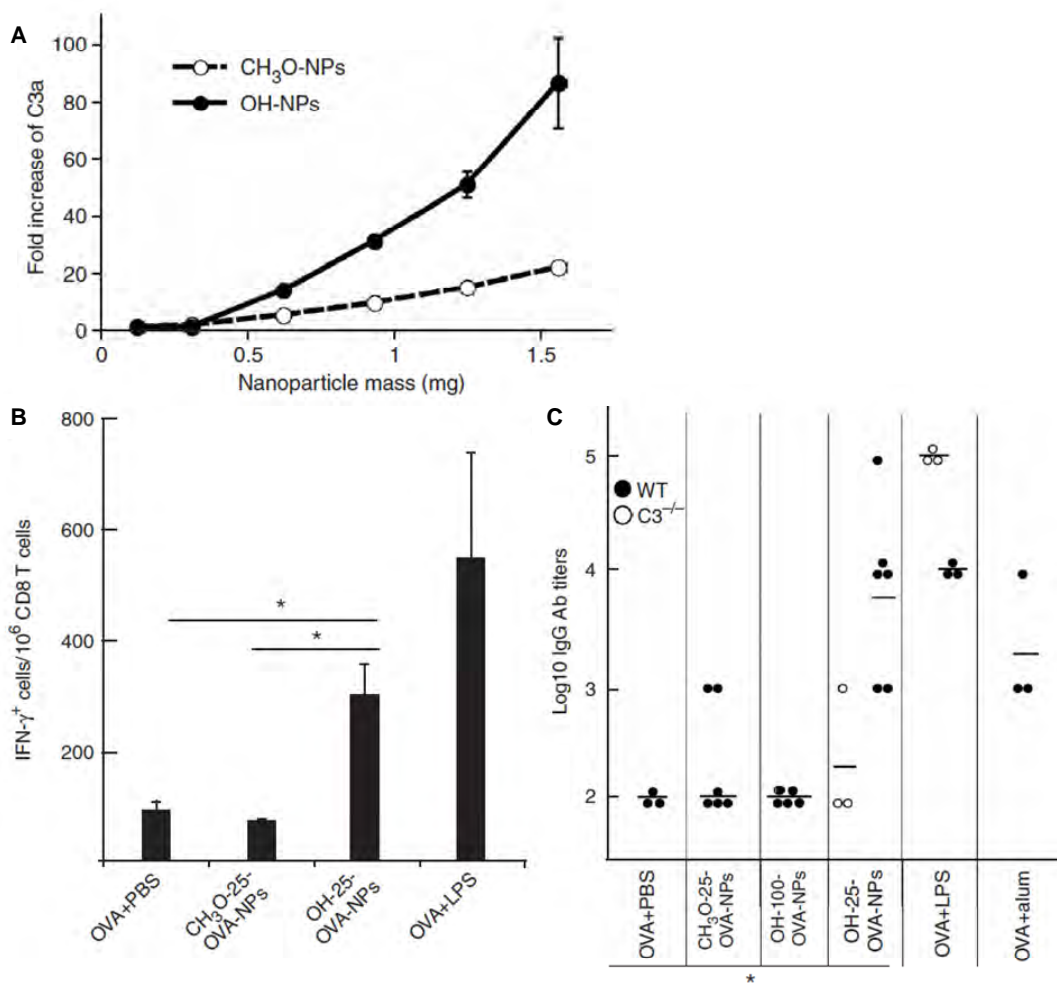


Figure 6. Immune responses upon NPs administration. **A)** NPs-induced complement activation. In the presence of as poly hydroxylated NPs the C3a concentration in human serum increases considerably but few after the incubation with polymethoxylated NPs (OH- and CH₃O-NPs, respectively). **B)** CD8 T-cell memory could be observed after treatment with OH-25-OVA-NPs but not CH₃O-25-OVA-NPs. **C)** Anti-ovalbumin IgG titers were observed only for OH-25-OVA-NPs, but not larger NPs or low-complement activating NPs. Injection of OH-25-OVA-NPs to C3^{-/-} mice (C3 defective), this response was abrogated (wild type, WT). [5]

THESIS PROJECTS

PROJECT-I: LASV ENTRY IN HUMAN ANTIGEN PRESENTING CELLS

A hallmark of fatal Lassa fever is a marked immunosuppression of the patient. Early and preferred targets of LASV infection are APCs, in particular DCs. Instead of being recognized and presented as a foreign antigen by DCs, LASV subverts the normal mechanisms of pathogen recognition, invades DCs and establishes a productive infection. Viral replication perturbs the DCs' ability to present antigens and to activate T cells and B cells contributing to the marked virus-induced immunosuppression observed in fatal disease. Considering their crucial role in the development of an anti-viral immune response, the characterization of LASV entry receptor(s) and the mechanisms by which LASV invades DCs is of particular interest to understand viral pathogenesis and represents a promising target for the development of novel anti-viral strategies. The first project of my thesis aimed therefore in the investigation of LASV interaction with antigen presenting cells, more precisely at the first and decisive steps, host cell attachment and entry.

PROJECT-II: EVALUATION OF A NOVEL NANOPARTICLE VACCINE PLATFORM AGAINST ARENAVIRUSES

Limited therapeutic options are currently available to treat arenaviruses infections and all the prophylactic approaches (use of immune sera, vaccines) developed until now have either failed or have major limitations, making them likely not feasible for human administration. The laboratories of Jeffrey Hubell and Melody Swartz have developed novel vaccination platforms based on the immobilization of a wide variety of antigens on PPS NPs. According to the promising results they obtained in the context of the model antigen (OVA), as well as, *Mycrobacterium* Mtb and influenza virus, we decided to evaluate the NPs platform for the development of a safe and efficacious recombinant vaccine against human pathogenic arenaviruses.

RESULTS OF PROJECT-I

LASV ENTRY IN HUMAN ANTIGEN PRESENTING CELLS

ORIGINAL MANUSCRIPT:**“Role of DC-SIGN in Lassa virus entry into human dendritic cells”**

Ana-Rita Goncalves¹, Marie-Laurence Moraz¹, Antonella Pasquato¹, Ari Helenius², Pierre-Yves Lozach³, and Stefan Kunz^{1*}

¹Institute of Microbiology, Lausanne University Hospital and University of Lausanne, Lausanne, Switzerland.

²Institute of Biochemistry, Federal Institute of Technology Zurich (ETHZ), Zurich, Switzerland.

³INRS-Institut Armand-Frappier, Université du Québec, Laval, Québec, Canada.

* Corresponding author. Mailing address: Institute of Microbiology, University Hospital Center and University of Lausanne, Lausanne CH-1011, Switzerland. Phone: +41 (0)21 314 77 43, Fax: +41 (0)21 314 40 60, E-mail: Stefan.Kunz@chuv.ch

In press at the Journal of Virology

AUTHORS' CONTRIBUTION:

*Conceived and designed the experiments: **Ana-Rita Goncalves**, Antonella Pasquato, Stefan Kunz

*Performed the experiments: **Ana-Rita Goncalves**

*Analyzed the data: **Ana-Rita Goncalves**, Stefan Kunz

*Contributed by providing reagents/materials: Marie-Laurence Moraz, Pierre-Yves Lozach, Ari Helenius

*Wrote the paper: **Ana-Rita Goncalves**, Stefan Kunz

ABSTRACT

The arenavirus Lassa (LASV) causes a severe hemorrhagic fever with high mortality in humans. Antigen-presenting cells, in particular dendritic cells (DC), are early and preferred targets of LASV and their productive infection contributes to virus-induced immunosuppression observed in fatal disease. Here we characterized the role of the C-type lectin DC-specific ICAM-3-grabbing non-integrin (DC-SIGN) in LASV entry into primary human DCs using a chimera of the prototypic arenavirus lymphocytic choriomeningitis virus (LCMV) expressing the LASV glycoprotein (rLCMV-LASVGP). We found that differentiation of human primary monocytes into DCs enhanced virus attachment and entry, concomitant with the up-regulation of DC-SIGN. LASV and rLCMV-LASVGP bound to DC-SIGN via mannose sugars located on the N-terminal GP1 subunit of LASVGP. We provide evidence that DC-SIGN serves as an attachment factor for rLCMV-LASVGP in MDDC and can accelerate capture of free virus. However, in contrast to the phlebovirus Uukuniemi virus (UUKV), which uses DC-SIGN as an authentic entry receptor, productive infection with rLCMV-LASVGP was less dependent on DC-SIGN. In contrast to DC-SIGN-mediated cell entry of UUKV, entry of rLCMV-LASVGP in MDDC was remarkably slow and depended on actin, indicating the use of different endocytotic pathways. In sum, our data reveal that DC-SIGN can facilitate cell entry of LASV in human MDDCs, but that its role seems distinct from the function as an authentic entry receptor reported for phleboviruses.

INTRODUCTION

The arenavirus Lassa (LASV) is endemic in Western Africa from Senegal to Cameroon and causes several hundred thousand infections per year with high mortality (1). There is currently no vaccine available and therapeutic intervention is limited to intensive care and the use of ribavirin, which shows some efficacy when given early in disease (2). Considering the number of people affected, the human suffering involved, and the unaddressed need for better therapeutics, LASV is arguably one of the most neglected tropical pathogens.

A highly predictive factor for the outcome of LASV infection in humans is the extent of viremia (3). Patients with fatal Lassa fever have higher viral loads at time of hospitalization and are unable to limit viral spread, whereas survivors have lower viral load and control infection progressively. The inability of the host to control viral infection in fatal Lassa fever cases is due to a marked virus-induced immunosuppression (1). The virus-induced immunosuppression likely involves infection of antigen-presenting cells (APCs), in particular dendritic cells (DCs) that are crucial for the development of the adaptive anti-viral immune response in a primary LASV infection (4). Accordingly, infection of human DCs with LASV fails to activate the cells and results in an impairment of their ability to present antigens to T cells (5, 6). However, the virus induced-mechanisms leading to immunosuppression remain largely unknown.

Arenaviruses are enveloped negative-strand RNA viruses with a cell cycle restricted to the cytoplasm (7-9). The viral genome is comprised of two RNA segments. The S segment encodes the envelope glycoprotein precursor (GPC) and the nucleoprotein (NP), and the L segment the matrix protein (Z) as well as the viral polymerase (L). The viral GPC is synthesized as a single polypeptide and undergoes processing by cellular proteases yielding the N-terminal GP1, the transmembrane GP2, and a stable signal peptide (SSP) (10). The GP1 binds to cellular receptors (11), whereas GP2 mediates viral fusion and structurally resembles other class I viral fusion proteins (12, 13). The first cellular receptor discovered for LASV was dystroglycan (DG), a ubiquitously expressed receptor for extracellular matrix (ECM) proteins (14, 15). Recent efforts to discover novel cellular receptors for LASV using an expression cloning approach identified the Tyro3/Axl/Mer (TAM) receptor tyrosine kinases Axl and Dtk (Tyro3), as well as the C-type lectins DC-specific ICAM-3-grabbing non-integrin (DC-SIGN) and LSECtin as novel candidate receptors (16).

DC-SIGN is a type II C-type lectin that contains a carbohydrate recognition domain that binds pathogen-derived high-mannose carbohydrates in a calcium-dependent manner. DC-SIGN is present on many classes of DCs and its expression can be subject to regulation by different factors (17, 18). In DCs, DC-SIGN is normally involved in endocytosis of antigens and delivery to late endosomes/lysosomes followed by processing and subsequent presentation in the context of MHC II (19). DC-SIGN can facilitate infection or transmission of a variety of enveloped viruses, such as HIV-1 (20, 21), the filoviruses Ebola and Marburg virus (22, 23), SARS coronavirus (24), the flaviviruses Dengue virus (25, 26) and West Nile virus (27). Recently, DC-SIGN has been identified as the cell entry receptor for arthropod-borne bunyaviruses of the genus *phlebovirus*, including Rift Valley fever (RVFV) and Uukuniemi viruses (UUKV) in human DCs (28). DC-SIGN was found to directly bind to high-mannose glycans on phlebovirus GPs and to be crucial for attachment and subsequent internalization, leading to productive infection. Considering the crucial role of human DCs in the development of an anti-viral immune response, the mechanisms by which LASV invades these cells are of particular interest to understand the viral pathogenesis. In our present study we investigated the role of known candidate receptors for LASV cell entry into human DCs.

MATERIALS AND METHODS

Antibodies and reagents

Monoclonal antibodies (mAbs) 113 (anti-LCMVNP) and 83.6 (anti-LCMVGP) have been described (29, 30). Mouse monoclonal antibodies (mAb) B-ly6 anti-CD11c conjugated to phycoerythrin (PE), mouse mAb 2331 anti-CD86-PE, mouse mAb DCN46 anti-CD209 (DC-SIGN)-PE, and mouse mAb M5E2 anti-CD14-PE were from BD Pharmingen. Purified polyclonal goat IgG anti-hAxl, mAb 125518 anti-hMer-PE, mAb 96201 anti-hDtk-PE, mAb 120507 anti-DC-SIGN and mAb DC28 anti-DC-SIGN/DC-SIGNR were from R&D Systems. Polyclonal guinea pig anti-LCMV NP serum was provided by Dr. Juan Carlos de la Torre (Scripps Research Institute, La Jolla). The rabbit polyclonal antibody U2 is directed against all UUKV proteins and was generated as previously described (31). Mouse mAb B-5-1-2 anti- α -tubulin, rabbit anti-goat IgG, goat anti-mouse IgG secondary antibodies conjugated to PE and biotinylated anti-guinea pig IgG were purchased from Sigma-Aldrich. Horseradish peroxidase (HRP) conjugated polyclonal rabbit anti-mouse IgG was from Dako, Rhodamine Red-X-AffiniPure F(ab')₂ Fragment Goat Anti-Rabbit IgG (H+L) from Jackson ImmunoResearch (EU), while Alexa Fluor® 594 goat anti-mouse IgM (μ chain), Alexa Fluor® 594 streptavidin and 4',6-diamidino-2-phenylindole (DAPI) were purchased from Molecular Probes® (Invitrogen). Human FcR blocking reagent (MACS Miltenyi Biotec) was used during surface staining of immature dendritic cells with “whole” IgG primary antibodies.

Recombinant human granulocyte-macrophage colony-stimulating factor (GM-CSF) and recombinant human interleukin-4 (IL-4) were obtained from Gibco. Recombinant human DC-SIGN/CD209/Fc chimera was from R&D Systems, β 1-2 N-Acetylglucosamine-mannose (GlcNAc β 1-2man) was from Dextra Inc. LIVE/DEAD® fixable dead cell stain kit was from Molecular probes®, Invitrogen. Recombinant DG fused to human IgG Fc (DG-Fc) was produced as described (32).

Cells and viruses

Peripheral blood mononuclear cells (PBMCs) were isolated from human blood obtained from healthy volunteers (protocol approved by the Commission cantonale d'éthique de la recherche sur l'être humain from de canton de Vaud, #106/10), from buffy coats (provided by the Service Régional Vaudois de Transfusion Sanguine, Epalinges, Switzerland), or purchased as frozen aliquots from Clonethics/Lonza (Walkersville, MD). Briefly, blood samples or buffy coats were diluted 2-4x volume in PBS supplemented with 2mM EDTA Utrapure™ (Gibco®)

and transferred in Leucosep® tubes (Greiner Bio-One GmbH, Huber) previously loaded with Biocoll Separating Solution 1.077g/ml density (Biochrom AG) according to the manufacturer instructions. The Leucosep® tubes were then centrifuged at 1000xg for 10 minutes at 20°C in a swinging-bucket rotor without brake. The plasma layer was discarded and the PBMCs “ring” collected, washed once with PBS-EDTA and centrifuged 10 min. at 300xg. Red blood cells were lysed using sterile ACK Lysis buffer (1mM KHCO₃, 0.15M NH₄Cl, 0.1mM EDTA, HCl, pH 7.2-7.4) for 3-4 min. Cells were washed again with PBS-EDTA and centrifuged at 200 x g for 15 min at 4°C. CD14⁺ monocytes were isolated from PBMCs by CD14⁺ positive selection using a magnetic cell sorting (MACS®, Miltenyi Biotec) according manufacturer’s instructions. Monocytes derived immature dendritic cells (MDDCs) were obtained by culturing CD14⁺ monocytes in RPMI 1640 medium + GlutaMAX™ (Gibco®) supplemented with 10 % FCS, antibiotics (100 U/mL penicillin and 0.1 mg/mL streptomycin), 100 ng/ml GM-CSF and 50 ng/ml IL-4 for 3-5 days as described (33). A549 and HEK293 cells were cultured in DMEM, 10 % (vol/vol) FBS, supplemented with glutamine, and penicillin/streptomycin. Jurkat cells were maintained in RPMI, 10 % (vol/vol) FBS, supplemented with glutamine, and penicillin/streptomycin. Raji cell lines expressing DC-SIGN WT, DC-SIGN wild-type and DC-SIGN-LL mutant were maintained in RPMI 1640 medium + GlutaMAX™ supplemented with 10% FCS and 100 U/mL penicillin and 0.1 mg/mL streptomycin as shown before (34). The Raji-derived B-THP-1 cells expressing LSECTin were a gift from the laboratory of Dr. Stefan Pöhlmann, Deutsches Primatenzentrum, Göttingen and were maintained as reported (35)

The recombinant rLCMV-LASVGP and rLCMV-VSVG have been described elsewhere (36, 37). According to the institutional biosafety guidelines of the Lausanne University Hospital, the chimera rLCMV-LASVGP has been classified as a BSL2 pathogen for use in cell culture. The generation of recombinant VSVΔG* expressing GFP pseudotyped with VSV G (rVSVΔG*-VSVG) has been reported (38, 39). Viruses were produced and the titers determined as previously described (40). UUKV strain S23 was used in this study (41). UUKV production, purification and titration were performed in mammalian BHK-21 cells as described (28, 31). LASV (strain Josiah) was produced at the Special pathogens Branch of the Centers for Disease Control and Prevention (Atlanta, GA) and inactivated by gamma irradiation using a dose of 2 x 10⁶ rads as described (42).

Flow cytometry analysis

For cell surface staining, cells were detached, when adherent, with enzyme-free cell dissociation solution, resuspended in FACS buffer (1% (vol/vol) FCS, 0.1% (wt/vol) sodium azide, PBS), and plated in conical 96-well plates, followed by one hour on ice with FACS buffer diluted with corresponding primary antibody. Cells were then washed twice in FACS buffer and labeled with secondary antibodies (as needed) for 45 min on ice in the dark. After two wash-steps in 1% (vol/vol) FBS in PBS, cells were fixed with 1/10 CellFix® solution for 10 min at room temperature in the dark. The cells were washed twice with PBS, and fluorescence intensity assessed using a FACSCalibur flow cytometer (Becton Dickinson) using the CellQuest Pro® acquisition and analysis software. Intracellular FACS staining of LCMV NP and UUKV antigens was performed as described (43).

Solid phase binding assays

For binding of virus to DC-SIGN-Fc and DG-Fc fusion proteins, 20 µg/ml purified proteins in PBS were immobilized in microtiter plates for 2 h and nonspecific binding blocked with 1% (wt/vol) bovine serum albumin (BSA) in PBS. Inactivated LASV or rLCMV-LASVGP (10⁷ PFU/ml) in 1% (wt/vol) BSA, PBS were applied for 12 h at 6°C. Bound viruses were detected with mAb 83.6 (20 µg/ml) in 1% (wt/vol) BSA, PBS using an HRP-conjugated secondary antibody. For binding of DC-SIGN and DG-Fc fusion proteins to rLCMV-LASVGP, purified viruses (10⁷ PFU/ml) were immobilized in microtiter plates and incubated with the Fc fusion proteins for 2 hours at 4 °C. Bound Fc-proteins were detected with a combination of mouse anti-human IgG Fc (1:500) and HRP-conjugated goat anti-mouse IgG (1:500). Assays were developed with ABTS [2,2α-azinobis(3-ethylbenzthiazolinesulfonic acid)] substrate and the optical density at 405 nm recorded in an enzyme-linked immunosorbent assay (ELISA) reader. Background binding to BSA was subtracted.

Virus binding to monocytes and MDDC

For biotinylation of rLCMV-LASVGP, we used a modified version of the protocol described (44). Briefly, purified virus was dialyzed against reaction buffer (0.1 M NaHCO₃, 100 mM NaCl, pH 8.0) and reacted twice with 1 mM NHS-X-biotin (Calbiochem) for 20 min on ice. The reaction was quenched by adding cold 50 mM glycine (final concentration) pH 8.0 for 10 min, the virus dialyzed against PBS and infectivity checked by IFA on VeroE6 cells. Only biotinylated virus retaining >50% of infectivity was used in experiments. For virus

binding assay, single cell suspensions of monocytes and MDDC were prepared in 1% (vol/vol) FBS, 0.1% (wt/vol) sodium azide, PBS supplemented with 1 mM MgCl₂ and 0.5 mM CaCl₂ (binding buffer) and blocked for 15 min on ice. Cells (5×10^4 per well) were transferred to M96 plates, centrifuged for 5 min at 1200 rpm, and resuspended in 50 μ l binding buffer containing biotinylated rLCMV-LASVGP at the indicated particle/cell ratios in presence or absence of inhibitors. Incubation was for 1 hour on ice under shaking. After two wash-steps in binding buffer, cells were re-suspended in 4% (wt/vol) paraformaldehyde in PBS with 1 mM MgCl₂ and 0.5 mM CaCl₂ and fixed for 20 min on ice. After three washes in binding buffer, biotinylated virus was detected by adding FITC-conjugated streptavidin (1:100 in binding-buffer) for 45 min in the dark. After three wash-steps, cells were fixed with 4% (wt/vol) paraformaldehyde, PBS for 10 min at room temperature, washed twice with PBS, and analyzed with a FACS Calibur flow cytometer (Becton Dickinson, San Jose CA) using Cell Quest software.

Infection and inhibitor studies in Raji and B-THP-1 cells

Raji cells were seeded in round bottom 96 well plates (Costar) pretreated for 30 min in the presence of mannan, anti-DC-SIGN antibodies (120507 or DC28), 5 mM EDTA/EGTA at the indicated concentrations at 37 °C followed by 1 hour infection at 37°C with rLCMV-LASVGP or UUKV at the indicated multiplicity of infection (MOI) in the presence of the inhibitors at 37 °C. Unbound virus was removed by washing the cells. At 4 hours post infection 20 mM ammonium chloride was added to prevent secondary infection. At 16 hours post-infection, cells were fixed (BD cellFix™). Infection with rLCMV-LASVGP was assessed by intracellular staining of LCMV NP with mAb 113 and a PE-conjugated secondary antibody, followed by analysis in flow cytometry as described (43). Infection with UUKV was assessed by flow cytometry at 7 hours post infection as described (28). B-THP-1 cells were seeded at 10^4 cells/well in round bottom 96 well plates and incubated with the indicated concentrations of inhibitors for 30 minutes. Cells were infected with rLCMV-LASVGP and rLCMV-VSVG at MOI = 10 as described above and infection assessed after 16 hours by flow cytometry.

Determination of viral attachment and entry kinetics in MDDC

To assess the kinetics of viral attachment, MDDCs were seeded in round bottom 96 well plates. After 16 hours, cells were chilled in ice and pre-treated with mAb DC28 or a control IgG at the indicated concentrations. After two washes in cold medium, fresh ice cold medium

containing rLCMV-LASVGP (MOI 10) in presence of antibodies was added and cells incubated on ice. At the indicated time points, unbound virus was removed by two rapid wash steps in cold medium, followed by addition of pre-warmed medium and incubation at 37 °C. At four hours after the temperature shift, 20 mM ammonium chloride was added to prevent secondary infection. At a total of 16 hours, cells were fixed and infection detected by intracellular staining of LCMV NP.

For measurement of the viral entry kinetics, rLCMV-LASVGP and UUKV (MOI 3) were added to cells on ice for 1 hour. Unbound virus was removed by washing with cold medium. Pre-warmed complete medium was added and cells rapidly shifted to 37 °C at 5% CO₂. 20 mM ammonium chloride was added at 0, 5, 10, 20, 40, 60, 120 and 240 min. After 7 (UUKV) or 16 (rLCMV-LASVGP) hours infection were quantified by intracellular staining of the viral proteins by flow cytometry as described above.

Immunoblotting

Proteins were separated by SDS-PAGE and transferred to nitrocellulose. After blocking in 3% (wt/vol) skim milk in PBS, membranes were incubated with 1–10 µg/ml primary antibody in 3% (wt/vol) skim milk, PBS overnight at 4°C or 2 hours at RT. After several washes in PBS, 0.1% (wt/vol) Tween-20 (PBST), secondary antibodies coupled to HRP were applied 1:6000 in PBST for 1 h at room temperature. Blots were developed by enhanced chemiluminescence (ECL) using Super Signal West Pico ECL Substrate (Pierce).

Inhibitor studies in MDDC

MDDCs cells were seeded in round bottom 96 well plates (Costar) pretreated for 30 min in the presence of sugars (mannan, GlcNAcβ(1-2)Man), anti-DC-SIGN antibodies (mAb 120507 or mAb DC28) on ice, or for 2 hours in the presence of chlorpromazine, or for 30 minutes in presence of nocodazole, the actin inhibitors cytochalasin B, latrunculin A, and jasplakinoline, dynasore, EIPA, and IPA-3 at the indicated concentrations at 37 °C. Cells were then infected in the presence of inhibitors for 1 hour with rLCMV-LASVGP, UUKV and rLCMV-VSVG at 37 °C. At 4 hours post infection 20 mM ammonium chloride was added to prevent secondary infection. Infection was detected after 7 (UUKV) or 16 (rLCMV-LASVGP) hours by flow cytometry as mentioned above. The viability of drug-treated cells was determined by staining of single-cell preparations with Live and dead staining.

RESULTS

Up-regulation of DC-SIGN in MDDC correlates with enhanced LASV entry

Previous studies demonstrated that primary human monocyte-derived DCs (MDDC) are highly susceptible to infection with different LASV isolates and that productive infection caused virus-induced perturbation of their antigen presenting function (5, 6). To investigate LASV cell entry into human DCs, we therefore used primary human MDDCs as a model. Since LASV is a BSL4 pathogen, work with the live virus is restricted to laboratories with high security containment. To circumvent these biosafety concerns, we used a recombinant form of the genetically and structurally closely related prototypic arenavirus LCMV expressing the envelope GP of LASV (rLCMV-LASVGP) (36). The chimera rLCMV-LASVGP does not show significant attenuation *in vitro* when compared to the parental LCMV strain and grows to robust titers. Since receptor binding and host cell entry of arenaviruses are mediated exclusively by the viral GP, rLCMV-LASVGP adopts the receptor binding characteristics of LASV. The rLCMV-LASVGP has been used extensively to study LASV cell entry and cell tropism in cultured cells *in vitro* (36, 45, 46) and recently *in vivo* using a small animal model (47). Notably, rLCMV-LASVGP showed a marked tropism for DCs *in vitro* and *in vivo* and showed a tissue distribution reminiscent of LASV in human patients (47, 48). The rLCMV-LASVGP chimera represents therefore a powerful BSL2 surrogate for studies on LASV-receptor interaction and cell entry in the context of productive arenavirus infection.

In a first step, we evaluated productive infection of our rLCMV-LASVGP chimera in human MDDCs. For this purpose, primary human monocytes were isolated from peripheral blood of healthy donors and differentiated *in vitro* in the presence of GM-CSF and IL-4 as described (5). Differentiation of monocytes into MDDCs resulted in up-regulation of DC-SIGN, as detected by flow cytometry and Western-blot (Fig. 1A, B). To assess susceptibility to rLCMV-LASVGP, monocytes, and MDDCs were infected at different multiplicities. Cells were fixed and infection was detected by immunostaining for the intracellular viral nucleoprotein (NP) and quantification by flow cytometry. As a negative control, human CD4 T cells (Jurkat), which are refractory to LASV infection, were included. When compared to monocytes, MDDCs showed increased susceptibility to rLCMV-LASVGP (Fig. 1C). In line with previous studies, CD4 T cells were highly resistant (Fig. 1C). Next, we determined virus production from infected monocytes and MDDC. Briefly, cells were infected with rLCMV-LASVGP at high multiplicity (3) and virus production monitored by determination of

infectious viral titers in the cell supernatants over time using immunofocus assay (IFA). When compared to monocytes, MDDCs produced >10-fold higher amounts of infectious virus (Fig. 1D).

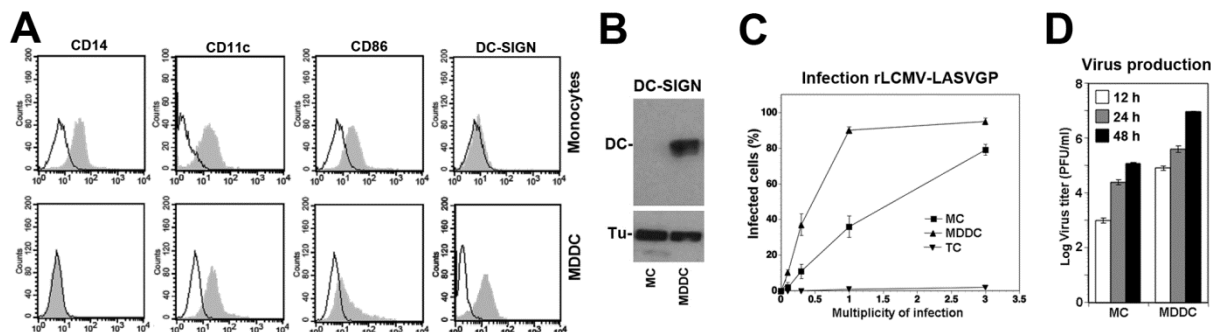


FIG. 1. Up-regulation of DC-SIGN in MDDC correlates with enhanced LASV entry. (A) Primary human monocytes were isolated from peripheral blood of healthy donors and differentiated in presence of GM-CSF and IL4 as described in Materials and Methods. The indicated markers were detected by immunostaining on live, non-permeabilized cells and analyzed by flow cytometry as described in Materials and Methods. Empty peaks: secondary antibody only, shaded peaks: primary and secondary antibody. One representative example is shown out of three experiments with different donors. (B) Detection of DC-SIGN in monocytes and MDDC. Monocytes (MC) and MDDC differentiated as in (A) were lysed, total proteins separated by SDS-PAGE, and blotted to nitrocellulose. Blots were probed with mAb 120507 to DC-SIGN and an HRP-conjugated secondary antibody using enhanced chemiluminescence (ECL) for development. As a loading control, α -tubulin was detected. The positions of DC-SIGN (DC) and α -tubulin (Tu) are indicated. One representative example is shown out of two experiments with different donors. (C) Infection of monocytes and MDDC with rLCMV-LASVGP. Primary human blood monocytes were either kept as monocytes (MC) or differentiated into MDDC. As a control, Jurkat cells (TC) were used. Cells were infected with rLCMV-LASVGP at the indicated multiplicities. After 24 hours, cells were fixed and infection detected by intracellular staining of LCMV NP in flow cytometry. Results are means \pm SD, $n = 3$. For monocytes and MDDCs, three different donors were used. (D) Virus production. Monocytes (MC), and MDDC were infected with rLCMV-LASVGP at high multiplicity (3). After the indicated time points, supernatants were collected and infectious virus titers determined by immunofocus assay (IFA) on monolayers of VeroE6 cells. Data are means \pm SD of three experiments with different donors.

The increased susceptibility to rLCMV-LASVGP of MDDC when compared to monocytes closely resembled previous observations made with live LASV isolates (5) and correlated with the strong up-regulation of DC-SIGN. Recent studies showed the absence of the TAM kinases Axl and Dtk from MDDC (33). We confirmed these previous findings by probing TAM receptor expression in monocytes and MDDC by flow cytometry (Fig. 2) and Western blot (not shown). While primary human monocytes express low levels of Dtk, none of the TAM receptors was detected in MDDC.

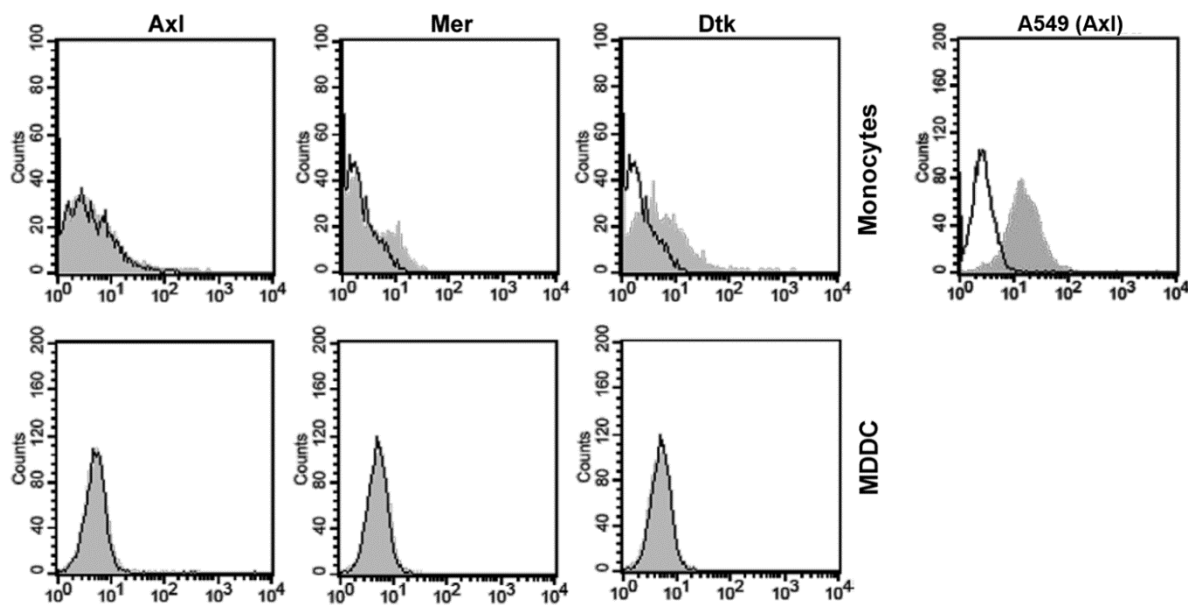


FIG. 2. MDDC lack the TAM receptors Axl, Dtk, and Mer. Live, non-permeabilized monocytes and MDDC were stained for the TAM receptors Axl, Dtk, and Mer with specific antibodies, followed by fixation, detection with PE-conjugated secondary antibodies, and analysis by flow cytometry. As a positive control for Axl, A549 cells were included. Empty peaks: secondary antibody only, shaded peaks: primary and secondary antibody. One representative example is shown out of three experiments with different donors.

LASV GP binds DC-SIGN via mannose glycans on the receptor-binding GP1

Considering the correlation between DC-SIGN expression and susceptibility to rLCMV-LASVGP infection in monocytes vs. MDDC, DC-SIGN represented an interesting candidate LASV receptor in MDDC. To further characterize the molecular interaction between LASV GP and DC-SIGN, we used authentic inactivated LASV strain Josiah, provided by the Special Pathogens Branch of the Centers for Disease Control and Prevention. To define the LASVGP part involved in DC-SIGN binding, we first addressed the relative contributions of the N-terminal GP1 and the transmembrane GP2. For this purpose, the virus was immobilized in microtiter plates and treated with 1M NaCl, which results in complete dissociation of GP1 from virions, but does not affect GP2 (49). Virus stripped with high salt and untreated control virus were incubated with C-terminal fusion proteins of recombinant DG, known to bind GP1, and DC-SIGN with human IgG Fc (DG-Fc and DC-SIGN-Fc). Virus-bound DG-Fc and DC-SIGN-Fc were then detected with an HRP-conjugated secondary antibody in a color reaction. The presence of mannose glycans in the viral glycoproteins was detected with the lectin *Galanthus nivalis* agglutinin (GNA) that specifically binds to $\alpha(1-3)$ -linked mannose. To monitor possible detachment of virus due to high salt treatment, the membrane-associated

GP2 was detected with mAb 83.6. High salt treatment of inactivated LASV markedly reduced binding of DG-Fc, DC-SIGN-Fc, and the mannose-specific lectin GNA, whereas the signal for GP2 was unaffected (Fig. 3A). The results indicate that DC-SIGN binds to LASV GP1, which bears mannose glycans. The very similar DC-SIGN binding characteristics observed with authentic LASV and rLCMV-LASVGP further confirmed that our chimera virus is an adequate model to study LASV-DC-SIGN interactions.

The binding of DC-SIGN to mannose-rich glycans present on pathogens critically depends on divalent cations and can be blocked by the sugar polymer mannan and the mAb DC28 to DC-SIGN (20, 22, 23, 25, 28). To assess the effects of these inhibitors on the interaction between LASV GP1 and DC-SIGN, DG-SIGN-Fc was immobilized and pre-treated with mannan, EDTA/EGTA and mAb DC28, followed by incubation with rLCMV-LASVGP in the presence of inhibitors. Bound virus was then detected in ELISA using mAb 83.6 to GP2 as described (32). As a control, the effect of inhibitors on virus binding to DG-Fc was examined. Binding of rLCMV-LASVGP to DC-SIGN-Fc, but not DG-Fc was specifically reduced by mannan, chelators, and mAb DC28 to DC-SIGN (Fig. 3B), suggesting a role of LASV GP1-derived mannose sugars in recognition of DC-SIGN. To corroborate a role of LASV GP1-linked mannose sugars in DC-SIGN binding, immobilized rLCMV-LASVGP was treated with EndoH, which specifically removes high-mannose *N*-glycans, but not hybrid- and complex *N*-glycans. Subsequent probing with DC-SIGN-Fc and GNA revealed a significant reduction of binding, whereas attachment of DG-Fc and mAb 83.6 to GP2 was unaffected (Fig. 3C). Taken together, our data reveal that LASV GP binds to DC-SIGN via mannose glycans on GP1.

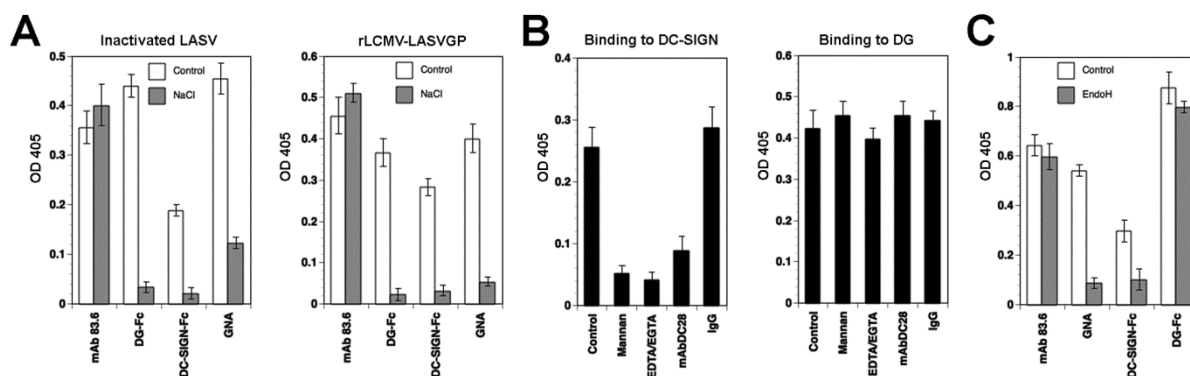


FIG. 3. Characterization of the interaction of LASV GP with DC-SIGN. (A) DC-SIGN binds to LASV GP1. Inactivated LASV and rLCMV-LASVGP purified over a renografin gradient were immobilized in microtiter plates and treated with 1 M NaCl for one hour (NaCl) or left in PBS (Control). After several washes in PBS, recombinant DC-SIGN-Fc, DG-Fc, the mAb 83.6 to LASV GP2, and biotinylated GNA were added. Bound Fc-fusion proteins were detected with HRP-conjugated anti-human IgG Fc, mAb 83.6 with an HRP-conjugated anti-mouse IgG, and GNA with HRP-linked streptavidine in a color reaction. Data represent OD values with background subtraction, means \pm SD, $n = 3$. (B) Binding of DC-SIGN to rLCMV-LASVGP is blocked by mannan, EDTA/EGTA, and mAb DC28. DC-SIGN-Fc (left panel) and DG-Fc (right panel) were immobilized in microtiter plates and treated with mannan (25 μ g/ml) 5 mM EDTA/EGTA, 20 μ g/ml mAb DC28, and IgG isotype control (IgG) at 20 μ g/ml for one hour. Purified rLCMV-LASVGP was added at 10^7 PFU/ml in presence of inhibitors for 2 hours in the cold. Bound virus was detected with mAb 83.6 to LASV GP2, combined with an HRP-conjugated secondary antibody in a color reaction as in (A) (means \pm SD, $n = 3$). (C) Removal of mannose sugars from LASV GP reduces binding to DC-SIGN. Purified rLCMV-LASVGP was immobilized and subjected to treatment with EndoH glycosidase for 12 hours at room temperature (EndoH) or left untreated (Control). After several washes, binding to DC-SIGN-Fc, DG-Fc, GNA, and mAb 83.6 were assessed as in (A) (means \pm SD, $n = 3$).

DC-SIGN mediates attachment of rLCMV-LASVGP to MDDC

In a next step, we addressed a possible role of DC-SIGN in attachment of LASV to human DCs. For this purpose, we performed a well-established virus-cell binding assay that had been previously used to characterize cellular receptors for LCMV (11, 44). Briefly, rLCMV-LASVGP was purified over a renografin gradient and labeled with biotin using the reagent NHS-X-biotin. Biotinylated virus was tested for infectivity and only preparation that retained $>50\%$ of infectious virus titers were used for further experimentation. Monocytes, MDDC, and CD4 T cells were incubated with biotinylated virus at increasing particle/cell ratios in the cold. Unbound virus was removed by washing and cells fixed. Bound virions were detected with streptavidine conjugated to Alexa 488 in flow cytometry. The binding curves displayed in Fig. 4A revealed a marked increase in virus binding to MDDC when compared to monocytes, consistent with the enhanced susceptibility for productive infection (Fig. 1C). As expected, CD4T cells showed negligible virus binding. To address the role of DC-SIGN in virus attachment to MDDC, cells were pre-treated with mannan and mAb DC28, prior to exposure to biotin-labeled virus. Treatment with both mannan and mAb DC28

resulted in a dose-dependent reduction of virus binding to MDDCs (Fig. 4B), implicating DC-SIGN in virus attachment. To complement these studies, labeled virus was pre-treated with DC-SIGN-Fc, followed by binding to MDDC. Exposure of virus to DC-SIGN-Fc, but not an isotype Fc control resulted in a dose-dependent reduction of virus binding (Fig. 4C). Together, the data indicate a role for DC-SIGN in attachment of free virus to MDDC.

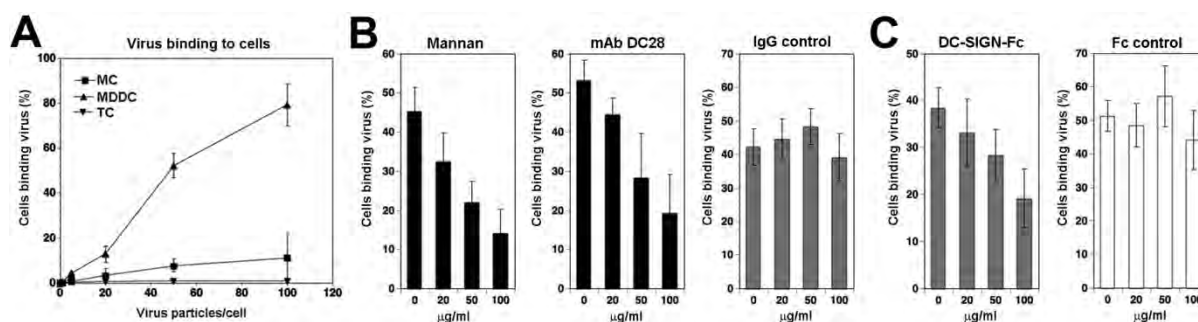


FIG. 4. DC-SIGN is an attachment factor for rLCMV-LASVGP in MDDC. (A) Binding of rLCMV-LASVGP to monocytes and MDDC. Biotinylated rLCMV-LASVGP was added to monocytes, MDDC, and Jurkat cells at the indicated particle/cell ratios for one hour at 4 °C. Unbound virus was removed, cells fixed and bound virus detected with streptavidin labeled with Alexa488. Virus-binding cells were detected in flow cytometry. Data are means \pm SD, of three experiments with different donors. (B) Blocking of virus binding to MDDC. MDDC were treated with the indicated concentrations of mannan, mAb DC28 to DC-SIGN, and control IgG for 2 hours on ice, followed by incubation with biotinylated rLCMV-LASVGP at 50 particles/cell for one hour in the cold. Bound virus was detected as in (A) and the percentage of virus-binding cells displayed. Data are means \pm SD, of three experiments with different donors. (C) Blocking of virus binding with DC-SIGN-Fc. Biotinylated rLCMV-LASVGP was incubated with the indicated concentrations of DC-SIGN-Fc and Fc control for 2 hours on ice and then added to MDDC for one hour in the cold. Virus-binding cells were assessed as in (A). Results are means \pm SD, of three experiments with different donors.

DC-SIGN facilitates productive infection of rLCMV-LASVGP in MDDC

The apparent role of DC-SIGN in attachment of rLCMV-LASVGP to MDDC (Fig. 4) opened the possibility that DC-SIGN could function as an entry receptor for LASV, similar to what has been observed for the phleboviruses UUKV and RVFV (28). In a next step, we therefore compared the role of DC-SIGN in productive infection of rLCMV-LASVGP and UUKV in MDDC. In a first step, cells were pre-treated with the DC-SIGN ligand mannan, followed by infection with rLCMV-LASVGP and UUKV in presence of the inhibitor. At four hours post infection, 20 mM ammonium chloride was added to avoid secondary infection. Infected cells were detected by intracellular staining for LCMV NP and UUKV antigen in flow cytometry after 16 and 7 hours, respectively. Blocking with mannan resulted in an only mild reduction (<30%) of infection with rLCMV-LASVGP, whereas UUKV infection was diminished by > 90% (Fig. 5A). To more specifically block DC-SIGN-mediated infection, MDDC were pre-treated with mAbs DC28 and 120507 to DC-SIGN, prior and during

infection with rLCMV-LASVGP and UUKV. Pre-treatment of MDDC with mAbs DC28 and 120507 reduced infection with rLCMV-LASVGP by circa 60% and 40%, respectively. In contrast, infection with UUKV was consistently reduced by >90% (Fig. 5C). The only partial blocking of rLCMV-LASVGP infection in MDDC by anti-DC-SIGN antibodies suggested that DC-SIGN somehow facilitated viral entry and productive infection, but was not strictly required.

Another candidate receptor identified for LASV is the C-type lectin LSECTin, identified in a recent expression cloning approach (16). Since LSECTin can be present on MDDC under some conditions (50), we addressed a potential role of LSECTin in LASV entry into MDDCs. For this purpose, cells were pre-treated with increasing concentrations of the LSECTin ligand GlcNac β (1-2)Man, followed by infection with rLCMV-LASVGP and UUKV. Treatment of MDDCs with up to 100 μ g/ml GlcNac β (1-2)Man did not affect infection with the two viruses (Fig. 5A). To confirm the efficiency of our inhibitor treatment, we used B-THP-1 cells expressing recombinant LSECTin (35). In line with previous studies (16), pre-treatment with 100 μ g/ml GlcNac β (1-2)Man, but not mannan significantly reduced infection with rLCMV-LASVGP. As a negative control, we included a recombinant LCMV expressing the G protein of vesicular stomatitis virus (rLCMV-VSVG), which is not dependent on LSECTin and was not affected by the inhibitor treatment (Fig. 5B). Together, our data make a major contribution of LSECTin for cell entry of rLCMV-LASVGP in MDDC appear unlikely.

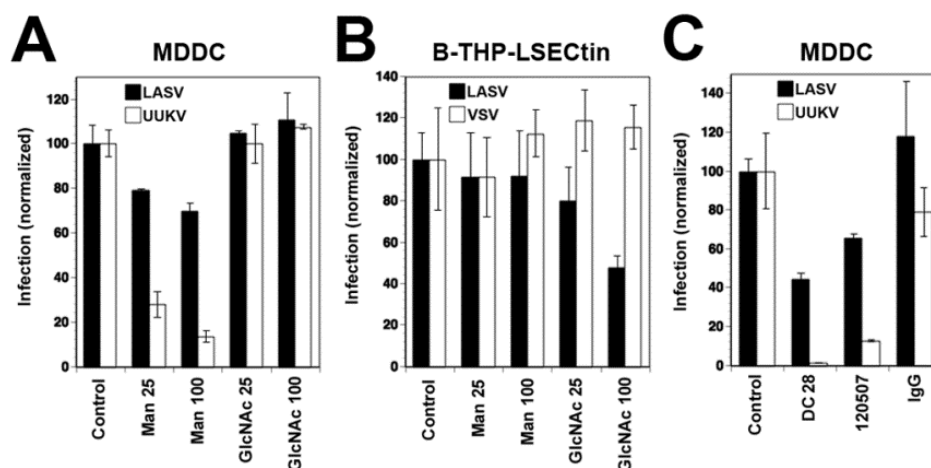


FIG. 5. DC-SIGN facilitates cell entry of rLCMV-LASVGP. (A) Blocking of virus infection in MDDC. MDDC were treated with 25 μ g/ml mannan (Man 25), 100 μ g/ml mannan (Man 100), 25 μ g/ml GlcNAc β (1-2)Man (GlcNAc 25), 100 μ g/ml GlcNAc β (1-2)Man (GlcNAc 100), and PBS vehicle control (Control) for 30 minutes at 37 $^{\circ}$ C. Cells were then infected with rLCMV-LASVGP (LASV) and UUKV at multiplicity of 3 for one hour in presence of inhibitors. Cells were washed and at four hours post infection, 20 mM ammonium chloride added to prevent secondary infection. Infection was assessed by FACS. Infection was normalized setting control specimens at 100%. Data are means \pm SD, of three experiments with different donors (6 donors in total). (B) B-THP-LSEctin cells were treated with inhibitors as in (A), followed by infection with rLCMV-LASVGP (LASV) and rLCMV-VSVG (VSV) at MOI = 10. Infection was assessed by IFA after 16 hours and data normalized as in (A). (C) Blocking of virus infection in MDDC with mAb to DC-SIGN. MDDC were treated with 20 μ g/ml of mAb DC28 (DC28), mAb 120507 (120507), isotype control IgG (IgG), or PBS (control) for 30 minutes at 37 $^{\circ}$ C, followed by infection with rLCMV-LASVGP and UUKV as in (A). Infection was normalized setting control specimens at 100%. Data are means \pm SD, of two experiments with different donors (4 donors in total).

Different efficiency of DC-SIGN in mediating entry of rLCMV-LASVGP and UUKV

The data at hand indicated that DC-SIGN can facilitate attachment and entry of rLCMV-LASVGP in MDDC. In contrast, UUKV, RVFV, and other bunyaviruses can use DC-SIGN alone for binding and infectious uptake, suggesting different roles of DC-SIGN in entry. To assess the relative efficiency of DC-SIGN in mediating productive infection by rLCMV-LASVGP and UUKV, we utilized Raji cells stable transfected with wild-type DC-SIGN and a DC-SIGN mutant containing a mutation in the cytoplasmic LL motif that is impaired in endocytosis (34). Parental Raji cells lacked TAM receptors (Fig. 6A), and expressed only negligible levels of DC-SIGN (Fig. 6B), making them refractory to rLCMV-LASVGP and UUKV. The Raji-DC-SIGN and Raji-DC-SIGN-LL stable transfectants expressed similar amounts of DC-SIGN at their surface (Fig. 6B). Parental Raji cells, Raji-DC-SIGN, and Raji-DC-SIGN-LL were infected with rLCMV-LASVGP and UUKV. Productive infection was assessed after one round of replication and normalized to the untransfected parental line. In line with previous studies, expression of DC-SIGN increased infection with UUKV by >40-

fold (28), whereas only circa 4-fold enhancement of rLCMV-LASVGP infection was observed (Fig. 6C). When compared to wild type DC-SIGN, DC-SIGN-LL was less efficient in mediating infection with rLCMV-LASVGP and UUKV (Fig. 6C). Infection of rLCMV-LASVGP and UUKV in Raji-DC-SIGN cells was blocked upon treatment with mannan and the chelators EDTA/EGTA (Fig. 5C), confirming a role of DC-SIGN in enhancement of infection. The data obtained with Raji cells expressing recombinant DC-SIGN are in line with our findings in MDDC (Fig. 7). That rLCMV-LASVGP and UUKV present significant difference in their ability to infect DC-SIGN⁺ cells may reflect distinct roles of the lectin in mediating cell entry of these viruses.

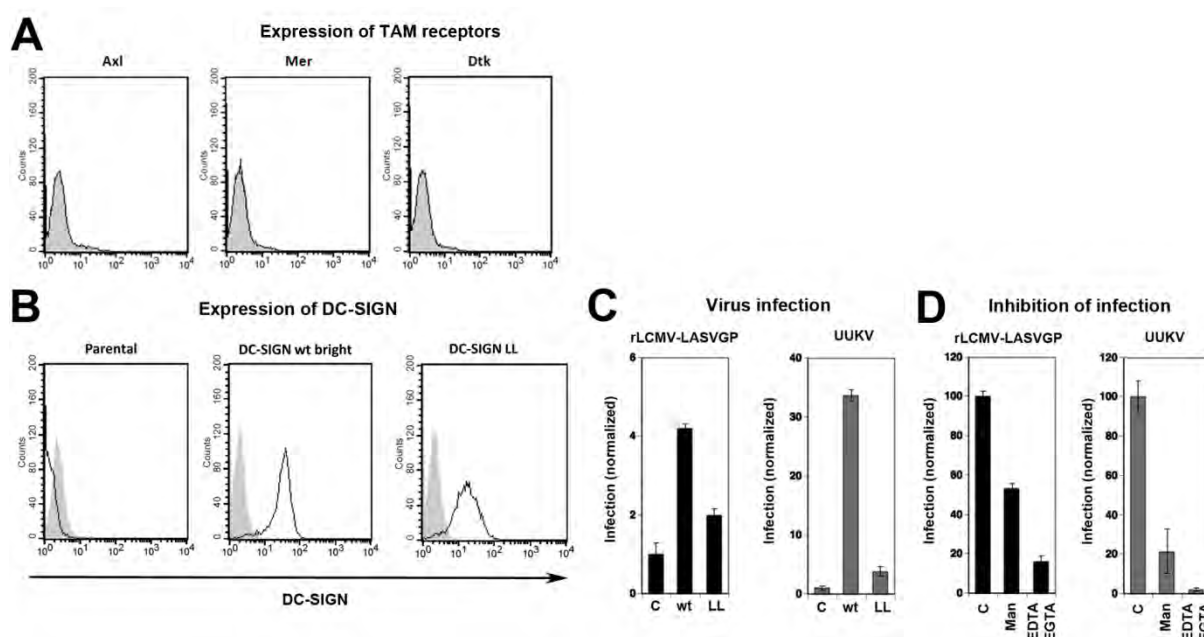


FIG. 6. Different efficiencies of DC-SIGN in cell entry of rLCMV-LASVGP and UUKV. (A) Detection TAM receptors in parental Raji cells by flow cytometry as in Fig 2. Empty peaks: secondary antibody only, shaded peaks: primary and secondary antibody. (B) Detection of DC-SIGN in Raji cell lines. Raji parental cells, Raji-DC-SIGN, and Raji-DC-SIGN-LL cells were stained with mAb 120507 to DC-SIGN combined with a PE-conjugated secondary antibody and analyzed in flow cytometry. (C) Virus infection of Raji cell lines. Raji parental cells (C), Raji-DC-SIGN (wt), and Raji-DC-SIGN-LL (LL) were infected with rLCMV-LASVGP and UUKV at a multiplicity of 3. At 4 hours post infection, 20 mM ammonium chloride was added to avoid secondary infection. Infection was assessed by intracellular staining for LCMV NP and UUKV antigen after 18 hours, respectively, and infected cells detected by flow cytometry (means \pm SEM, $n = 2$). (D) Inhibition of infection of Raji-DC-SIGN cells. Raji-DC-SIGN cells were treated with 50 μ g/ml mannan (Man), 5 mM EDTA/EGTA, or PBS vehicle control (C) for 30 minutes, followed by infection with rLCMV-LASVGP and UUKV. Infection was assessed as in (B) and normalized setting control specimens at 100% (means \pm SEM, $n = 2$).

DC-SIGN accelerates capturing of free rLCMV-LASVGP by MDDCs

A hallmark of lectin-type carbohydrate-protein interactions are their relatively fast on-rates, opening the possibility that DC-SIGN may be involved in capturing free rLCMV-LASVGP by human DCs. To address this possibility, we investigated the role of DC-SIGN in the attachment kinetics of rLCMV-LASVGP in MDDCs. Cells were chilled on ice and pre-incubated with mAb CD28 to DC-SIGN or a control IgG in the cold. rLCMV-LASVGP was then added at MOI 10 in presence of the antibodies. At the indicated time points, unbound virus was removed by washing and the cells rapidly shifted to 37°C. After 4 hours, ammonium chloride was added and infection detected after 16 hours by flow cytometry. In presence of control IgG, the virus rapidly attached to cells and reached saturation with half-maximal binding after <15 minutes (Fig. 7A). Blocking of DC-SIGN with mAb DC28 resulted in slower virus attachment that hardly reached saturation after 45 min. After < 45 min of attachment, we noticed reduced viral titers produced from cells treated with anti-DC-SIGN antibody (Fig. 7B). The data suggest that DC-SIGN can accelerate capture of free virus, facilitating productive infection.

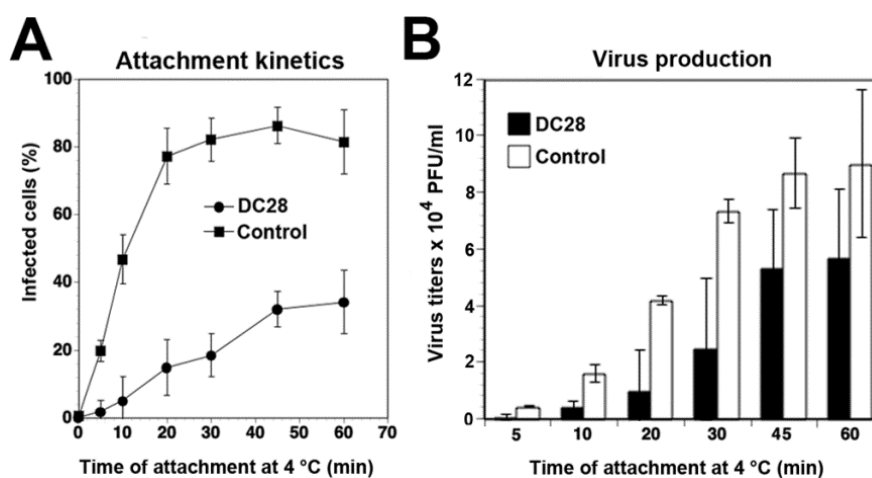


FIG. 7. Attachment and entry kinetics of rLCMV-LASVGP in MDDC. (A) DC-SIGN accelerates capture of free virus. MDDCs were pre-treated with mAb DC28 to DC-SIGN and control IgG (Control) for 1 hour in the cold, followed by binding of rLCMV-LASVGP at MOI of 10. At the indicated time points, unbound virus was removed by washing and cells shifted to 37°C. Productive infection was detected after a total of 16 hours by FACS (means \pm SEM, n = 3). (B) Conditioned cell culture supernatants from A were assessed for infectious virus titers by IFA as in Fig. 1D. Data are means \pm SD, of three experiments with different donors.

rLCMV-LASVGP enters MDDC via a slow actin-dependent pathway

The apparently different role of DC-SIGN in productive infection of rLCMV-LASVGP and UUKV opened the possibility that the viruses may use distinct pathways for cell entry. In a first step, we compared the entry kinetics of rLCMV-LASVGP and UUKV in MDDC. Both viruses require a pH of < 6.0 for fusion indicating delivery to late endosomes for productive cell entry (28, 45). To assess how fast receptor-bound rLCMV-LASVGP and UUKV trafficked to late endosomes, we determined the time required for the viruses to become resistant to ammonium chloride. When added to cells, ammonium chloride raises the endosomal pH rapidly and blocks low pH-dependent membrane fusion without causing overall cytotoxicity (51, 52). The viruses were bound to MDDC in the cold, allowing receptor attachment without internalization. Unbound virus was removed and cells shifted to 37°C to restore membrane movements. Ammonium chloride was added at different time points post infection and kept throughout the experiment. Cells were fixed and infection assessed by flow cytometry. In line with published data, 50% of UUKV had escaped from the late endosome after circa 20 minutes (28). In contrast, cell entry of rLCMV-LASVGP was markedly slower with < 50% of the virus having escaped from the endosome after one hour (Fig. 8A).

To test the involvement of actin-dependent pathways, like macropinocytosis or phagocytosis that are present in MDDC, we treated cells with cytochalasin D or latrunculin A, which disrupt actin fibers, as well as jasplakinolide, an actin-polymer stabilizing drug that blocks the dynamics of actin filaments. When added to cells for 30 minutes prior to infection, cytochalasin D, latrunculin A, and jasplakinolide significantly reduced infection of rLCMV-LASVGP, but not UUKV (Fig. 8B). Previous studies revealed that UUKV associates in MDDC with clathrin-coated pits (28). A possible role of clathrin-mediated endocytosis (CME) in cell entry of rLCMV-LASVGP into MDDC was therefore addressed using chlorpromazine (CPZ), a drug that perturbs the assembly of clathrin-coated pits at the plasma membrane. As a positive control, we included a recombinant VSV pseudotype that contains a GFP reporter and bears VSVG (rVSVΔG*-VSVG) in its envelope, which mediates cell entry in a clathrin- and dynamin-dependent manner (53). The VSV pseudotype lacks endogenous G and is limited to one round of replication, limiting viral spread. Treatment of MDDC with up to 8 μM CPZ did not significantly affect infection with rLCMV-LASVGP, but reduced infection of rVSVΔG*-VSVG in a dose-dependent manner (Fig. 8C). To address the involvement of dynamin in rLCMV-LASVGP cell entry, MDDC were treated with the dynamin inhibitor dynasore prior to infection. As control, we again included rVSVΔG*-

VSVG. As shown in Fig. 8D, infection of MDDC with rLCMV-LASVGP was not affected by up to 100 μ M dynasore, whereas infection of rVSV Δ G*-VSVG was reduced.

The actin-dependence and apparent clathrin- and dynamin-independence of rLCMV-LASVGP cell entry into MDDC suggested a possible role of macropinocytosis in the process (54). Treatment of cells with the Na⁺/H⁺ exchanger inhibitor ethylisopropyl amiloride (EIPA) reduced infection with rLCMV-LASVGP, but only at relatively high concentrations (Fig. 8E). We further used the PAK1 inhibitor IPA-3, which plays a central role in macropinocytosis of some viruses, e.g. vaccinia (55). As shown in Fig. 8F, IPA-3 had no significant effect on infection of rLCMV-LASVGP in MDDC, but reduced infection of HeLa cells with vaccinia virus, in line with published data (55). Since vesicular transport to late endosomes in many cell types depends on microtubules (56), we tested the effect of nocodazole, a drug that dissociates microtubular structures on rLCMV-LASVGP entry into MDDCs. Pretreatment of cells with nocodazole to some extent reduced infection with rLCMV-LASVGP, indicating a role of microtubules in the process (Fig. 8G).

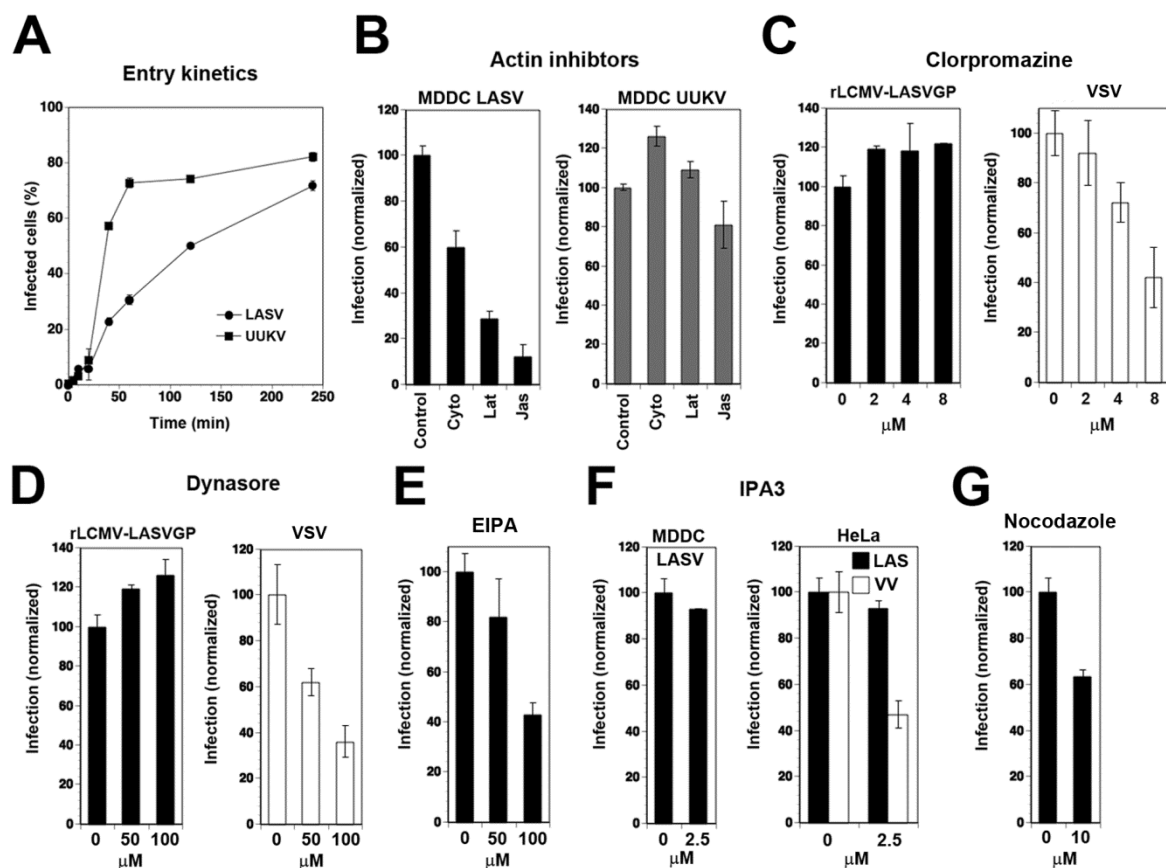


FIG. 8. Characterization of rLCMV-LASVGP entry into MDDC. (A) Entry kinetics of rLCMV-LASVGP and UUKV in MDDC. MDDC were incubated with rLCMV-LASVGP and UUKV at multiplicity of 3 for one hour in the cold. Unbound virus was removed and cells shifted to 37 °C. At the indicated time points, 20 mM ammonium chloride was added and left throughout the experiment. After 16 hours (rLCMV-LASVGP) and 7 hours (UUKV), cells were fixed and infection detected as in Fig. 6. The percentage of infected cells was plotted against time, data are means \pm SEM of three experiments with three different donors. (B) Infection of rLCMV-LASVGP in MDDC is actin-dependent. MDDC were treated with 20 μ M cytochalasin D (Cyto), 5 μ M latrunculin A (Lat), and 1 μ M jasplakinolide (Jas), or solvent control (control) for 30 minutes, followed by infection with rLCMV-LASVGP and UUKV as in (A). Data are means \pm SD, of three experiments with three different donors. (C) Effect of CPZ on the infection of rLCMV-LASVGP. MDDC were treated with the indicated concentrations of CPZ or PBS only (0) for one hour, followed by infection with rLCMV-LASVGP or rVSV Δ G*-VSVG (VSV) at a multiplicity of 10. After 4 hours, 20 mM ammonium chloride were added to prevent secondary infection, and rLCMV-LASVGP infected cells detected after 16 hours as in (A). Cells infected with rVSV Δ G*-VSVG were fixed after 6 hours and GFP detected by direct fluorescence. At 6 hours post infection, MDDC infected with rVSV Δ G*-VSVG, but not rLCMV-LASVGP started to show signs of activation. Infection was normalized setting untreated specimens at 100%. Data are means \pm SD, of three experiments with three different donors. (D) Blocking of infection of rLCMV-LASVGP with dynasore. MDDC were pre-treated with the indicated concentrations of dynasore or vehicle control (0), followed by infection with rLCMV-LASVGP or rVSV Δ G*-VSVG (VSV) as in (C). Data are means \pm SD, of three experiments with three different donors. (E) Inhibition of rLCMV-LASVGP infection in MDDC by EIPA. MDDC were pre-treated with the indicated concentrations of EIPA or vehicle control (0) for 30 minutes, prior to infection with rLCMV-LASVGP as in (B). Data are means \pm SD, of three experiments with three different donors. (F) Effect of the PAK1 inhibitor IPA-3 on infection of rLCMV-LASVGP. MDDC and HeLa cells were pre-treated with the indicated concentration of IPA-3 or vehicle control (0) for 30 minutes, followed by infection with rLCMV-LASVGP (LASV) or recombinant vaccinia virus expressing GFP (VV). Infection with rLCMV-LASVGP was assessed as in (B) and infection with VV by detection of the GFP reporter in direct fluorescence microscopy at 12 hours post infection. Data are means \pm SD, of three experiments with three different donors. (G) The role of microtubules in rLCMV-LASVGP infection in MDDC. MDDC were pre-treated with nocodazole (10 μ M) or solvent control (0) and infection with rLCMV-LASVGP performed as in (B). Data are means \pm SD, of three experiments with three different donors.

DISCUSSION

Here we studied the role of the C-type lectin DC-SIGN in cell entry of LASV into human MDDC using a recombinant LCMV expressing LASV GP (rLCMV-LASVGP) as a BSL2 surrogate for LASV. We found that differentiation of primary human monocytes into MDDC enhanced susceptibility to rLCMV-LASVGP infection, a situation similar to the one observed with live LASV isolates (5). The up-regulation of DC-SIGN in MDDC correlated with markedly stronger virus attachment and enhanced productive infection suggesting a role of DC-SIGN in attachment and/or infection of rLCMV-LASVGP, similar to its function in cell entry of the arthropod-borne phleboviruses UUKV and RVFV (28)

Previous studies on the role of DC-SIGN in entry of UUKV and RVFV showed that these viruses bind to DC-SIGN via high mannose N-glycans present on their glycoproteins (28). Our present studies revealed a similar binding mechanism for LASV involving N-linked mannose sugars on GP1, in line with the previously reported observation that LASV GP1 contains high proportion of mannose sugars (57), similar to the glycoproteins of arthropod-borne viruses. To investigate the role of DC-SIGN in different steps of LASV cell entry, we first performed virus-cell binding assays and found that DC-SIGN is involved in attachment of the virus to MDDCs. To address the function of DC-SIGN in productive infection, we compared rLCMV-LASVGP with UUKV that uses DC-SIGN as an authentic entry receptor (28). Blocking of DC-SIGN on MDDCs with mannan and antibodies almost completely abolished UUKV infection, but only partially reduced infection with rLCMV-LASVGP. Using Raji cells stable expressing DC-SIGN, we confirmed the different efficiency of DC-SIGN in mediating infection of rLCMV-LASVGP and UUKV. While recombinant DC-SIGN greatly enhanced productive infection with UUKV, as shown previously (28), the effect on rLCMV-LASVGP was more modest.

The data at hand supported a role of DC-SIGN as an entry factor for rLCMV-LASVGP, raising the question about the possible physiological relevance of the LASV-DC-SIGN interaction. In early LASV infection, the virus infects DCs at the site of inoculation and the kinetics of free virus capture by DCs may thereby be an important determinant for efficient productive infection. To address the role of DC-SIGN in virus capture by MDDC, we determined the kinetics of virus-cell attachment in presence and absence of function-blocking anti-DC-SIGN antibodies. Using productive infection as readout, we provide first evidence that DC-SIGN can accelerate capture of free virus by MDDC.

The data at hand suggest that DC-SIGN can facilitate LASV infection of MDDC at the level of virus-cell attachment. However, its role in the subsequent cell entry process was unclear. UUKV and LASV require a similarly low pH for fusion, indicating that both viruses escape from a late endosomal compartments (31, 58, 59). Previous live cell microscopy studies performed with UUKV revealed that, upon virus attachment, the virus-DC-SIGN complex is rapidly internalized and delivered to early endosomes, followed by transport of the virus to the late endosome, where fusion occurs after only 9-15 minutes (28). Monitoring of viral entry kinetics in MDDC revealed that UUKV escaped from the endosome with a half-time of less than 20 minutes, whereas < 50% of rLCMV-LASVGP had escaped after one hour. Using a combination of actin inhibitors, we found that entry of rLCMV-LASVGP, but not UUKV was actin-dependent. In contrast to UUKV that associated with clathrin-coated pits in MDDC (28), studies with inhibitors provided first evidence that entry of rLCMV-LASVGP was independent of clathrin and dynamin. The strong actin-dependence of rLCMV-LASVGP entry into MDDCs and its sensitivity to the amiloride EIPA, a potent inhibitor of the Na/H⁺ exchanger rather suggest an entry pathway related to macropinocytosis that is constitutively active in MDDCs. The distinct entry pathways used, together with the substantial DC-SIGN-independent infection of rLCMV-LASVGP, suggest rather different roles of DC-SIGN in cell entry of LASV compared to phleboviruses like UUKV and RVFV. In contrast to phleboviruses that use DC-SIGN as an entry receptor, DC-SIGN seems to serve primarily as an attachment factor for LASV in MDDC involved in virus capture. The partial independence of rLCMV-LASV entry from DC-SIGN suggests the existence of additional LASV entry factors in MDDCs. Of particular importance in this context is the role of DG, which represents a major LASV receptor. LASV binding to DG critically depends on functional glycosylation of the receptor, in particular specific O-linked glycans present on α -DG synthesized by the glycosyltransferase LARGE that are also crucial for recognition of DG's ECM ligands (32, 60). While the core protein of DG is ubiquitously expressed, the functional glycosylation of the receptor is under tight tissue-specific control (61). In previous studies, we found that many human cell types targeted *in vivo* by LASV, such as epithelial cells, vascular endothelial cells, and hepatocytes express functionally glycosylated DG able to bind LASV with high affinity (62). However, the functional glycosylation of DG in human DCs, including MDDC, is currently unknown. Our initial attempts to detect functional DG in primary human MDDC in this study gave unclear results, suggesting possible differences in the extent or nature, or both, of functional glycosylation of DG compared to other cell types. In-depth characterization of the post-translational modification of DG in human DCs, and its

possible role as an entry factor for LASV, are currently under way in our laboratory and will contribute to a better understanding of LASV entry into this pivotal cell type

ACKNOWLEDGEMENTS

The authors thank Prof. Stefan Pöhlmann (Deutsches Primatenzentrum, Göttingen) for providing us with the B-THP-1 cell line expressing LSECtin. We acknowledge Christelle Pythoud, Jillian M. Rojek, and Laetitia Basterra for their contributions to these studies. This research was supported by Swiss National Science Foundation grant FN 310030_132844 (S.K.). The antibody IIH6 to dystroglycan was provided by Kevin P. Campbell, Howard Hughes Medical Institute, University of Iowa.

REFERENCES

1. **McCormick JB, Fisher-Hoch SP.** 2002. Lassa fever. *Curr Top Microbiol Immunol* **262**:75-109.
2. **McCormick JB, King IJ, Webb PA, Scribner CL, Craven RB, Johnson KM, Elliott LH, Belmont-Williams R.** 1986. Lassa fever. Effective therapy with ribavirin. *N Engl J Med* **314**:20-26.
3. **Johnson KM, McCormick JB, Webb PA, Smith ES, Elliott LH, King IJ.** 1987. Clinical virology of Lassa fever in hospitalized patients. *The Journal of infectious diseases* **155**:456-464.
4. **Geisbert TW, Jahrling PB.** 2004. Exotic emerging viral diseases: progress and challenges. *Nature medicine* **10**:S110-121.
5. **Baize S, Kaplon J, Faure C, Pannetier D, Georges-Courbot MC, Deubel V.** 2004. Lassa virus infection of human dendritic cells and macrophages is productive but fails to activate cells. *J Immunol* **172**:2861-2869.
6. **Mahanty S, Hutchinson K, Agarwal S, McRae M, Rollin PE, Pulendran B.** 2003. Cutting edge: impairment of dendritic cells and adaptive immunity by Ebola and Lassa viruses. *J Immunol* **170**:2797-2801.
7. **Buchmeier MJ, de la Torre JC, Peters CJ.** 2007. Arenaviridae: the viruses and their replication, p. p. 1791-1828. *In* Knipe DL, Howley PM (ed.), *Fields Virology*, 4th ed. Lippincott-Raven, Philadelphia.
8. **de la Torre JC.** 2009. Molecular and cell biology of the prototypic arenavirus LCMV: implications for understanding and combating hemorrhagic fever arenaviruses. *Ann N Y Acad Sci* **1171 Suppl 1**:E57-64.
9. **Meyer BJ, de La Torre JC, Southern PJ.** 2002. Arenaviruses: Genomic RNAs, Transcription, and Replication, p. 139-149. *In* Oldstone MB (ed.), *Arenaviruses I*, vol. 262. Springer-Verlag, Berlin Heidelberg.
10. **Burri DJ, da Palma JR, Kunz S, Pasquato A.** 2012. Envelope glycoprotein of arenaviruses. *Viruses* **4**:2162-2181.
11. **Borrow P, Oldstone MB.** 1992. Characterization of lymphocytic choriomeningitis virus-binding protein(s): a candidate cellular receptor for the virus. *J Virol* **66**:7270-7281.
12. **Eschli B, Quirin K, Wepf A, Weber J, Zinkernagel R, Hengartner H.** 2006. Identification of an N-terminal trimeric coiled-coil core within arenavirus glycoprotein 2 permits assignment to class I viral fusion proteins. *J Virol*. **80**:5897-5907.
13. **Igonet S, Vaney MC, Vonhrein C, Bricogne G, Stura EA, Hengartner H, Eschli B, Rey FA.** 2011. X-ray structure of the arenavirus glycoprotein GP2 in its postfusion hairpin conformation. *Proc Natl Acad Sci U S A* **108**:19967-19972.
14. **Cao W, Henry MD, Borrow P, Yamada H, Elder JH, Ravkov EV, Nichol ST, Compans RW, Campbell KP, Oldstone MB.** 1998. Identification of alpha-dystroglycan as a receptor for lymphocytic choriomeningitis virus and Lassa fever virus [see comments]. *Science* **282**:2079-2081.
15. **Oldstone MB, Campbell KP.** 2011. Decoding arenavirus pathogenesis: essential roles for alpha-dystroglycan-virus interactions and the immune response. *Virology* **411**:170-179.
16. **Shimojima M, Stroher U, Ebihara H, Feldmann H, Kawaoka Y.** 2012. Identification of cell surface molecules involved in dystroglycan-independent lassa virus cell entry. *J Virol* **86**:2067-2078.
17. **van Kooyk Y.** 2008. C-type lectins on dendritic cells: key modulators for the induction of immune responses. *Biochem Soc Trans* **36**:1478-1481.
18. **Svajger U, Anderluh M, Jeras M, Obermajer N.** 2010. C-type lectin DC-SIGN: an adhesion, signalling and antigen-uptake molecule that guides dendritic cells in immunity. *Cellular signalling* **22**:1397-1405.
19. **McGreal EP, Miller JL, Gordon S.** 2005. Ligand recognition by antigen-presenting cell C-type lectin receptors. *Curr Opin Immunol* **17**:18-24.
20. **Geijtenbeek TB, Kwon DS, Torensma R, van Vliet SJ, van Duijnhoven GC, Middel J, Cornelissen IL, Nottet HS, KewalRamani VN, Littman DR, Figdor CG, van Kooyk Y.**

2000. DC-SIGN, a dendritic cell-specific HIV-1-binding protein that enhances trans-infection of T cells. *Cell* **100**:587-597.
21. **Kwon DS, Gregorio G, Bitton N, Hendrickson WA, Littman DR.** 2002. DC-SIGN-mediated internalization of HIV is required for trans-enhancement of T cell infection. *Immunity* **16**:135-144.
 22. **Alvarez CP, Lasala F, Carrillo J, Muniz O, Corbi AL, Delgado R.** 2002. C-type lectins DC-SIGN and L-SIGN mediate cellular entry by Ebola virus in cis and in trans. *J Virol* **76**:6841-6844.
 23. **Simmons G, Reeves JD, Grogan CC, Vandenberghe LH, Baribaud F, Whitbeck JC, Burke E, Buchmeier MJ, Soilleux EJ, Riley JL, Doms RW, Bates P, Pohlmann S.** 2003. DC-SIGN and DC-SIGNR bind ebola glycoproteins and enhance infection of macrophages and endothelial cells. *Virology* **305**:115-123.
 24. **Jeffers SA, Tusell SM, Gillim-Ross L, Hemmila EM, Achenbach JE, Babcock GJ, Thomas WD, Jr., Thackray LB, Young MD, Mason RJ, Ambrosino DM, Wentworth DE, Demartini JC, Holmes KV.** 2004. CD209L (L-SIGN) is a receptor for severe acute respiratory syndrome coronavirus. *Proc Natl Acad Sci U S A* **101**:15748-15753.
 25. **Tassaneetrithep B, Burgess TH, Granelli-Piperno A, Trumfheller C, Finke J, Sun W, Eller MA, Pattanapanyasat K, Sarasombath S, Birx DL, Steinman RM, Schlesinger S, Marovich MA.** 2003. DC-SIGN (CD209) mediates dengue virus infection of human dendritic cells. *J Exp Med* **197**:823-829.
 26. **Navarro-Sanchez E, Altmeyer R, Amara A, Schwartz O, Fieschi F, Virelizier JL, Arenzana-Seisdedos F, Despres P.** 2003. Dendritic-cell-specific ICAM3-grabbing non-integrin is essential for the productive infection of human dendritic cells by mosquito-cell-derived dengue viruses. *EMBO Rep* **4**:723-728.
 27. **Davis CW, Nguyen HY, Hanna SL, Sanchez MD, Doms RW, Pierson TC.** 2006. West Nile virus discriminates between DC-SIGN and DC-SIGNR for cellular attachment and infection. *J Virol* **80**:1290-1301.
 28. **Lozach PY, Kuhbacher A, Meier R, Mancini R, Bitto D, Bouloy M, Helenius A.** 2011. DC-SIGN as a receptor for phleboviruses. *Cell Host Microbe* **10**:75-88.
 29. **Buchmeier MJ, Lewicki HA, Tomori O, Oldstone MB.** 1981. Monoclonal antibodies to lymphocytic choriomeningitis and pichinde viruses: generation, characterization, and cross-reactivity with other arenaviruses. *Virology* **113**:73-85.
 30. **Weber EL, Buchmeier MJ.** 1988. Fine mapping of a peptide sequence containing an antigenic site conserved among arenaviruses. *Virology* **164**:30-38.
 31. **Lozach PY, Mancini R, Bitto D, Meier R, Oestereich L, Overby AK, Pettersson RF, Helenius A.** 2010. Entry of bunyaviruses into mammalian cells. *Cell Host Microbe* **7**:488-499.
 32. **Kunz S, Rojek JM, Kanagawa M, Spiropoulou CF, Barresi R, Campbell KP, Oldstone MB.** 2005. Posttranslational modification of alpha-dystroglycan, the cellular receptor for arenaviruses, by the glycosyltransferase LARGE is critical for virus binding. *J Virol* **79**:14282-14296.
 33. **Scutera S, Fraone T, Musso T, Cappello P, Rossi S, Pierobon D, Orinska Z, Paus R, Bulfone-Paus S, Giovarelli M.** 2009. Survival and migration of human dendritic cells are regulated by an IFN-alpha-inducible Axl/Gas6 pathway. *J Immunol* **183**:3004-3013.
 34. **Lozach PY, Burleigh L, Staropoli I, Navarro-Sanchez E, Harriague J, Virelizier JL, Rey FA, Despres P, Arenzana-Seisdedos F, Amara A.** 2005. Dendritic cell-specific intercellular adhesion molecule 3-grabbing non-integrin (DC-SIGN)-mediated enhancement of dengue virus infection is independent of DC-SIGN internalization signals. *J Biol Chem* **280**:23698-23708.
 35. **Gramberg T, Soilleux E, Fisch T, Lalor PF, Hofmann H, Wheeldon S, Cotterill A, Wegele A, Winkler T, Adams DH, Pohlmann S.** 2008. Interactions of LSECtin and DC-SIGN/DC-SIGNR with viral ligands: Differential pH dependence, internalization and virion binding. *Virology* **373**:189-201.

36. **Rojek JM, Sanchez AB, Nguyen NT, de la Torre JC, Kunz S.** 2008. Different mechanisms of cell entry by human-pathogenic Old World and New World arenaviruses. *J Virol* **82**:7677-7687.
37. **Pinschewer DD, Perez M, Sanchez AB, de la Torre JC.** 2003. Recombinant lymphocytic choriomeningitis virus expressing vesicular stomatitis virus glycoprotein. *Proc Natl Acad Sci U S A* **100**:7895-7900.
38. **Perez M, Watanabe M, Whitt MA, de la Torre JC.** 2001. N-terminal domain of Borna disease virus G (p56) protein is sufficient for virus receptor recognition and cell entry. *J Virol* **75**:7078-7085.
39. **Takada A, Robison C, Goto H, Sanchez A, Murti KG, Whitt MA, Kawaoka Y.** 1997. A system for functional analysis of Ebola virus glycoprotein. *Proc Natl Acad Sci U S A* **94**:14764-14769.
40. **Dutko FJ, Oldstone MB.** 1983. Genomic and biological variation among commonly used lymphocytic choriomeningitis virus strains. *The Journal of general virology* **64**:1689-1698.
41. **Pettersson R, Kaariainen L.** 1973. The ribonucleic acids of Uukuniemi virus, a noncubical tick-borne arbovirus. *Virology* **56**:608-619.
42. **Elliott LH, McCormick JB, Johnson KM.** 1982. Inactivation of Lassa, Marburg, and Ebola viruses by gamma irradiation. *J Clin Microbiol* **16**:704-708.
43. **Rojek JM, Campbell KP, Oldstone MB, Kunz S.** 2007. Old World Arenavirus Infection Interferes with the Expression of Functional {alpha}-Dystroglycan in the Host Cell. *Mol Biol Cell* **29**:29.
44. **Kunz S, Sevilla N, Rojek JM, Oldstone MB.** 2004. Use of alternative receptors different than alpha-dystroglycan by selected isolates of lymphocytic choriomeningitis virus. *Virology* **325**:432-445.
45. **Pasqual G, Rojek JM, Masin M, Chatton JY, Kunz S.** 2011. Old world arenaviruses enter the host cell via the multivesicular body and depend on the endosomal sorting complex required for transport. *PLoS Pathog* **7**:e1002232.
46. **Rojek JM, Moraz ML, Pythoud C, Rothenberger S, Van der Goot FG, Campbell KP, Kunz S.** 2012. Binding of Lassa virus perturbs extracellular matrix-induced signal transduction via dystroglycan. *Cell Microbiol* **14**:1122-1134.
47. **Lee AM, Cruite J, Welch MJ, Sullivan B, Oldstone MB.** 2013. Pathogenesis of Lassa fever virus infection: I. Susceptibility of mice to recombinant Lassa Gp/LCMV chimeric virus. *Virology*.
48. **Walker DH, McCormick JB, Johnson KM, Webb PA, Komba-Kono G, Elliott LH, Gardner JJ.** 1982. Pathologic and virologic study of fatal Lassa fever in man. *Am J Pathol* **107**:349-356.
49. **Burns JW, Buchmeier MJ.** 1991. Protein-protein interactions in lymphocytic choriomeningitis virus. *Virology* **183**:620-629.
50. **Dominguez-Soto A, Aragoneses-Fenoll L, Martin-Gayo E, Martinez-Prats L, Colmenares M, Naranjo-Gomez M, Borrás FE, Muñoz P, Zubiaur M, Toribio ML, Delgado R, Corbi AL.** 2007. The DC-SIGN-related lectin LSECtin mediates antigen capture and pathogen binding by human myeloid cells. *Blood* **109**:5337-5345.
51. **Ohkuma S, Poole B.** 1978. Fluorescence probe measurement of the intralysosomal pH in living cells and the perturbation of pH by various agents. *Proc Natl Acad Sci U S A* **75**:3327-3331.
52. **Ohkuma S, Poole B.** 1981. Cytoplasmic vacuolation of mouse peritoneal macrophages and the uptake into lysosomes of weakly basic substances. *J Cell Biol* **90**:656-664.
53. **Johannsdottir HK, Mancini R, Kartenbeck J, Amato L, Helenius A.** 2009. Host cell factors and functions involved in vesicular stomatitis virus entry. *J Virol* **83**:440-453.
54. **Mercer J, Helenius A.** 2009. Virus entry by macropinocytosis. *Nat Cell Biol* **11**:510-520.
55. **Mercer J, Helenius A.** 2008. Vaccinia virus uses macropinocytosis and apoptotic mimicry to enter host cells. *Science* **320**:531-535.
56. **Raiborg C, Stenmark H.** 2009. The ESCRT machinery in endosomal sorting of ubiquitylated membrane proteins. *Nature* **458**:445-452.

57. **Illick MM, Branco LM, Fair JN, Illick KA, Matschiner A, Schoepp R, Garry RF, Guttieri MC.** 2008. Uncoupling GP1 and GP2 expression in the Lassa virus glycoprotein complex: implications for GP1 ectodomain shedding. *Virology journal* **5**:161.
58. **Klewitz C, Klenk HD, ter Meulen J.** 2007. Amino acids from both N-terminal hydrophobic regions of the Lassa virus envelope glycoprotein GP-2 are critical for pH-dependent membrane fusion and infectivity. *J Gen Virol.* **88**:2320-2328.
59. **Cosset FL, Marianneau P, Verney G, Gallais F, Tordo N, Pecheur EI, ter Meulen J, Deubel V, Bartosch B.** 2009. Characterization of Lassa virus cell entry and neutralization with Lassa virus pseudoparticles. *J Virol* **83**:3228-3237.
60. **Kanagawa M, Saito F, Kunz S, Yoshida-Moriguchi T, Barresi R, Kobayashi YM, Muschler J, Dumanski JP, Michele DE, Oldstone MB, Campbell KP.** 2004. Molecular recognition by LARGE is essential for expression of functional dystroglycan. *Cell* **117**:953-964.
61. **Barresi R, Campbell KP.** 2006. Dystroglycan: from biosynthesis to pathogenesis of human disease. *J Cell Sci.* **119**:199-207.
62. **Rojek JM, Spiropoulou CF, Campbell KP, Kunz S.** 2007. Old World and clade C New World arenaviruses mimic the molecular mechanism of receptor recognition used by alpha-dystroglycan's host-derived ligands. *J Virol* **81**:5685-5695.

RESULTS OF PROJECT-II:

EVALUATION OF A NOVEL NANOPARTICLE VACCINE PLATFORM AGAINST ARENAVIRUSES

SUMMARY OF PROJECT-II

Arenaviruses are the causative agents of severe viral HF with high mortality in humans and represent a threat to public health. Considering the lack of effective treatment against these viruses and the limited public health infrastructure in affected regions, the development of protective vaccines against arenaviruses is an urgent need. To address this issue, we initiated the evaluation of a novel and promising recombinant vaccine platform based on NPs for the development of a safe recombinant vaccine against pathogenic arenaviruses.

The first part of my second thesis project aimed at the engineering of a vaccine formulation capable to induce an antibody response against the highly pathogenic NW arenavirus MACV. Based on available structural data on the MACV envelope GP, in particular its receptor-binding GP1 moiety, we engineered suitable MACV GP1-derived immunogens with the potential to induce a protective humoral response. Specifically, we produced recombinant forms of MACV GP1 that comprise the binding site to the cellular receptor hTfR1. In a complementary approach, we designed a synthetic peptide immunogen mimicking MACV GP loop 10 (L10), which represents a key GP1 structure implicated in receptor binding. MACV GP1-derived immunogens were produced in mammalian cells, conjugated to PPS NPs and evaluated *in vivo* in a mouse model. Vaccination of mice with NPs conjugated to MACV GP1 fragments induced strong and specific Abs responses, demonstrating efficient delivery and presentation of the antigens. However, based on the available neutralization assays only weak and transient nAbs titers were detected in the first attempt.

Since recombinant subunit vaccines may not be able to elicit nAbs titers that can confer protective immunity *per se*, we undertook a complementary approach and evaluated our NPs platform for its ability to induce cellular anti-viral immunity. In a proof-of-concept study, we employed the infection of LCMV in its natural host, the mouse. Well-defined peptides derived from defined MHC class I restricted CD8 T cell epitopes derived from LCMV were conjugated to NPs. First assessment of anti-viral T cell responses indicated that NPs are able to elicit a potent CD8 T cell response to immunodominant epitopes with a markedly weaker response to sub-dominant epitopes. Viral challenge experiments are currently performed to assess the protective potential of the anti-viral memory CD8 T cell response elicited by NPs.

INTRODUCTION

Arenaviruses have emerged as a growing public health problem in many countries of Africa and South America [37]. Considering the number of people affected and the current lack of efficacious treatments and licensed vaccines, arenaviruses like LASV, JUNV, and MACV belong arguably to the most neglected tropical pathogens. Taking into account the limited public health infrastructure in the affected regions and the limited resources at hand, the development of a protective vaccine that is safe, easy to administer and does not require a continued cold chain is of highest priority. Extensive work over the past decades resulted in the development of a live attenuated vaccine against JUNV, Candid-1 [49] that is currently administered in high-risk populations in Argentina, but has not been approved for broader use. A LASV/MOPV reassortant vaccine (ML29) showed promising characteristics when tested in NHP, but has not yet been tested in man [112]. Despite being promising, the use of such live-attenuated vaccines will be severely restricted in the affected regions of the world due to the high prevalence of immunocompromising conditions and biosafety concerns. The development of a safe recombinant vaccine that can be produced at low costs remains therefore the major goal of current arenavirus vaccine development.

Several lines of evidence indicate that neutralizing antibodies (nAbs) represent an important correlate of protection for a number of anti-viral vaccines [113,114]. By neutralizing free virus, nAbs can act as “gatekeepers” either providing sterilizing immunity or at least limiting the initial burst of viral replication, providing a window of opportunity for the host’s cellular immunity to control infection and eliminate the virus. In the case of arenaviruses, clinical and experimental evidence revealed important differences in the quality of the antibody response in primo-infection with pathogenic OW (LASV) and NW (JUNV and MACV) arenaviruses. Human primary LASV infection seems mainly controlled by the anti-viral CD8 T-cell response, whereas nAbs appear late during convalescence and are frequently of low titers [34,41]. However, if provided at sufficient titers, nAbs to LASV proved to be protective in post-exposure prophylaxis in animals [47,48], and in some human cases [115,116]. In contrast, nAbs appear earlier after infection with JUNV and MACV[117], and the development of nAbs in the second week of disease correlates with positive clinical outcome [118]. The robust nAbs titers in JUNV and MACV convalescent plasma provide the basis for the current immune plasma therapy of human JUNV and MACV infection that markedly reduces mortality from > 30 to $< 0.1\%$ [119]. The strong nAbs responses against NW arenaviruses indicates that the viral GP1 is immunogenic and a recombinant vaccine

capable of inducing sufficient nAbs titers seems in principle feasible. Moreover, in contrast to other viral HF, there is currently no evidence for enhancement of human arenavirus disease by sub-neutralizing antibodies [23,26]. The reasons for the striking difference in quality of the antibody response against OW and NW arenaviruses are currently unknown. Although NW arenavirus HF is widespread in endemic regions, there is no evidence for repeated infection in survivors [120]. This suggests that a vaccine would likely be protective.

PART 1: INDUCTION OF A PROTECTIVE ANTIBODY RESPONSE

1.1. Design and production of the vaccine antigen

A large body of evidence supports the notion that antibodies targeting viral attachment proteins are of particular importance for protection as they prevent host cell attachment and entry [114,121,122]. The arenavirus envelope GP is initially synthesized as a single polypeptide that is processed into the N-terminal GP1 and the membrane-associated GP2 (Fig. 1A, B), which forms trimers, similar to other class I fusion-active viral GPs [123] (Fig. 1C). Structural studies on MACV GP1 showed that arenavirus GP1 represents an independent folding unit with a globular structure [124,125] (Fig. 1D). Examination of the complex between MACV GP1 and its receptor revealed that trimerization of MACV GP1 is not required for receptor binding (Fig. 1E) [12,125]. The MACV GP1 monomer thus represents the “functional unit” of receptor recognition, which involves conserved peptide loops protruding from its surface (Fig.1F).

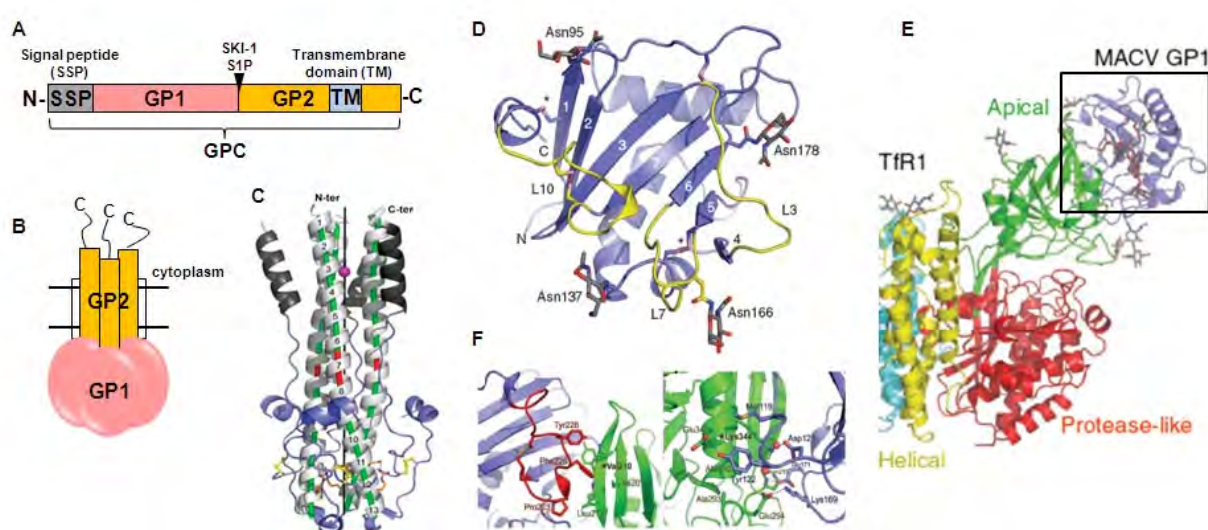


Figure 1. Structure of arenavirus glycoproteins. **A)** Schematic representation of arenavirus GPC: The N-terminal receptor-binding GP1 subunit, the C-terminal GP2 subunit, the transmembrane domain and the signal peptide SSP are indicated. The S1P processing site is depicted with a black arrow. **B)** In the virion membrane, mature arenavirus GP forms a trimer. **C)** X-ray crystallographic structure of the trimeric GP2 of LCMV taken from [123]. **D)** Structure of MACV GP1 with two receptor-binding loops (L3 and L10) highlighted in yellow. **E)** Structure of the complex of MACV GP1 (blue) with its cellular receptor TfR1. Only one monomer of the TfR1 dimer is shown with the individual domains indicated. **F)** Details on the molecular contact between loops L3 and L10 of MACV GP1 (blue) with the apical domain of TfR1 (green). (D-F taken from [125]).

In line with these structural data, nAb were found to be directed exclusively against GP1 [126,127], and GP1 purified from JUNV virions was able to elicit a nAb response [128]. Based on these data we designed soluble recombinant “GP1 only” fragments. Considering the

wealth of structural data available and its similarity to JUNV, we initially chose MACV GP1 for our studies on NW arenaviruses.

The studies by Bowden and colleagues revealed that the GP1 of MACV consists of a novel α/β fold (Fig.1D) and that deletion of the first 87 amino acids from the full-length GP1 protein greatly enhances protein expression in HEK293 cells [124]. Using a PCR cloning approach (see material and methods for details), we constructed an analogous truncated form of MACV GP1 containing an N-terminal HA-tag and a C-terminal FLAG-tag, HA-MACVGP1-88-262-FLAG (MACV Δ GP1) shown in Fig. 2A. The construct was cloned in a pcDNA 3.1(+) expression vector containing the cytomegalovirus major immediate early promoter, followed by an intron (intron A) sequence and expressed in HEK293T cells by transient transfection. Protein expression and secretion was assessed by SDS-PAGE and Western blot (Fig. 2B).

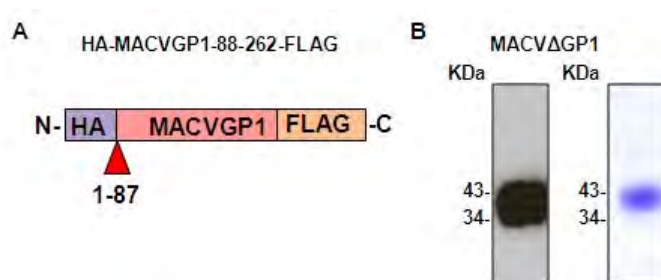


Figure 2. The MACV GP1 fragment: A) Recombinant MACV GP1 variant HA-MACVGP1-FLAG, containing a deletion of amino acids 1-87, an N-terminal HA-tag and a C-terminal FLAG-tag B) Purified HA-MACVGP1-FLAG detected with an anti-HA antibody in Western blot (left) and by Coomassie blue staining (right).

Affinity purification using an anti-HA column followed by HA-peptide competitive elution yielded around 0.5-1 mg of protein of >95% purity per liter of supernatant. Sequential anti-HA purifications of the same supernatant batch were performed in order to increase the protein recovery.

1.2. Conjugation of the vaccine antigen MACV Δ GP1 onto PPS NPs

In a first approach to conjugate our MACV Δ GP1 immunogen to PPS NPs, we tried to generate NPs bearing anti-FLAG Fab fragments at their surface, allowing immobilization of our immunogen via its C-terminal FLAG-tag. The advantage of this conjugation scheme was the defined orientation of the immunogen on the NPs and the coupling without prior modification. Nevertheless, this approach turned out to be not feasible due to technical and cost restrictions.

The modular chemistry for conjugating antigens onto the surface of pyridyl disulfide activated PPS NPs via a disulfide link between the NPs surface and the thiol (SH) functional

group of cysteine residue(s) on the antigen has been recently described [129]. MACVΔGP1 has 8 cysteines, organized in four intra-molecular disulfide bonds that stabilize the overall conformation of the protein, but no free sulfhydryl (S-S) groups (Fig.1D) [130]. In order to accomplish conjugation via thiol groups, an unpaired cysteine residue was inserted into MACVΔGP1 by PCR cloning resulting in the form MACVΔCGP1. Although MACVΔCGP1 was efficiently expressed in HEK293T cells, the purified protein spontaneously formed high molecular weight aggregates, perturbing the protein conjugation. The aggregates could only be partially dissociated in the presence of strong reducing agents resulting in a loss of protein conformation (data not shown).

In a second approach, a partial reduction scheme of the wild type MACVΔGP1 was considered, where the solvent accessible disulfide bonds would be reduced preferentially. For this purpose, we tested two different reducing agents: β-mercaptoethylamine (2-MEA) and Tris(2-carboxyethyl) phosphine (TCEP) covalently linked to 4% crosslinked beaded agarose. The latter having the advantage of being easily removable from the initial reduction reaction by centrifugation without any additional purification steps. To assess MACVΔGP1 conformation preservation we performed an *in vitro* binding assay to its receptor hTfR1. MACVΔGP1 reduced with 2-MEA was not retained for further conjugation on the NPs as more than 80% of the protein was lost during the pre-conjugation purification step. The partial reduction of MACVΔGP1 with TCEP was carried out in two ways, using TCEP beads with or without guanidinium hydrochloride (GuHCl). At low concentrations, the chaotropic agent GuHCl allows the protein to “swell” without actual denaturation of its tertiary structure, thus enhancing accessibility of disulfide bonds to TCEP. Although GuHCl treatment enhanced conjugation efficiency (Fig. 3A), it also impaired the binding of the protein to hTfR1, whereas treatment with TCEP alone retained > 50% of receptor bind capacity (Fig. 3B). Since our objective was the production of nAbs, the TCEP/ without GuHCl formulation was chosen as reduction method for MACVΔGP1 prior to conjugation on the NPs.

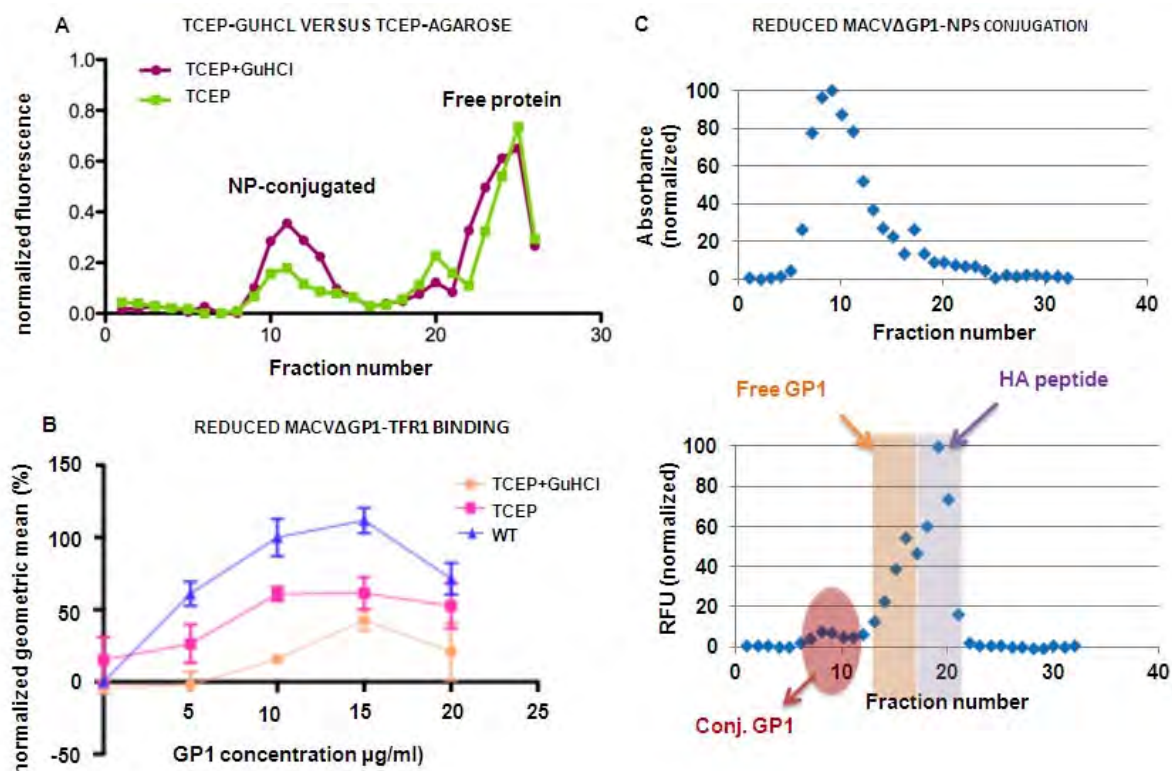


Figure 3. MACVΔGP1 partial reduction and conjugation. **A)** Comparison of TCEP+GuHCl and TCEP agarose reduced proteins conjugation efficiency to PPS NPs. MACV GP1 was partially reduced by TCEP + 1M guanidium hydrochloride, conjugated to PPS NPs and purified by gel filtration. Peaks corresponding to NP-conjugated and free protein are indicated. **B)** hTfr1 binding assay. GP1 binding at various concentrations to CHO.K1 cells transiently transfected with hTfr1 was assessed by flow cytometry on a CyAn™ ADP Analyzer (Beckman Coulter). MACVΔGP1 was detected by a polyclonal rabbit anti-FLAG antibody against its C-terminal FLAG tag, followed by a secondary anti-rabbit antibody conjugated with Alexafluor 647. Only live (Live/Dead violet, Invitrogen), hTfr1+ (PE-anti hTfr1 clone M-A712) cells are depicted for the normalized geometric mean of the FL8 channel, which reflects the AF647 fluorescence intensity. Analysis was done using FlowJo (version 7.5.5, Tree Star) software. **C)** MACVΔGP1 NPs' conjugation profile. MACVΔGP1 was reduced with TCEP beads at 37°C (1h). Reduced MACV GP1 was mixed with NPs in a 1:1 reaction (v/v) and reacted over night at RT, purified by size exclusion chromatography and eluted with H₂O. NPs and protein presence was assessed in each elution fraction by iodine staining (absorbance at 342nm upper graph) and fluorescamine reactivity (lower graph) respectively.

1.3. Evaluation of MACV Δ GP1 NPs *in vivo*

To evaluate the ability of our GP1-conjugated NPs to elicit an anti-viral antibody response *in vivo*, we performed a proof-of-principle study using the MACV Δ GP1-NPs produced above. For this purpose, groups of five age and sex-matched C57Bl/6 mice were vaccinated with our MACV Δ GP1-NPs. For comparison, we applied purified MACV Δ GP1 protein alone. As a negative control, unconjugated NPs were used. Since previous studies had shown a positive effect of stimulators of Toll-like receptors (TLRs) on the quality and magnitude of immune responses in the context of the NP platform [104], we added the TLR9 agonist CpG to our vaccine formulations. Mice were injected following the vaccination schedule shown in Fig. 4A. At the indicated time points, mice were bled and serum obtained. Detection of specific antibodies (IgG) against MACV GP1 in ELISA revealed a strong and specific antibody response against MACV GP1 in mice immunized with MACV Δ GP1-conjugated NPs (Fig. 4B). Notably, the IgG titers obtained with the NP platform were significantly higher than those obtained with the purified protein. As expected, pre-immune sera and sera from mice vaccinated with unconjugated NPs showed no detectable titers of anti-MACV GP1 antibodies. To assess the presence of nAbs, we employed a neutralization test, as described in materials and methods [131]. In animals vaccinated with MACV Δ GP1-conjugated NPs, we were able to detect nAbs (Fig. 4C). However, the neutralizing activity of the antibodies was low and the extent of neutralization would likely provide insufficient protection.

Until now our data have shown that the NPs platform could induce a strong humoral immune response, which was specific for the antigen used for vaccination. However, the weak and transient nAbs titers detected suggested that the majority of the antibodies detected in figure 4 were directed to non-neutralizing epitopes displayed by our immunogen. During natural infection, MACV GP1 is displayed in its native conformation on virion surfaces and on infected cells. In contrast, our MACV GP1 immunogen displays peptide structures that are either not present or inaccessible in the native GP, such as the peptide tags (HA, FLAG) and structures of GP1 that are normally hidden within the mature GP trimer.

To detect antibodies directed against the accessible surface of MACV GP1 in the native protein, we expressed full-length MACV GP in human HEK293 cells. At 48 hours post-transfection, live, non-permeabilized cells were incubated with sera and bound antibodies detected in flow cytometry. Notably, no significant binding of serum antibodies to native MACV GP1 was detectable in NPs-MACV Δ GP1 immunized animals (data not shown). This

suggests, that the antibodies generated by our vaccine were either unable to recognize MACV GP1 in its native form or had low affinity. The absence of high affinity antibodies to native MACV GP1 is in line with the lack of a robust neutralizing activity in mice sera shown in Fig.4.

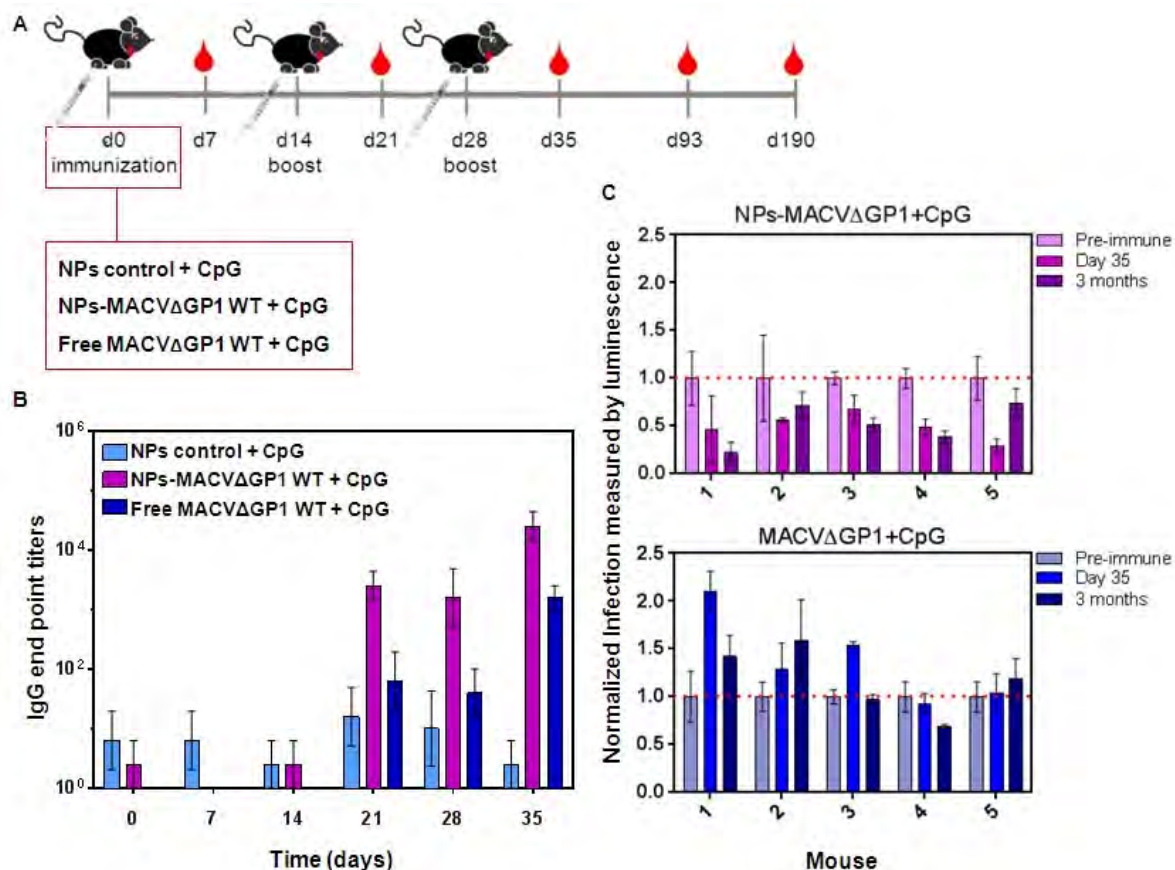


Figure 4. NPs conjugated to MACVGP1 elicit strong antibody responses. A) Groups of five age- and sex-matched C57BL/6 mice were immunized with MACVGP1 conjugated NPs (NPs-MACVGP1, 1.6 μ g of protein/mouse), unconjugated NPs (NP), or MACVGP1 protein (MACVGP1), all in combination with 10 μ g of CpG-B. At days 14 and 28, mice were given vaccine boosts. Blood draws were performed at the indicated time points (red drops). B) Antibody titers (IgG) in vaccinated mice over time. Titers of specific anti-MACV GP1 IgG were determined by ELISA using purified MACVGP1 immobilized in microtiter plates and IgG specific secondary antibodies. Note that the specific IgG titers after vaccination with the NPs conjugated antigen were consistently higher than those obtained with the soluble protein. Data shown are means \pm SD, n = 5. C) Neutralization assay. Preimmune sera and immune sera from d35 and d93 (40 x dilution) were mixed with MACV pseudotypes virus carrying the reporter gene luciferase. The inoculums were added to susceptible human cells (A549) and infection detected by luciferase assay. Signals were normalized to preimmune sera. Data shown are means \pm SEM, n = 2.

In order to further characterize the antibody responses induced by our vaccine, we sought to identify MACV GP1 peptide structures recognized by the antibodies present in the sera of vaccinated mice. To this end, we employed the peptide array technology described in Fig.5A.

This technique allowed us to identify peptides of MACVΔGP1 that are bound by antibodies and thus to obtain information about structures on the immunogen that are recognized. The results of a study are shown in Fig.5B. We observed that the major peptides recognized by sera from both mice immunized with NPs-MACVΔGP1 and MACVΔGP1 located to the N-terminal part of the protein, in particular to a region encompassing the HA-tag (DYPYDVDPDYAGAQPASPGGL, HA epitope in bold) (Fig.5).

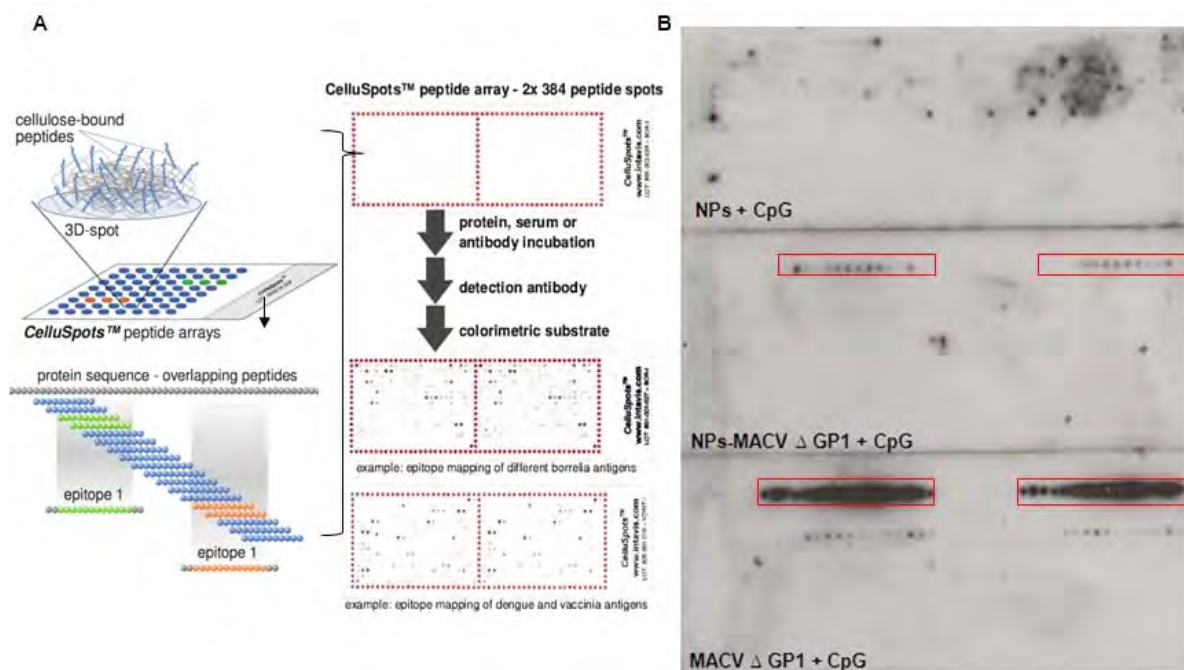


Figure 5. A) CelluSpots™ technology. CelluSpots™ are array of cellulose-bound peptide spotted on glass slides. The cellulose support can be dissolved after peptide synthesis. The solutions of individual peptides covalently linked to macro molecular cellulose are then spotted onto a surface of choice. After evaporation of the solvent a three-dimensional layer is formed which is not dissolved in aqueous reagents used for standard assays. B) Epitope mapping array. The whole sequence of MACVΔGP1 protein was displayed on a peptide slide array (201 x 20-mer peptides with one amino acid overlap, in duplicate). The peptide slides were then incubated with the sera of one mouse of each vaccination group: 1) nanoparticles; 2) NPs-MACVΔGP1; 3) MACVΔGP1 only. Bound antibodies were detected with a HRP-conjugated goat anti-mouse secondary antibody with enhanced chemiluminescence. Red squares: linear B-cell epitopes detected in both MACVGP1-NPs and MACVGP1 only immunized mice.

The preferential recognition of the HA-tag by antibodies from sera of vaccinated mice was confirmed by flow cytometry and ELISA (data not shown).

1.4. A “Second generation” of MACVΔGP1 constructs

The strong antibody response obtained against the HA-tag indicates efficient antigen delivery and presentation upon vaccination with NPs conjugated to PPS NPs. The lack of nAbs may be due, at least in part, to the loss of conformational epitopes on MACV GP1

caused by the conjugation chemistry and the associated treatments of the immunogen with reducing agents. In order to circumvent these problems, we evaluated an alternative conjugation strategy. The recently developed aldehyde-tag strategy allows single site modification of native bioactive proteins for further conjugation to fluorochromes, antibodies, etc [132,133]. In our context, “aldehyde tags” would allow coupling of the immunogen via a specific chemical functional group without affecting the MACV GP1-derived part under mild conditions that allow retention of the native conformation. This technique requires the insertion of a formylglycine generating enzyme (FGE) recognition site (**LCTPSRAALLTGR**, minimal sequence recognized by the FGE in bold) either at the N- or C-terminus of the target protein (Fig.6A). The FGE post-translationally converts the cysteine within recognition site into a formylglycine containing a reactive aldehyde group (Fig.6A and B). As the FGE is naturally present and active in the endoplasmic reticulum (ER) of mammalian cells, the engineered protein can be directly produced in mammalian cells. Nevertheless, the addition of exogenous FGE (by co-transfection with the target protein) generally increases the cystein-formylglycine conversion yield. From our previous studies, we have learned that the HA-tag was recognized as major epitope and we were concerned that the strong antibody response to these apparently highly immunogenic sequences could interfere with a potential weak MACV GP1 response. Therefore we decided to include a thrombin (TH) cleavage site between the GP1 and the HA sequence (Fig.6A). This would allow us to remove the HA-tag after purification and prior to conjugation. The aldehyde-tag should then allow the conjugation of the antigen to hydrazide/aminooxy functionalized NPs under mild conditions (room temperature, pH 6-7.5) allowing retention of the native conformation of MACV GP1.

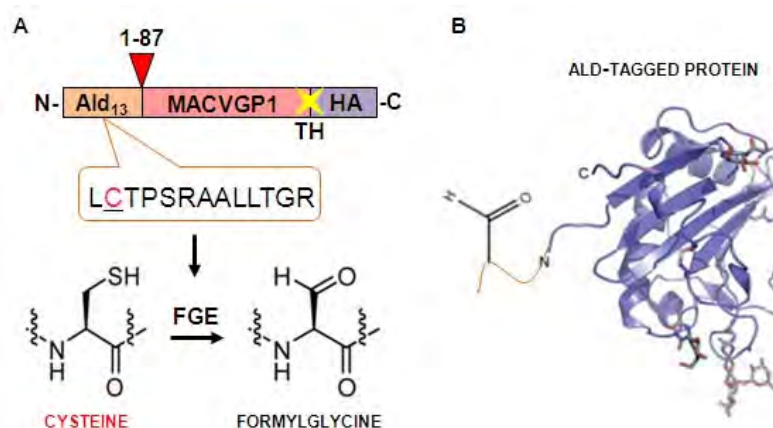


Figure 6. Site-specific modification using the genetically encoded aldehyde-tag. **A)** Schematic representation of Ald-tagged MACVΔGP1 and the FGE recognition sequence. After recognition of a specific sequence inserted in the antigen sequence, FGE oxidizes the Cys in the tag to formylglycine leading to the site specific labeling of the functionalized protein (ald-tagged protein). **B)** Schematic representation of the Ald-tagged MACVΔGP1.

The aldehyde (Ald)-tagged MACVΔGP1 constructs were successfully produced in HEK293T cells (Fig.7A) and purified using an anti-HA affinity matrix (Fig.7B) in analogy to the first generation of MACVΔGP1 constructs. After purification, the HA tag was removed by treating the protein with agarose-bound thrombin as described in the material and methods section, allowing cleavage of >90% of the HA tag (Fig.7C). The extent of cysteine to formylglycine conversion was determined by reaction of the Ald-tagged MACVΔGP1 with aminoxy biotin (see material and methods). Based on the results obtained, we estimate 80-90% Cys-formylglycine conversion efficiency for the N-terminal Ald-tagged protein (Ald-MACVΔGP1) (Fig.7D, AldΔGP1) and 50-70% for the C-terminal Ald-tagged protein (MACVΔGP1-Ald). As the conversion efficiency was higher for the Ald-MACVΔGP1 than for the MACVΔGP1-Ald, we decided to use the N-terminal Ald-tagged construct for further conjugation on the NPs and *in vivo* testing.

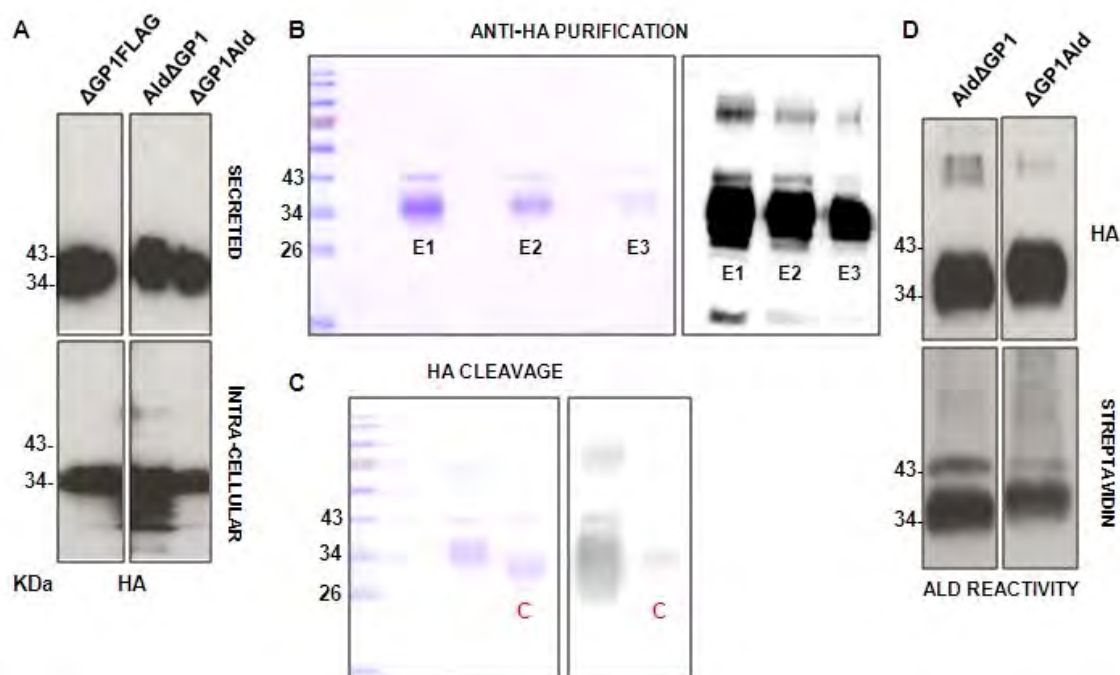


Figure 7. Ald-tagged MACVΔGP1 expression in mammalian cells. **A)** Total protein extraction from HEK293T cells supernatant and cell lysates. Total cell supernatants and cell lysates (intracellular) proteins (secreted) were recovered by methanol/chloroform extraction, resuspended in SDS sample buffer and detected using anti-HA Ab in western blot. ΔGP1FLAG: non Ald-tagged protein used as control. AldΔGP1 and ΔGP1Ald correspond to the N and C terminal Aldehyde tagged proteins respectively. **B)** Anti-HA affinity matrix purified Ald-MACVΔGP1 protein. Supernatant from a large scale (1-3 liters) protein's production was loaded on an anti-HA affinity matrix (0.5ml/min), the column was eluted for 15 min at 37°C (3 sequential elutions) and a sample of each eluate (E1-E3) was mixed with SDS sample buffer. The purification efficiency was assessed by coomassie staining (left) and specific protein detection was achieved using an anti-HA Ab (right). **C)** HA cleavage efficiency. Buffer exchanged Ald-MACVΔGP1 was mixed with 3U/mg of protein of thrombin-agarose and incubated over night at R.T. (23-25°C) on a wheel. Agarose-bound thrombin was removed using a spin column. The cleavage efficiency was determined by coomassie staining (left) and anti-HA detection (right). **C** stands for cleaved protein. **D)** Aldehyde reactivity assessment. Ald-MACVΔGP1 was reacted with aminoxy-biotin for 2h at RT. The Ald-MACVΔGP-aminooxy-biotin binding was determined using and a streptavidin - HRP coupled. KDa: kilo Dalton.

Two different conjugation strategies were simultaneously tested for the coupling of the Ald-tagged protein on PPS NPs. 1) NPs containing reactive amines were functionalized with a hydrazino-nicotinamide (HyNIC) linker and then reacted with the Ald-tagged protein (Fig.8A). Succinimidyl-6-hydrazino-nicotinamide (S-HyNIC), an aromatic hydrazine and 4-succinimidyl-formylbenzamide (S-4FB), an aromatic aldehyde allow the linking of diverse molecule types (proteins, oligos and peptides) through primary amines, thiols or maleimides to a variety of compounds resulting in an UV-traceable, stable bis-arylhydrazone bond. 2) Oxyamine-pluronic (aminooxy) NPs were synthesized and directly reacted with the Ald-tagged protein (Fig.8B). The conjugation data with Ald-tagged OVA showed almost 100% coupling efficiency to the NPs (data not shown). In contrast to Ald-OVA, only 16% of the Ald-MACVΔGP1 was coupled to the NPs in both conjugation strategies (Fig.8C). The Ald-MACVΔGP1-NPs conjugation procedure needs further optimization and is currently ongoing in the laboratory of our collaborator at the EPFL.

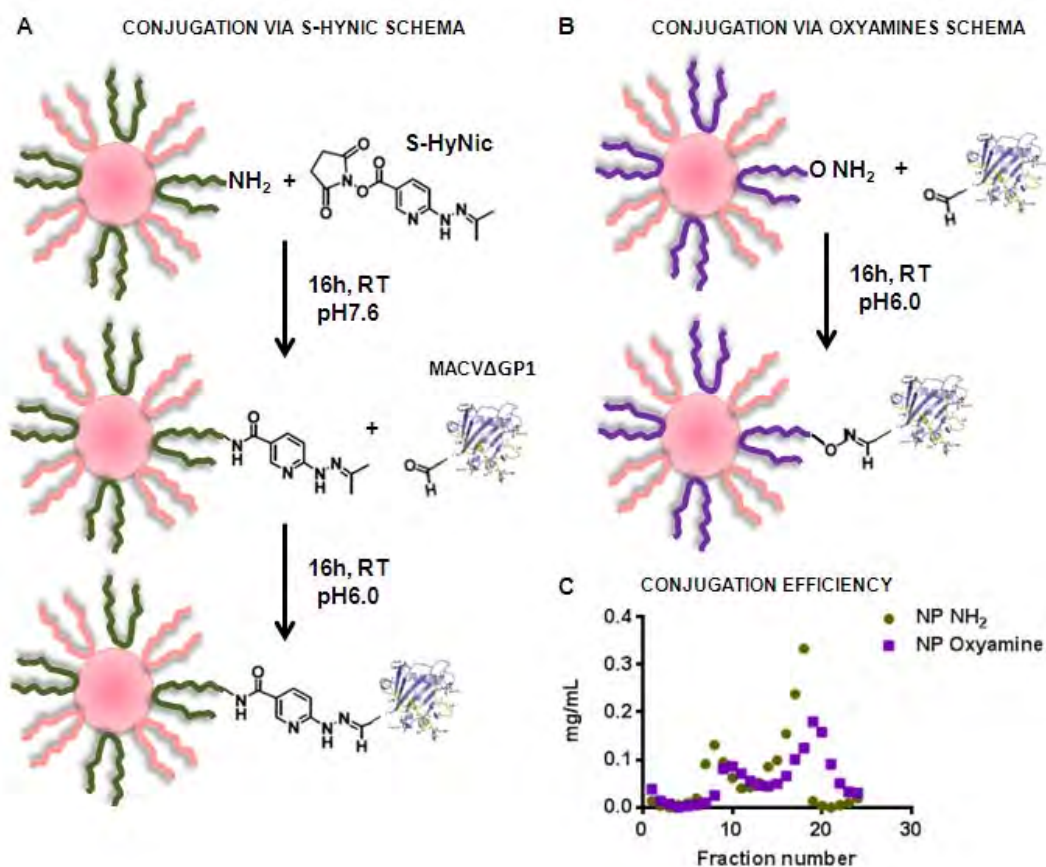


Figure 8. Schematic representation of Ald-MACVΔGP1 conjugation to NPs. A) Conjugation via hydrazine. **B)** Conjugation via oxyamine. **C)** Ald-MACVΔGP1 NPs' conjugation profile. Ald-MACVΔGP1 was mixed either with hydrazine or oxyamine functionalized NPs in a 1:1 reaction (v/v) and reacted over night at RT, purified by size exclusion chromatography and eluted with H₂O. NPs and protein presence was assessed in each elution fraction by iodine staining (not shown) and fluorescamine reactivity respectively. For more details about the conjugation conditions see materials and methods section.

1.5. The receptor-binding MACVGP1 loop 10 as antigen

In our first approach to generate nAbs against MACV, we adopted a rather conventional protein-based vaccine strategy using the major part of the viral envelope GP targeted by nAbs *in vivo*. Protein-based vaccines have proved to be efficient and are routinely used in clinics. Nevertheless, they are not always cost-effective and straightforward to produce due to the fact that many viral proteins are toxic for mammalian cells and thus difficult to produce in high amounts. The use of bacterial or insect expression systems is not always feasible as they are devoid of some enzymes crucial for the correct post-translational modifications of mammalian proteins. A cost-effective alternative to protein-based vaccines is the use of peptide-based antigens. Peptides can be easily produced by liquid or solid phase synthesis. Moreover, they can display single, multiple and/or combined T or B cells epitopes allowing targeting the immune response towards a specific region of interest within a previously identified on the native protein.

“First generation” peptide-based vaccines are frequently potent inducers of T cell immune responses. Indeed, most of the T cells epitopes are composed of linear continuous amino acid (aa) sequences with an average length of circa 10 aa for MHC I and 13-20 aa for MHC II epitopes. In contrast, B cell epitopes required for the induction of nAbs are frequently discontinuous sequences, which in some cases adopt secondary and/or tertiary structures, thus limiting the use of linear peptides for the induction of nAbs. However, a “new generation” of peptides, which were engineered to adopt a tertiary conformation allowed overcoming some of these limitations. Several strategies for the generation of conformational peptides are now available. Another concern regarding peptide-based vaccines is their lack of immunogenicity. However, this can, at least in part, be compensated by appropriate vaccine formulations, including the addition of adjuvants.

In a complementary strategy, we sought to identify MACV GP1-derived peptide structures that would be suitable for the design of immunogenic peptides with the potential to elicit nAbs. As shown in Fig. 1D and E, structural studies revealed that MACV GP1 binds to its receptor hTfR1 via distinct peptide loops that protrude from the surface of the GP1 and virtually “grab” the receptor surface in a finger-like fashion. Subsequent structure-function analysis and mutagenesis pinpointed in particular the peptide loops L3 and L10 as crucial structures implicated in receptor recognition [12]. We hypothesize that binding of an IgG molecule with sufficient affinity to any of these loops would drastically perturb the attachment of MACV GP1 to hTfR1 obstructing host cell attachment of the virus. First, we

employed molecular modeling to predict the structure of the peptides derived from L3 and L10 in solution, when separated from their protein core. These studies performed with the help of Prof. Matteo Dal Peraro from the laboratory of Biomolecular Modeling of EPFL, revealed that a peptide derived from L3 adopted with a high probability a linear undefined and non-conformational structure. In contrast, the peptide sequence corresponding to L10 spontaneously adopted a loop-like structure similar to that observed in the crystal structure of the MACV GP1-hTfR1 complex. Thus only L10 was selected as a candidate immunogen. The binding efficiency of the S-4FB linker to L10 is currently ongoing. Once obtained 4FB functionalized L10 will be conjugated to HyNIC functionalized NPs as described in Figure 9. Then we will proceed with the *in vivo* testing in mice as described for MACVΔGP1-NPs immunization.

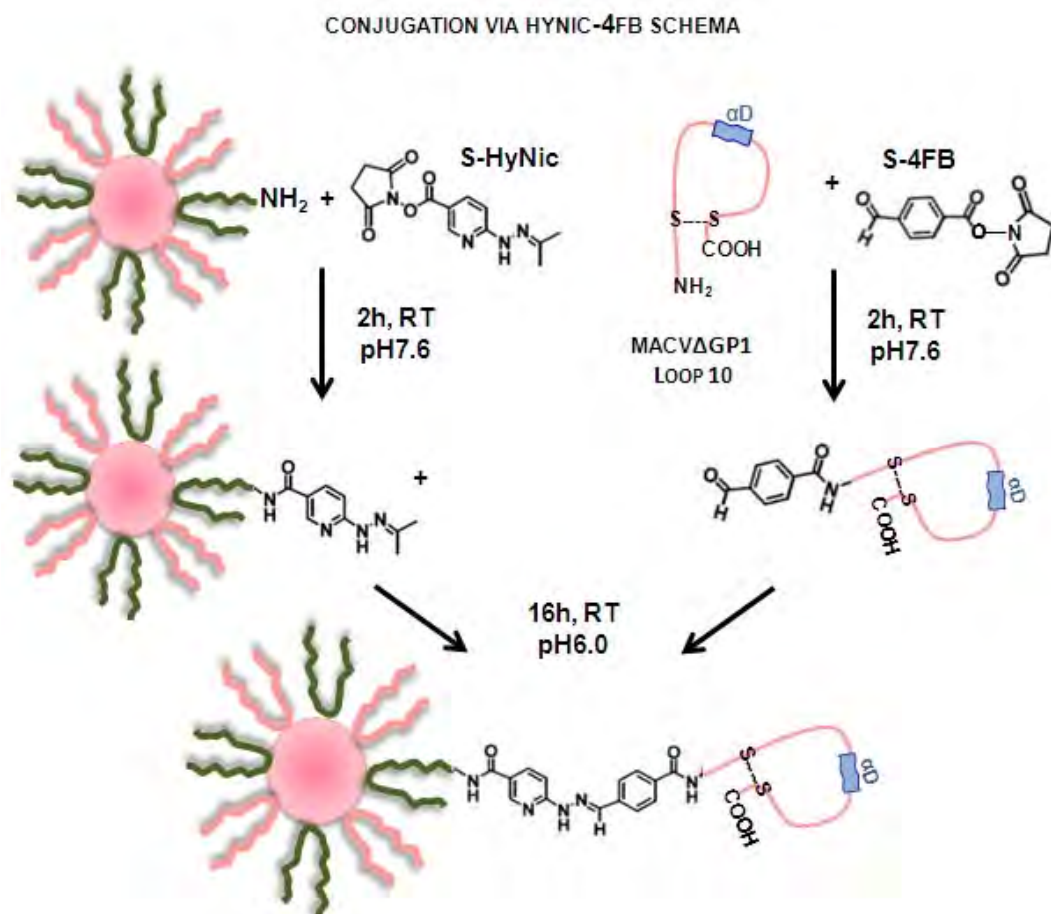


Figure 9. Loop 10 conjugation to NPs' schema.

PART 2: INDUCTION OF A PROTECTIVE T CELL RESPONSE

While nAbs would significantly contribute to protection against virus challenge, we are aware that nAbs titers conferring sterile immunity against virulent arenaviruses may be difficult if not impossible to achieve. As a complementary strategy, we therefore evaluated the NPs platform for its capacity to induce anti-viral T cells. The focus on receptor-binding GP1 fragments for the development of a NPs vaccine able to elicit a protective Abs response resulted in removal of major CD8 T cell epitopes. For this reason, we wanted to complement the GP1-conjugated NPs with NPs displaying MHC I-restricted CD8 T cell epitopes with the goal to elicit an anti-viral CD8 T cell response. To this end, we used the infection of the prototypic arenavirus LCMV in the mouse, which is one of the best experimental models to study anti-viral CD8 T cell responses [134,135]. The major dominant and subdominant MHC I-restricted CD8 T cell epitopes of LCMV are well-defined and are derived for the structural proteins NP and GPC.

Infection of mice with LCMV results in a strong CD8 T cell response that has been extensively characterized, including the identification of CD8 T cell epitopes, as well as their functional hierarchy. For our studies we used C57/Bl6 mice and selected H2-D^b-restricted CD8 T cell epitopes. We chose two dominant CD8 T cell epitopes, LCMV GP₃₃₋₄₁ and NucP₃₉₆₋₄₀₄, and a less dominant one LCMV GP₂₇₆₋₂₈₆, in order to check if the hierarchy between the CD8 T cell epitopes was conserved upon immunization with NPs-conjugated peptides. The peptides were synthesized by solid phase synthesis. For conjugation, we used a peptide design known to allow the targeting of peptides to MHC I cross-presentation by antigen presenting cells [104]. This new strategy ensures efficient uptake of the NPs, and intra-endoplasmic reticulum processing to reveal the immunogenic epitope, excluding non-specific attachment to surface MHC I. The GP₃₃₋₄₁ and GP₂₇₆₋₂₈₆ peptide epitopes were successfully conjugated to NPs, whereas conjugation of NucP₃₉₆₋₄₀₄ requires further optimization. As proof-of-principle, LCMV GP₃₃₋₄₁ and LCMV GP₂₇₆₋₂₈₆-conjugated NPs were evaluated and compared to the well-characterized H2-K^b restricted OVA peptide SIINFEKL for their efficacy to trigger a cellular immune response.

2.1. Conjugation of MHC I LCMV peptides onto PPS NPs

As described in a previous publication, peptide epitopes can be readily conjugated to the core sulfhydryls of the Pluronic stabilized PPS NPs via disulfide bonds [104]. Briefly, the native cysteines of the peptides LCMV GP₃₃₋₄₁, LCMV GP₂₇₆₋₂₈₆ and OVA₂₅₀₋₂₆₄ (used as a

control) were activated with a 2-pyridylthiol group (Fig.10). Conjugation was verified by analytical HPLC/MS.

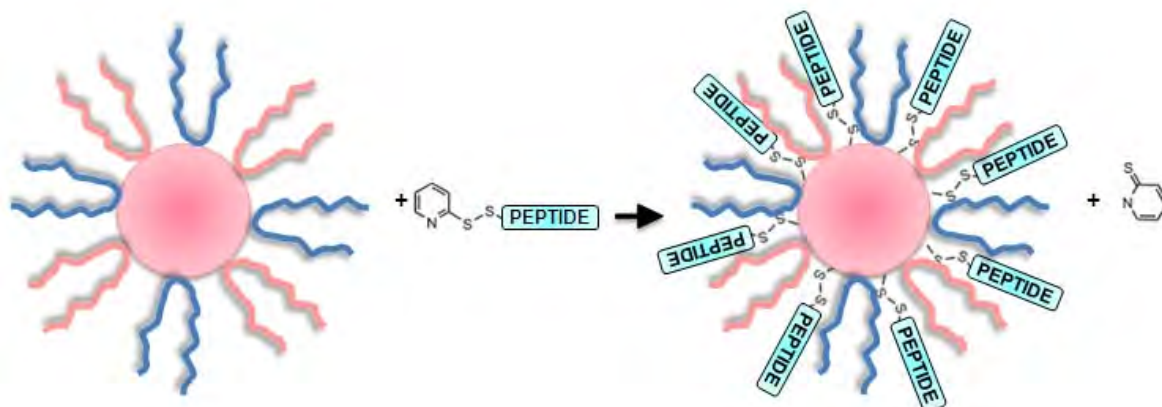


Figure 10. Peptide conjugation. LCMV peptides epitopes can be readily conjugated to the core sulfhydryls of the pluronic stabilized PPS NPs via disulfide bonds. The native cysteines LCMV peptides were activated with a 2-pyridylthiol group. Extent of peptide conjugation was monitored by absorbance of pyridine-2-thione at 340nm, and free peptide removed by size exclusion.

2.2. Evaluation of NPs bearing CD8 T cell epitope peptides *in vivo*

To evaluate the ability of the peptide-conjugated NPs to elicit a cellular anti-viral immune response *in vivo*, groups of three age- and sex-matched C57Bl/6 mice were vaccinated with NPs conjugated to the peptides LCMV GP₃₃₋₄₁ and LCMV GP₂₇₆₋₂₈₆, either individually or in combination (Mix), or NPs bearing the peptide OVA₂₅₀₋₂₆₄, which includes the immunodominant SIINFEKL, as shown in Figure 11A. The induction of a specific MHC I-restricted CD8 T cell response to the different epitopes was assessed on days 14 (data not shown) and 21 by detection of interferon (IFN)- γ producing CD8 T cells in enzyme-linked immunospot (ELISPOT) assay (Fig.11B) and by intracellular cytokine staining of CD8 T cells producing IFN- γ and TNF- α (Fig. 11C). As shown in Figure 11B and C, a robust CD8 T cell response to the immunodominant epitope GP₃₃₋₄₁ could be measured, which was comparable in magnitude to the OVA peptide SIINFEKL. However, we were unable to detect a significant response to the less dominant epitope GP₂₇₆₋₂₈₆. When applied in combination, the epitopes GP₃₃₋₄₁ and GP₂₇₆₋₂₈₆ resulted in CD8 T cells response comparable to the GP₃₃₋₄₁ alone, indicating lack of a synergistic effect between the two peptides. This gave first hints that the NP platform maintains the functional epitope hierarchy between GP₃₃₋₄₁ and GP₂₇₆₋₂₈₆. As expected, responses measured at day 14, after single immunization were weaker than those measured at day 21, after a boost. Examination by intracellular cytokine staining in flow cytometry (Fig.11C) revealed 1-2% of GP₃₃₋₄₁ epitope specific IFN- γ producing CD8 T cells,

which is in the order of magnitude of the GP₃₃₋₄₁ epitope-specific CD8 T cell frequencies observed in natural infection (6-8%) [136].

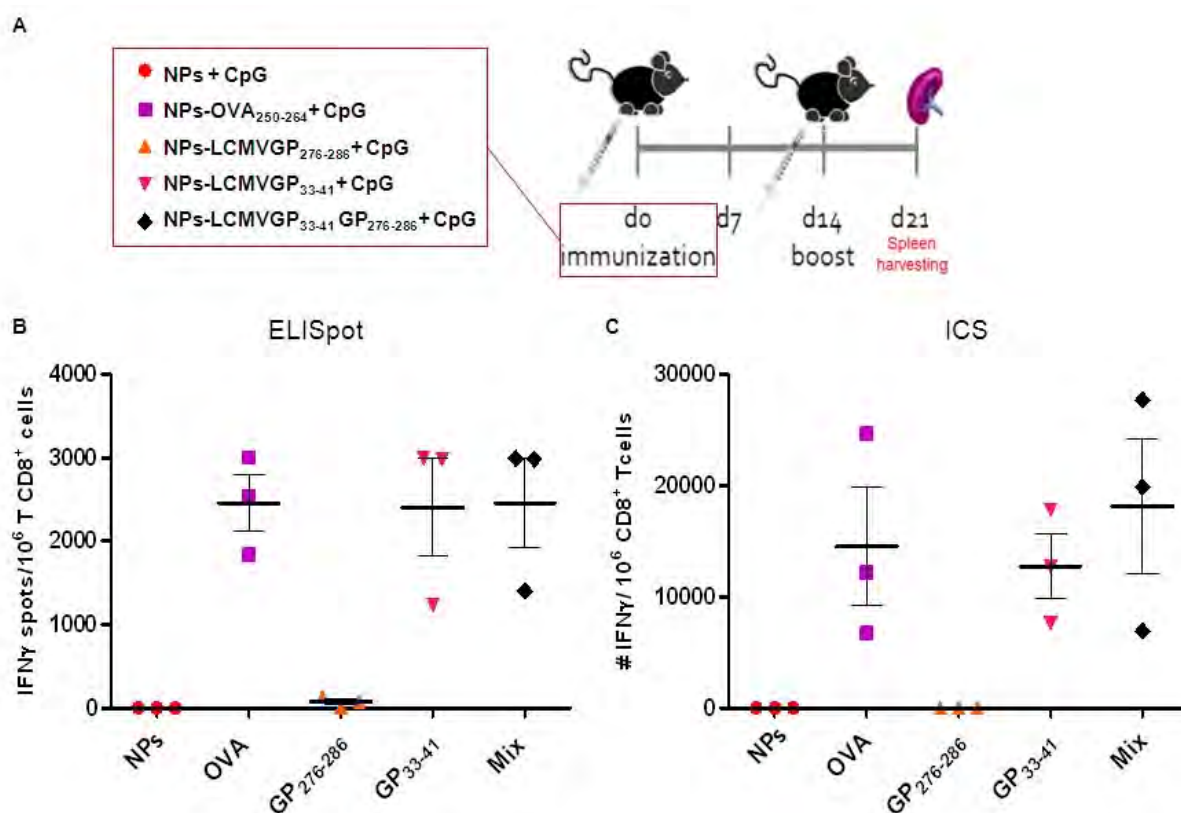


Figure 11. CD8 T cell responses after vaccination **A)** Vaccination schematic. Six age- and sex-matched C57Bl/6 mice were vaccinated intradermally on their hind legs on day 0, followed by a boost vaccination on day 14. Mice were vaccinated with 10 μ g of CpG-B and with the following formulations at 2.2 nmol total immunodominant peptide per mouse: NPs conjugated to the C-OVA₂₅₀₋₂₆₄; NPs conjugated to LCMV GP₃₃₋₄₁; LCMV GP₂₇₆₋₂₈₆; or a mix of LCMV GP₃₃₋₄₁ and LCMV GP₂₇₆₋₂₈₆ (Mix). CD8 T cell responses were assessed on days 14 (n=3) (data not shown) and 21 (n=3). **B)** Detection of IFN- γ producing CD8 T cells at day 21 by ELISPOT. 10^5 splenocytes were plated and restimulated with corresponding peptides, and developed according to the manufacturer's instructions (eBioscience ELISPOT READY-SET-GO!). Note that the numbers of IFN- γ producing cells for the mouse groups immunized with LCMV GP₃₃₋₄₁ and the OVA₂₅₀₋₂₆₄ are likely underestimated due to the high number of spots in the assay. **C)** Frequencies of epitope-specific CD8 T cells producing IFN- γ at day 21, analysis by flow cytometry. d21 splenocytes were restimulated in vitro with respective peptides for 6 h and Brefeldin A was added for the last 3 h of incubation for intracellular cytokine staining. Splenocytes were surface stained for CD8 T cells with CD3 ϵ and CD8 α , and intracellular stained for IFN- γ by analysis by flow cytometry. ICS: intracellular staining.

DISCUSSION AND OUTLOOK

1. PROJECT-I

In the first project of this thesis, we focused on the role of the recently identified candidate receptors DC-SIGN and LSECtin, as well as the TAM receptor tyrosine kinases, Axl and Tyro3, combined with the rLCMV-LASV chimera entry into DCs, using human primary MDDC as a model. We identified DC-SIGN as an attachment factor for LASV in human MDDC. DC-SIGN enhanced the binding of free virions to this crucial immune cell type *in vitro*. This binding was mediated by high mannose N-glycans present on the LASV GP1 and facilitated capture of free virus by MDDC. However, we observed significant residual infection in MDDC after treatment with mannan and function-blocking anti-DC-SIGN antibodies, indicating that other factors, in addition to DC-SIGN, contribute to LASV entry. In follow-up studies to this work, I propose to address the following questions/points:

- 1) What is the exact role of DC-SIGN in the LASV entry process in MDDC?
- 2) What is the role of the LASV receptor DG in LASV infection in MDDC?
- 3) What is the intracellular trafficking route of LASV in MDDC?

1.1. What is the exact role of DC-SIGN in the LASV entry process in MDDC?

The studies during my thesis revealed that DC-SIGN can facilitate LASV entry, but the underlying mechanisms are unknown. I propose to use a microscopic approach to further investigate the role of DC-SIGN in LASV entry using rLCMV-LASVGP as a model. In human DCs, DC-SIGN forms dynamic clusters at the plasma membrane that are associated with signaling molecules and seem to represent the functional units of pathogen recognition and endocytosis [137]. In a first step, confocal microscopy could be used to visualize the interaction of rLCMV-LASVGP with DC-SIGN clusters at the level of the plasma membrane and subsequent steps of viral entry into MDDC. Briefly, MDDCs cultured on coverslips will be incubated with fluorescence-labeled rLCMV-LASVGP at a high particle/cell ratio (100 particles/cell) in the cold. Unbound virus will be removed and the temperature shifted to 37°C. At different time points (e.g. 0, 5, 15, 30 min, 1, 2, and 4 h), cells will be fixed and permeabilized. Virus will be detected by direct fluorescence and DC-SIGN with an antibody [62]. Co-localization will be performed by combination with antibodies to markers for the plasma membrane and different intracellular compartments, including Rab5 (transport vesicles to early endosomes), EEA1 (early endosome), CD63/LBPA (MVB), Rab7 (transport vesicles to late endosomes), and LAMP1 (late endosome). Images will be acquired and reconstructed by Z-stack analysis. These studies will reveal if the virus attaches to pre-formed DC-SIGN clusters located at the plasma membrane, prior to uptake into the cell. Co-

localization studies with markers for intracellular compartments will reveal if DC-SIGN is internalized together with the virus or if the virus dissociates from DC-SIGN prior to or after internalization. These microscopic studies may help to understand if the slow LASV entry kinetics observed in MDDC is due to slow internalization of the virus-receptor complex or based on delayed intracellular transport with possible “temporary” sequestration of the virus in an intracellular compartment. Co-localization with Rab5/EEA1 and Rab7/LAMP-1 will reveal if LASV traffics through the classical endosomal pathway or uses a Rab5/EEA1-independent route, as previously shown for DG-mediated LASV entry in other cell types [14,138]. These studies will help to distinguish if DC-SIGN acts only as an attachment factor that concentrates virion particles at the cell surface prior to binding to the true entry receptor or if DC-SIGN is also involved in the internalization step. Based on previous studies on DC-SIGN-mediated entry of phleboviruses, we would expect that the virus separates from DC-SIGN at the level of the early endosome due to the low pH-induced dissociation of the DC-SIGN tetramers [62].

1.2. What is the role of the LASV receptor DG in LASV infection in MDDC?

We demonstrated that TAM receptor tyrosine kinases and the C-type lectin LSECtin are unlikely candidates for LASV receptors in MDDC. Neither of the TAM receptors was found on MDDC, in line with published studies [139]. Blocking of LSECtin with its carbohydrate ligands had no significant effect on MDDC infection with rLCMV-LASVGP and UUKV, but blocked LSECtin-mediated cell entry in a heterologous expression system, validating the inhibitor treatment.

A major receptor for LASV in many human cell types is DG. Functional DG is expressed in many cell types that are infected by LASV in humans *in vivo*, including, but not limited to epithelial cells, endothelial cells, and hepatocytes [140]. In the host cell, α -DG is subject to complex post-translational modifications that are crucial for its function as an ECM receptor [141,142]. Of particular importance are specific O-mannosyl-glycans found at the N-terminus of α -DG’s mucin-type domain produced by the glycosyltransferase LARGE that are crucial for binding to ECM proteins [143] and arenaviruses [140,144,145]. While the core protein of DG is ubiquitously expressed, the functional glycosylation of the receptor is under tight tissue-specific control [142]. Since the functional glycosylation of DG in human immune cells and in particular in human DCs is largely unknown, we started to characterize the expression of functional DG in human monocytes and MDDC. To detect functional DG in MDDC, cells were lysed and DG core protein enriched by affinity purification with the lectin wheat germ

agglutinin (WGA) as described [146]. As controls, we used the human lung epithelial cell line A549 rich in functional DG and the CD4 T cell line Jurkat that lacks functional receptor [145]. Lectin-bound proteins were separated by SDS-PAGE and probed with monoclonal antibody (mAb) I1H6 that recognizes the functional O-glycans on α -DG required for virus and ECM binding [143]. High amounts of glycosylated α -DG were present in A549 cells, whereas the expression levels in monocytes, MDDC, and Jurkat cells were below the detection limit of our assay (Fig.12A). Detection of glycosylated α -DG at the surface A549 cells, monocytes, and MDDC by flow cytometry gave similar results (Fig.12B). The lack of detection with the glycosylation-specific anti- α -DG antibody I1H6 in MDDC was unexpected and suggested either low levels of functional α -DG glycosylation or enhanced shedding of α -DG from β -DG. Previous studies demonstrated that over-expression of LARGE can rescue functional α -DG in cells bearing various genetic defects in DG glycosylation [147]. Using adenoviral (AdV) vectors, we over-expressed LARGE in MDDC, which resulted in detection of a band of 120-125 kDa by mAb I1H6, possibly functional α -DG (Fig.12C). No significant signals were detected in MDDC transduced with a control AdV expressing GFP. The appearance of a defined I1H6 reactive protein upon LARGE over-expression suggests the presence of α -DG core protein in MDDC, albeit with low endogenous levels of functional glycans. In a complementary approach, we tried to block infection of rLCMV-LASVGP in MDDC and A549 cells with mAb I1H6. Cells were pre-treated with increasing concentrations of mAb I1H6 and an isotype control, prior to addition of virus. After 16 hours, infection was assessed by flow cytometry. As expected, DG-mediated infection in A549 cells was blocked by I1H6 in a dose-dependent manner (Fig.12D). In contrast, no significant inhibition was observed in MDDC (Fig.12D). In sum, the data at hand suggest that human monocytes and MDDC express a form of DG that is only weakly recognized by the glycosylation-dependent mAb I1H6.

The expression of an underglycosylated DG form in MDDC with low virus-binding affinity seems to be in line with the significant contribution of DC-SIGN in virus attachment. However, our assays used so far are limited in their sensitivity and we cannot rule out that underglycosylated DG can still function as an entry receptor in MDDC, e.g. in concert with DC-SIGN. To address this possibility, I propose to perform depletion of the DG core protein in MDDC using RNA interference (RNAi). To this end, human monocytes will be transduced with lentiviral vectors expressing a validated shRNA targeting DG that is available in our group. Upon differentiation into MDDC, the absence of DG core protein can be validated by Western blot and RT-qPCR for DG mRNA. In case we are able to achieve > 95% depletion of

DG core protein, this RNAi approach would allow addressing a possible role of DG as a low affinity LASV receptor in MDDC.

Our finding that MDDC apparently express an underglycosylated form of α -DG is *per se* novel and interesting. I therefore propose to further study the glycosylation state of the α -DG form present on monocytes and MDDCs. In a first step, we could investigate, by real time PCR, the expression profile of the different enzymes responsible for the post-translational modifications of this protein, specifically LARGE (1 and 2) the proteins O-mannosyltransferases POMT1 and POMT2 [148], protein O-mannose β 1,2-N-GlcNAc transferase 1 (POMGnT1) [149], fukutin, and fukutin-related protein (FKRP) [150].

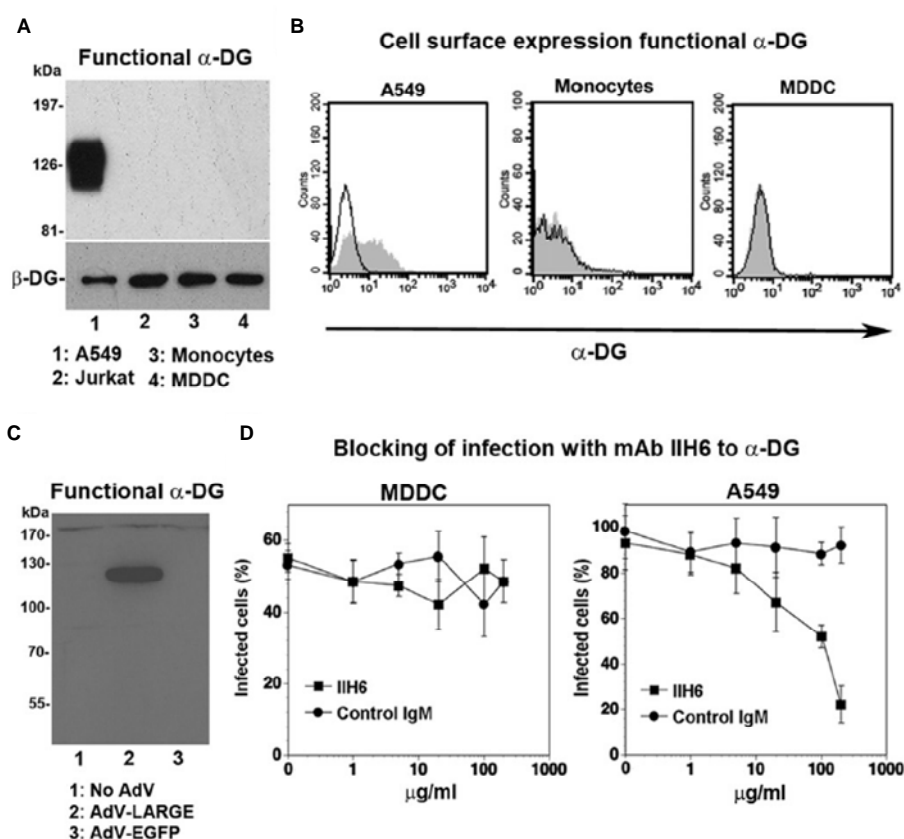


Figure 12. Detection of functional DG in human monocytes and MDDC. **A)** Monocytes, MDDC, A549 cells, and Jurkat cells (5×10^6 cells) were lysed and subjected to WGA affinity purification as described in Materials and Methods. Lectin-bound proteins were eluted by boiling in SDS-PAGE sample buffer. The whole eluates for monocytes, MDDC, and Jurkat cells and 1/10 of the eluate from A549 cells were analyzed in Western blot using mAb IIH6 to α -DG (upper blot) and mAb 8D5 to β -DG (lower blot). The position of β -DG and apparent molecular masses are indicated. **B)** Detection of functional DG at the cell surface. Monocytes, MDDC, and A549 cells were subjected to staining with mAb IIH6 on live, non-permeabilized cells. Cells were fixed and bound mAb IIH6 detected with a PE-conjugated secondary antibody in flow cytometry. Empty peaks: secondary antibody only, shaded peaks: primary and secondary antibody. **C)** Over-expression of LARGE rescues functional DG in MDDC. MDDC were infected with AdV-LARGE and AdV-GFP at MOI = 100. After 48 hours, total cell lysates were prepared and probed with mAb IIH6 as in (A). **D)** Blocking of infection of rLCMV-LASVGP with mAb IIH6. MDDC and A549 cells were blocked with mAb IIH6 or a control mouse IgM (Control IgM) at the indicated concentrations for 2 h at 4°C. Next, rLCMV-LASVGP (multiplicity of 1) was added for 45 min. Infection was assessed after 16 hours by flow cytometry for LCMV NP (means + SD, n = 3).

Moreover, we should exclude the possibility that the α -DG glycosylation profile observed in MDDCs was due to the *in vitro* procedure we use for differentiation. I propose to examine the functional α -DG expression on DCs directly isolated from human blood using negative or positive selection of blood cells with specific DCs markers coupled to magnetic beads. The investigation of additional DCs subtypes, in particular plasmacytoid DCs (pDCs) that are also targets for LCMV and LASV [151] would also be of great interest. From these experiments we could acquire a better knowledge about the expression of functional DG in human primary DCs and further validate MDDCs as an experimental model. Preliminary data from studies I performed on PBMC, which include T (45-70%), B (15%) and NK (15%) lymphocytes, monocytes (10-30%) and several types of DCs (1-2%) directly isolated from human blood, tended to confirm the absence of functional α -DG on primary human DCs (data not shown), but need to be confirmed.

1.3. What is the intracellular trafficking route of LASV in MDDC?

We have observed that the entry kinetics and characteristics of LASV in MDDC were remarkably different from those of DG-mediated LASV entry in other cell types as well as DC-SIGN-mediated cell entry of phleboviruses. This unusual entry pathway may be related to the ability of LASV to evade innate detection in MDDC and the ability of the virus to perturb antigen presentation by MHC I and II. The examination of the intracellular trafficking route used by LASV in MDDC is therefore of great importance. The microscopic studies on the role of DC-SIGN in LASV attachment and/or internalization mentioned above will give first hints about the events taking place at the plasma membrane and during internalization. In a next step, we will try to identify the initial compartment that is reached by the virus upon internalization. To detect the virus in putative early endosomal structures, we will perform 19°C trapping experiments. At 19°C, uptake of cargo takes place to some extent, whereas membrane maturation and vesicular sorting from early endosomal compartments are markedly slowed down [152]. Fluorescence-labeled virus (rLCMV-LASVGFP) will be added to cells on ice followed by a temperature shift to 19°C for 30 min, 1, 2, and 4 h. Cells will be virus co-localized with Rab5, EEA1, Rab7, LBPA, CD63, LAMP1, and DAPI (nuclei). In case we observe accumulation of virus at intracellular sites distinct from classical early Rab5/EEA1 positive endosomes or the MVB/late endosome, I propose to assess the size, shape and luminal pH of the compartment. For this, one could use LysoSensor™ probes (Invitrogen) that exhibit a pH-dependent increase in fluorescence in acidic environments and allow measuring the intraluminal pH of a given compartment. These studies will reveal if the

virus-receptor complex passes through an early acidified compartment in which it is retained for some time, or if it is directly transported to the MVB/late endosome. Apart from classical Rab5/EEA1 positive early endosomes, other early endosomal compartments have more recently been identified, such as clathrin-independent carrier compartments (CLIC) or GPI-protein enriched early endosomal pathway (GEECs), which may be involved in the process [153]. Interestingly, entry via CLIC and GEECs critically depends on actin, but is clathrin- and dynamin independent [154]. To further address a possible role of CLIC/GEECs, one could study the role of regulatory proteins implicated in the pathway, including the small GTPases Cdc42 and Arf1 using a combination of RNAi and dominant negative (DN) mutants. Co-localization with microtubules will visualize possible microtubular transport of virus-containing vesicles from early to late endosomes, suggested by the sensitivity of LASV entry to nocodazole.

1.4. Identification of novel LASV entry factors in human DCs

The significant residual infection of rLCMV-LASVGP upon blocking of DG and DC-SIGN in my studies suggests the existence of yet unknown LASV entry factors in MDDC. The expression cloning approaches performed by the laboratory of Prof. Kawaoka to identify LASV entry factors [13] were carried out in a sophisticated manner and I do not propose to repeat or to duplicate this work. Instead, I would like to suggest a complementary strategy, based on quantitative proteomics. This approach may allow the discovery of LASV entry factors in MDDC, whose identification may not be feasible by expression cloning. For the proteomic analysis, I propose to use stable isotope labeling of amino acids in culture (SILAC). This method is based on the *in vivo* incorporation of a non-radioactive isotope label into proteins in cultured cells to allow analysis by mass spectrometry (MS). SILAC allows the discrimination of two experimental conditions by the relative mass of proteins labeled with different isotopes present in the samples. This can be achieved by labeling cellular proteins by adding isotope-labeled amino acids, typically Lys and Arg, containing ^{15}N and ^{13}C isotopes (Lys-8 and Arg-10) to the cell culture medium during several passages. A key feature and advantage of SILAC is the possibility to detect specific changes in protein interactions by subtractive analysis, greatly reducing non-specific background and increasing the signal/noise ratio [155]. To assess feasibility of a SILAC proteomic approach in the follow-up of my project, I have performed a first set of preliminary studies that will be briefly summarized.

The putative LASV entry factors on human DCs are proteins or protein-bound entities:

A major restriction of SILAC for the identification of viral entry factors is that the method works only with proteins, but not sugars or lipids. In a first step, we sought to validate the protein nature of LASV entry factors in MDDCs. Cells were treated with a series of proteases, lipases, or glycosidases, and the effect of treatment on subsequent infection assessed. Treatment with the proteases trypsin and proteinase K resulted in >98% reduction of rLCMV-LASVGP infection, but hardly affected infection with rLCMV-VSVG, which uses a non-protein receptor. Treatment of cells with different phospholipases, PNGaseA, which remove all types of N-glycans and O-glycosidase, which hydrolyzes most O-linked sugars, had no significant effect on infection. These data suggest that the putative LASV entry factor(s) on MDDC are likely proteins or protein-linked entities, supporting a SILAC-based proteomic approach.

THP-1-derived MDDC are a suitable DC model: SILAC requires labeling of cells with heavy amino acids during several passages, limiting the use of primary cells. The human monocyte-derived cell line THP-1 can be differentiated in presence of PMA and IL-4 into a DC-like phenotype that shows key features of MDDC, including up-regulation of DC-SIGN [156]. Comparing receptor use and entry of rLCMV-LASVGP in THP-1-derived MDDC with primary cells revealed that the virus enters both cell types in a DG-independent manner facilitated by DC-SIGN. Blocking of DC-SIGN with antibodies reduced productive infection of rLCMV-LASVGP by <50%, suggesting the presence of alternative receptor(s) in THP-1-derived MDDC. However, I am aware of the limitations of the model and recommend validating candidate entry factors in primary MDDC.

The bait: recombinant LASVGP1 immunoadhesins: Fusion proteins that combine the receptor-binding region of a viral GP with the Fc region of an IgG, so-called “immunoadhesins”, have been successfully used as baits to identify virus receptors by proteomics [157,158]. The laboratory of Dr. Erica Ollman Saphire (Scripps, La Jolla) provided us with a fusion protein of LASV GP1 with the Fc part of rabbit IgG. The LASVGP1-Fc immunoadhesin was produced in HEK293T cells with good yields (>1 mg/l) and purified by protein A affinity chromatography. The purified protein formed dimers, showed the expected molecular mass, and bound to α -DG with high affinity, proving biological activity.

To identify candidate LASV entry factors, THP-1 cells will be cultured for 10 passages in medium supplemented with Lys-8/Arg-10 resulting in labeling of > 95% of cellular proteins, or normal medium. Cells will then be differentiated into MDDC-like cells for 3-4 days. Membrane lysates of cells labeled with heavy amino acids will be incubated with LASVGP1-Fc and cells kept in normal medium with a control IgG. Co-IP will be performed with protein A matrix and proteins will be analyzed by MS. In case the binding affinity of LASV GP1 for candidate cellular receptors is too low to allow co-IP, the GP1-receptor complexes could be stabilized by chemical cross-linking. To this end, hydrophilic, membrane-impermeable cross-linkers with short spacers (0.5-1.5 nm) between their reactive groups may be applied. The use of cleavable reagents allows the recovery of cross-linked proteins after their isolation. Upon cross-linking, the resulting GP-receptor complexes will be immunoprecipitated prior to further processing. In case we are unable to detect any candidate proteins upon co-IP combined with cross-linking with S-DST or Sulfo-SADP, we will evaluate the new tripartite cross-linker TRICEPS, which has longer spacer arms and combines amino reactive functions with a carbohydrate-reactive moiety and a biotin tag [159].

For functional validation, candidate receptor proteins will be expressed in resistant Jurkat cells by electroporation of plasmids encoding the corresponding cDNAs. Transduction with a functional receptor will render cells more susceptible to infection with rLCMV-LASVGP, but not rLCMV-VSVG. Possible cooperation of candidate receptors with DC-SIGN will be addressed by co-expression with DC-SIGN. In a complementary approach, primary MDDC will be transfected with siRNA against candidates and control siRNAs using electroporation and the knock-down verified by Western blot or RT-PCR. Depletion of a functional receptor will increase resistance of transfected cells to rLCMV-LASVGP, but not rLCMV-VSVG. Validated receptors in MDDC could then be examined for their expression/role in LASV cell entry into other immune cells that are targeted by LASV *in vivo*, including pDCs and macrophages. Considering the pivotal role of DCs in LASV pathogenesis the identification of such entry factors is of great importance.

2. PROJECT-II

2.1. Induction of an efficient humoral immune response against MACV GP1

An initial evaluation of our MACV GP1-NPs vaccine revealed that the immunogen conjugated to the surface of the PPS NPs elicited a specific antibody response that was significantly stronger than the response obtained after delivery of the non-conjugated immunogen. The enhanced magnitude of the antigen-specific antibody response was in line with previous reports that demonstrated a strong adjuvant effect of the NPs platform. [5,160]. Monitoring of IgG titers as well as determination of the prevalence of IgG subtypes (data not shown) over time indicated that the total IgG titers were stable over 6 months. Initially IgG2c represented a major IgG subtype and IgG1 gradually decreased. However, despite the detection of robust IgG titers in ELISA, neutralization assays using a well-characterized pseudotype platform showed only low nAbs in sera of mice vaccinated with either NPs-conjugated or free immunogen. The nAbs titers were not only low, but also faded away over time, indicating an only weak and transient nAbs response. This was in contrast to the situation in the context of the natural MACV infection that is characterized by robust nAbs titers in convalescent serum [118,161]. The low nAbs titers observed in our system were also very different from the serological evidence obtained from studies on the live attenuated JUNV vaccine Candid 1, in which solid and long-lasting nAbs are detected in vaccinated individuals after one immunization [49]. The obvious discrepancy between the nAbs response observed in our NPs vaccine when compared to the natural infection or live vaccine raised serious concerns about the antigenic nature of our immunogen. In a next step, we therefore further investigated the nature of the antibodies present in the sera of vaccinated animals, in particular the question what parts of our immunogen are indeed recognized. For this purpose, we employed the technology of peptide arrays that have been widely used for epitope mapping. Display of the entire immunogen sequence in an array of 20 peptides with an off-set of only one aa allowed a comprehensive screen for antigenic peptides. The array data pinpointed sequences surrounding the N-terminal HA tag as major antigenic sites. The preferential recognition of the HA-tag and in particular the flanking sequences by the antibodies present in the sera of vaccinee mice was further confirmed by flow cytometry. Since nAbs frequently recognize conformational epitopes [122,162], a possible restriction of the peptide array format used in my studies is the presentation of the immunogen in the form of linear peptides. To close this gap we sought to test the ability of antibodies in sera of vaccinated animals to recognize MACV GP1 in its native conformation present at the virion

surface. To this end, we expressed recombinant full-length MACV GP in human HEK293 cells. Previous studies from our group showed that recombinant MACV GP is displayed at the surface of HEK293 cells in its native conformation and retains its biological activity [78]. Flow cytometry analysis revealed weak but consistent binding of antibodies derived from mice vaccinated with the non-conjugated protein to native MACV GP, but no detectable attachment of antibodies from mice vaccinated with the NPs-conjugated protein. Together, the data at hand suggest that the antibody response elicited by our NPs-conjugated MACV GP1 immunogen was mainly directed against sequences surrounding the HA-tag, but not the MACV GP1 part.

Together, our results indicated two major flaws in the design of our immunogen. First, the introduction of the N-terminal HA-tag generated highly immunogenic sequences at the junction between the tag sequence and the surrounding protein. We hypothesize that these artificial immunogenic sites present in our vaccine antigen may somehow divert the antibody response and may be, at least in part, responsible for the very weak response against the MACV GP1-derived structures. This problem has already been solved by the introduction of thrombin cleavable HA-tag into MACV Δ GP1. After efficient cleavage of thrombin, only a stub of two amino acids is retained, which is not expected to give rise to an aberrant antibody response.

Second, the initial procedure used to conjugate the MACV Δ GP1 immunogen to NPs likely resulted in the disruption of crucial antigenic sites of the protein. As pointed out in the results section, the MACV Δ GP1 antigen produced in HEK293 T cells does not contain free cysteine residues. In order to conjugate the protein to the NP surface with the classical thiol-based coupling chemistry, we performed partial reduction with TCEP in the cold. Assessment of receptor binding capacity of the protein after TCEP treatment indicated retention of circa 50% of its binding activity, suggesting that about half of the protein may have undergone irreversible denaturation. Since the coupling efficiency to NPs occurs with < 10% efficiency, we cannot exclude a preferential conjugation of the denatured protein that may display a higher number of free cysteine side chains. During the *in vivo* evaluation of our NPs vaccine a study was published that identified specific structures of MACV GP1 crucial for receptor binding. According to this work, the major interaction of MACV GP1 with TfR1 is mediated by two peptide loops that protrude from the MACV GP1 surface, L3 and L10 highlighted in Fig.13. Notably, L10 is stabilized by the disulfide bond C220-C229 that is essential for the correct orientation of the crucial contact residue F226 of MACV GP1 with TfR1 [12,125].

Since the disulfide bond C220-C229 is located closely to the water-accessible surface of MACV GP1, it may react preferentially with TCEP and be cleaved efficiently even under mild conditions, disrupting the conformation of L10, which represents a key structural element of the receptor binding site. Moreover, the free thiol groups liberated after cleavage of the disulfide-bridge C220-C229 may result in conjugation of MACV GP1 in an orientation that renders the receptor-binding face and thus putative “neutralizing surface” inaccessible (Fig.13).

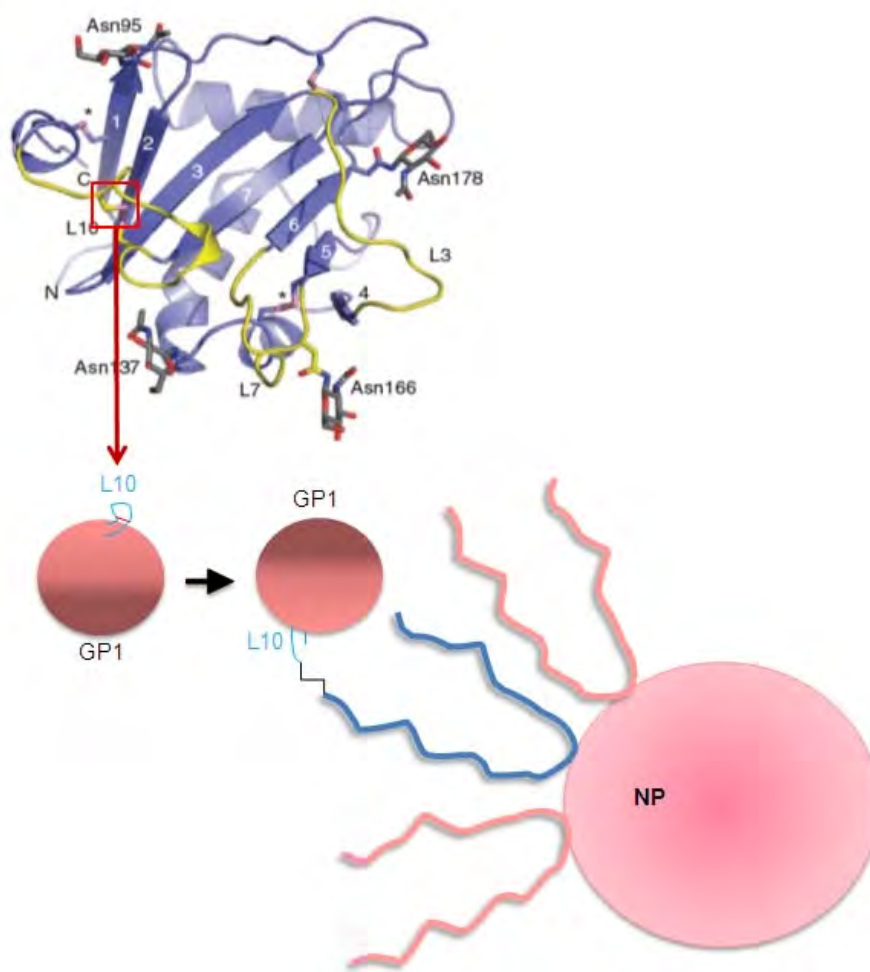


Figure 13. Structure of MACV GP1 with receptor-binding structures highlighted in yellow. The major receptor-binding L3 and 10 are highlighted. Note that L10 is stabilized by a disulfide bond formed by the Cys residues C220 and C229 (modified from [12]). Below: partial reduction of the disulfide bond C220-C229 and subsequent conjugation of MACV GP1 to the NPs surface (for details, please see text).

Considering the problem encountered with the partial reduction and subsequent thiol-conjugation of our vaccine antigen, we developed a novel strategy NPs coupling employing the recently developed “aldehyde (Ald)-tag” that allows site-specific conjugation of recombinant proteins under mild non-reducing conditions compatible with the retention of the

native conformation of MACV GP1. As outlined in the results section, we successfully engineered two new MACV Δ GP1 constructs containing Ald-tags either at their N- or C-terminus. Both constructs could be produced with similar efficiencies, however, the construct containing the C-term Ald-tag showed lower reactivity with oxyamines. We therefore decided to only use the N-terminally tagged protein for further studies. Ald-tagged MACV Δ GP1 readily reacted with oxyamine-biotin, indicating accessibility and reactivity of the aldehyde function. Initial attempts to conjugate the Ald-tagged MACV Δ GP1 to NPs resulted in around 16% conjugation efficiency. Although a good starting point, we are currently optimizing the individual conjugation steps to increase efficiency.

Taking into account the crucial role of the MACV GP1 L3 and L10 for receptor binding, we are currently evaluation these peptide sequences as possible vaccine antigens. Molecular modeling revealed that a synthetic peptide derived from loop 3 will unlikely adopt the correct conformation seen in the MACV GP1-TfR1 co-crystal structure. We therefore focus on L10. After successful synthesis of L10, preliminary data suggest sufficient conjugation efficiency and we anticipate no problems in the production of the NPs. In a next step, immunization will be performed analogous to our studies with MACV Δ GP1-NPs. Using the serological assays established during my thesis, vaccinated mice will be examined for the development of specific antibodies to the L10 sequence and possible nAbs will be tested in our neutralization assay with MACV GP pseudotypes. These studies could serve as proof-of-principle for the use of conformational peptides linked to NPs in the context of arenaviruses and other human pathogenic viruses. Upcoming crystal structures of other arenavirus GPs, in particular LASV and JUNV, could be used for the design of analogous peptides.

2.2. Towards a multivalent vaccine against the major pathogenic NW arenaviruses

Among the South American hemorrhagic fever viruses, JUNV represents the largest threat for human health. The rodent *Calomys musculus* and several other rodent species represent the natural reservoir of the virus. The exact mechanism of rodent to human transmission is not known, but there is strong experimental evidence that these viruses are infectious as aerosols [163]. While former endemic hot spots are currently cooling off, the disease area increases progressively, placing larger populations at risk [118]. Argentine hemorrhagic fever (AHF) is a severe illness with hemorrhagic and neurological manifestations and a case fatality of 15-30% [26,36,118]. With over 50,000 reported cases so far and considering the number of people at risk, JUNV currently represents one of the top priority BSL4 pathogens by the National Institute of Health (NIAID/NIH) and the Centers for

Disease Control and Protection (CDC). A major goal of the follow-up of my thesis project is therefore the development of a bivalent vaccine against MACV and JUNV, which combines the two most relevant pathogenic NW arenaviruses. JUNV and MACV are phylogenetically and antigenetically closely related. The study of receptor use by pathogenic and non-pathogenic Clade B arenaviruses showed that all viruses of this Clade use TfR1 orthologues, albeit with different species-specificities. The ability of a Clade B New World arenavirus to use human TfR1 is absolutely predictive for its potential to cause hemorrhagic fevers in man [164]. Virus binding was mapped to a specific region of the apical domain of hTfR1 that contained a conserved tyrosine in position 211 in humans, and the reservoir rodents, but not other species like rat and mouse [165]. The remarkable conservation of the receptor site recognized by MACV and JUNV suggests a similar conservation in the complementary receptor-binding site. In line with these recent findings, earlier serological studies indeed indicated cross-neutralization of MACV by anti-JUNV nAbs [166]. Together, the classical serological evidence and more recent structural data at hand suggest that the development of a bivalent JUNV/MACV vaccine is feasible. In a first step we will test our MACV NPs vaccine for its potential to generate nAbs that are cross-neutralizing between MACV and JUNV, as observed in the natural infection. If this is not the case, we will engineer and produce JUNV GP1-derived antigens analogous to our MACV GP1 antigen and produce NPs that display both antigens at their surface.

2.3. The challenge of generating a protective NPs vaccine against LASV

Although the South American hemorrhagic arenaviruses JUNV and MACV represent important public health problems, they are virtually dwarfed by the humanitarian impact of LASV that causes several hundred thousand infections annually in Western Africa [167]. The impact of LASV on public health in Western Africa is perhaps best illustrated by the fact that in some regions, >50% of the adult population are seropositive for LASV [168], making LASV likely a major cause of death in this part of the world [23]. However, as we have seen earlier, there are important differences in the quality of the antibody response between LASV and the NW arenaviruses JUNV and MACV [23,118]. While natural infections with JUNV and MACV result in robust nAbs titers that are fully protective against re-infection [118], the nAbs response against LASV in humans is normally delayed and rather weak [23]. Surveys in endemic regions revealed a high prevalence of non-neutralizing serum antibodies against LASV NP in survivors of LASV infection, but only low nAbs titers against GP that even seem to fade away over time [168]. Despite the only weak nAbs response observed in humans

after LASV infection, proof-of-concept studies in animal models demonstrated that nAbs are protective against LASV challenge, when given at sufficient titers [47,48,169]. The lack of a potent nAbs response against LASV seems reminiscent to the infection with the prototypic OW arenavirus LCMV in its natural host, the mouse [134]. Humans are not natural hosts of LASV and any extrapolation between the LCMV infection in the mouse and human Lassa fever appears therefore questionable. However, the lack of nAbs in both infection paradigms is intriguing and suggests that LASV and LCMV GP1 either lack inherent antigenicity or that the envelope GP1 of LASV and LCMV are presented to the host's immune system in the context of the natural primo infection in a way that prevents the production of potent nAbs.

Potential lower antigenicity of LASV GP1 could be due to different reasons. On many viral envelope GPs, N-glycans shield potential antigenic sites against the humoral immune response [162]. Indeed, when compared to the NW viruses JUNV and MACV, LASV GP1 contains more actual N-glycosylation sites, suggesting the presence of a more extensive "glycan shield" [170]. Another important difference between the GP1 of JUNV and MACV on the one hand and LASV on the other hand is receptor use. JUNV and MACV attach to the apical surface of hTfR1 via an extended molecular protein-protein interaction surface [125]. In contrast, LASV and LCMV recognize their receptor via conserved xylose/glucuronic acid co-polymer sugars attached to the N-terminal domain of DG by the glycosyltransferase LARGE [140,145,171] in a lectin-type binding. One might speculate that the extended molecular surface of MACV and JUNV GP1 interacting with hTfR1 could be easily recognized by antibodies, whereas this may be less the case for the sugar binding pocket of LASV GP1. To experimentally address these issues, I propose to use our PPS NPs in a comparative study testing the antigenicity of MACV GP1 and LASV GP1 in the context of a normalized vaccine platform. For this purpose, LASV GP1 analogues to our newest-generation MACV Δ GP1 are currently produced in the laboratory. The corresponding MACV Δ GP1 and LASV Δ GP1 containing Ald-tags and cleavable HA-tags will be conjugated to PPS NPs and evaluated side-by-side for their ability to elicit a nAbs response. We expect to see at least some nAbs development upon vaccination with MACV Δ GP1-NPs. Significantly lower nAbs titers in response to LASV Δ GP1-NPs would indicate an inherent difference in the antigenicity of MACV and LASV GP1. Comparable levels of nAbs generated upon vaccination with MACV Δ GP1-NPs and LASV Δ GP1-NPs would indicate that the apparent lack of nAbs in LASV primo infection is not an inherent property of the GP1, but likely due to important differences in antigen presentation and/or immunoregulation in the context of the two infections. In case we would observe marked differences between LASV and MACV

with LASV GP1 being less antigenic, we could try to improve the NPs platform and the LASV GP1 immunogen in an iterative way to achieve induction of nAbs. In a first step, we could perform peptide array analysis of the sera obtained from immunization with LASVΔGP1-NPs. The goal would be to identify potential neutralizing and in particular possible immunodominant non-neutralizing epitopes on LASVGP1. In case we would observe a predominantly non-neutralizing antibody response, we would try to define the dominant non-neutralizing epitopes, as they may act as “decoys” to divert the humoral immune response. Such “decoy” epitopes could be subjected to “silencing” by site-directed mutagenesis and introduction of novel N-glycosylation sites that will “shield” such epitopes allowing a more focused response to putative neutralizing epitopes.

2.4. Induction of an efficient T cell response

Our studies demonstrated that our PPS NPs conjugated to LCMV-derived MHC class I peptides were able to trigger a strong and specific anti-viral CD8 T cell response in mice. This response was much higher after a prime-boost vaccination strategy than after a unique immunization, which was somehow expected from the available literature. In addition, the functional hierarchy of the CD8 T cell epitopes seemed maintained upon vaccination with the conjugated NPs. However, more epitopes need to be tested to confirm this observation. To this end we will generate a complete set of NPs displaying known H2-D^b restricted CD8 T epitopes of LCMV in C57BL/6 mice. Specifically, we will study the epitopes GP₃₃₋₄₁, NP₃₉₆₋₄₀₄, and GP₂₇₆₋₂₈₆, as well as the subdominant epitope GP₉₂₋₁₀₁. This will allow us to monitor the frequencies of epitope-specific cells and conservation of CTL epitope hierarchy.

A crucial next step will be the systematic analysis of the CTL response to our NPs in comparison with a non-infectious vaccine paradigm (DNA vaccination) and the LCMV primo infection. The comparison with these systems will allow benchmarking the NPs platform’s T cell response against those of the DNA vaccine and natural infection. DNA immunization has been studied extensively in the LCMV model and, in general, plasmid DNA encoding LCMV proteins induced better CD8 T cell responses than antibody responses. Depending on the antigen, mouse strain, and route of inoculation, DNA vaccination using minigenes coding for immunodominant CTL epitopes conferred insufficient protection [172,173], whereas plasmid DNA encoding full-length NP or GP resulted in at least partial protection against LCMV infection [174,175,176]. I propose to use defined expression plasmids for full-length LCMV NP and GP that will be administered by intramuscular injections [175].

For benchmarking relative to the natural infection, mice will be infected with a low dose (10^5 PFU) of the low virulence LCMV ARM53b strain. In this classical paradigm, the CTL response peaks around day 8 post infection, following by a contraction period and memory formation. Mice clear virus after 15 days. Primo infection with LCMV ARM53b in C57BL/6 mice results in a CD8 T cell response with the following hierarchy of epitopes: NP₃₉₆₋₄₀₄ > GP₃₃₋₄₁ > GP₂₇₆₋₂₈₆ >> GP₉₂₋₁₀₁. Upon viral re-challenge, memory CD8 T cells rapidly activate and proliferate leading to a potent secondary anti-viral CTL response that confers life-long protection of the animal.

In a next step, our MHC I peptide NPs will be tested in a well-established challenge model *in vivo* at 8 weeks after vaccination. Specifically, vaccinated mice will be infected with high doses of the more virulent LCMV strain clone-13 (cl-13). When given at a dose of 2×10^6 PFU *i.v.* in naïve C57BL/6 mice, LCMV cl-13 induces a transient immunosuppression due to CTL exhaustion and establishes a persistent infection that lasts for 60-90 days. The quantity and quality of memory T cells will be monitored by MHC I tetramer staining. After 48 hours of challenge, splenocytes will be isolated and analyzed after peptide stimulation by intracellular cytokine staining (IFN- γ and TNF- α), and in a CTL killing assay. In naïve mice, upon primary infection, anti-viral CD8 T cells are undetectable at 48 hours of infection and any significant anti-viral CD8 T cell activity at this time point must stem from memory T cells induced by our vaccine. Kinetics of serum viral load will be monitored in blood of mice to assess protection against the viremia normally observed in the LCMV cl-13 paradigm.

This evaluation of the PPS NPs vaccine in the context of the LCMV model will represent the first extensive characterization of this platform with an infection of a pathogen in its natural host and close an important gap in our current knowledge about its possibilities. The extensive body of data available on the LCMV model, either in the natural infection or other vaccine systems, e.g. DNA vaccines, will allow a valid comparison of its future potential.

MATERIALS AND METHODS

PCR generation of MACVΔGP1 and LASVΔGP1 constructs DNA

MACVΔGP1 and MACVΔCGP1 (Carvalho NC_005078) fragments were produced by PCR using as template the respective full length glycoprotein precursors (GPC) subcloned in pCAGGS vector. All constructs were further subcloned in the the pcDNA 3.1 int A expression vector, kindly provided by Dr. Branco (Tulane University Health Sciences Center, New Orleans, LA, USA).

Amplification primers:

MACVΔGP1:

Forward: 5'-ATTCCCGGGCTCCCATCTCTCTGCATGCTT-3'

Reverse: 5'-CGATCTCGAGTCAGTCAGCCCTTGTCGTCGTCGTCCTTGTAGTCGGCAGCA
GACCTCTCAAAGTTGAGATG-3'

MACVΔCGP1:

Forward: 5'-ATTCCCGGGTGTCTCCCATCTCTCTGCATGCTT-3',

Reverse: 5'-CGATCTCGAGTCAGTCAGCCCTTGTCGTCGTCGTCCTTGTAGTCGGCAGC
AGACCTCTCAAAGTTGAGATG-3'

Ald-MACVΔGP1 construct sequence:

```
5' -AAGCTTGGTACCGAGCTCGGATCCACTAGTAACGGCCGCCAGTGTGCTGG
AATTCGGCTTGGGGATATCCACCATGGAGACAGACACTCCTGCTATGG
GTACTGCTGCTCTGGGTTCCAGGTTCCACTGGTGACCTGTGCACCCCCAG
CCGGGCCGCCCTGCTGACCGGCCGGCCCGGGCTCCCATCTCTCTGCATGC
TTAACAATAGTTTTTATTATATGAGGGGAGGTGTGAACACCTTCCTGATT
CGTGTCTTCTGATATTTTCAGTCCTCATGAAGGAGTATGATGTATCAATCTA
TGAACCAGAAGACCTTGGAAATTGTCTTAACAAGTCTGACTCAAGCTGGG
CTATTCATTGGTTCTCAAATGCTTTGGGACATGACTGGCTTATGGATCCT
CCAATGCTATGTAGAAACAAGACAAAGAAGGAGGGATCTAACATTCAATT
CAACATCAGCAAAGCTGATGATGCCAGAGTGTATGGAAAGAAGATAAGAA
ATGGTATGAGGCATCTCTTCAGGGGCTTCCATGACCCGTGTGAGGAAGGG
AAAGTGTGCTACCTGACCATCAATCAGTGTGGTGACCCAGTTTCTTTGA
CTACTGTGGCGTGAATCATCTTTCCAAATGTCAGTTTGACCATGTGAACA
CCCTTCATTTCTTGTGAGAAGTAAGACACATCTCAACTTTGAGAGGTCT
GCTGCCCTTGTCCCACGTGGTTCTTATCCATATGATGTTCCAGATTATGC
TTGACTGACTCGAGATCG-3'
```

Restriction sites HindIII, XmaI and XhoI are underlined. The red highlighted region corresponds to IgK sequence from pDisplay vector and is fused to the FGE full length recognition region in yellow (HindIII-XmaI). This sequence was synthesized by GeneArt® Gene Synthesis (Life technologies™). The rest of the construct (grey, green and violet highlight) was generated by PCR (XmaI-XhoI) using the following primers:

Forward: 5'-TTACCCGGGCTCCCATCTCTCTGCATGCTT-3',

Reverse: 5'CGATCTCGAGTCAGTCAAGCATAATCTGGAACATCATATGGATAAGAACCA

CGTGGGACAAGGGCAGCAGACCTCTCAAAGTTGAG-3'

MACVΔGP1-Ald construct sequence:

5' - AAGCTTGGTACCGAGCTCGGATCCACTAGTAACGGCCGCCAGTGTGCTGG
 AATTCGGCTTGGGGATATCCACC **ATGGAGACAGACACTCCTGCTATGG**
GTACTGCTGCTCTGGGTTCCAGGTTCCACTGGTGAC **TATCCATATGATGT**
TCCAGATTATGCTCTTGTGCCACGTGGTTCT **CCCGGG**CTCCCATCTCTCT
 GCATGCTTAACAATAGTTTTTATTATATGAGGGGAGGTGTGAACACCTTC
 CTGATTCGTGTTTCTGATATTTTCAGTCCTCATGAAGGAGTATGATGTATC
 AATCTATGAACCAGAAGACCTTGAAATTGTCTTAACAAGTCTGACTCAA
 GCTGGGCTATTCATTGGTTCTCAAATGCTTTGGGACATGACTGGCTTATG
 GATCCTCCAATGCTATGTAGAAACAAGACAAAGAAGGAGGGATCTAACAT
 TCAATTCAACATCAGCAAAGCTGATGATGCCAGAGTGTATGGAAAGAAGA
 TAAGAAATGGTATGAGGCATCTCTTCAGGGGCTTCCATGACCCGTGTGAG
 GAAGGGAAAGTGTGCTACCTGACCATCAATCAGTGTGGTGACCCAGTTC
 CTTTGACTACTGTGGCGTGAATCATCTTTCCAAATGTCAGTTTGACCATG
 TGAACACCCTTCATTTCTTGTGAGAAGTAAGACACATCTCAACTTTGAG
 AGGTCTGCTGCC **CTGTGCACCCCCAGCCGGGCCCTGCTGACCCGCCG**
GTGACTGACTCGAGATCG-3'

Restriction sites HindIII, XmaI and XhoI are underlined. The red highlighted region corresponds to IgK sequence from pDisplay vector and is fused to the HA tag (violet) followed by the thrombin cleavage site (green) (HindIII-XmaI). This sequence was synthesized by GeneArt® Gene Synthesis (Life technologies™). The rest of the construct (grey and yellow highlight) was generated by PCR (XmaI-XhoI) using the following primers:

Forward: 5'-TTACCCGGGCTCCCATCTCTCTGCATGCTT-3'

Reverse: 5'-CGATCTCGAGTCAGTCACCGGCCGGTCAGCAGGGCGGCCCGGCTGGGGGT
 GCACAGGGCAGCAGACCTCTCAAAGTTGAGATGTGTCTTACT-3'

Peptides and loops

LCMV glycoprotein derived peptides, LCMVGP₃₃₋₄₁ (KAVYNFATC), LCMVGP₂₇₆₋₂₈₆ (SGVENPGGYCL), and LCMVNP₃₉₆₋₄₀₄ (CAIFQPQNGQFI), the cysteine residue was artificially added to this peptide to allow further conjugation) and the ovalbumine peptide (CSIINFEKL, the cysteine residue was artificially added to this peptide to allow further conjugation) were obtained from PolyPeptide group (France).

The MACV GP1 loops 3 and 10 were synthesized by the Laboratory of Therapeutic Proteins and Peptides-LPPT at the EPFL.

Cell culture

HEK 293 T cells were grown and maintained in culture in complete Dulbecco's Modified Eagle Medium (DMEM) medium (DMEM-GlutaMAX™, 10 % fetal calf serum (FCS), 1% penicillin/streptomycin).

Antigen production

In house production:

HEK 293 T cells were grown in T75 flasks to 80-90 % confluence. One day before transfection 15 cm cell culture dishes were pre-treated with poly-lysine (~ 5 ml/ plate, 100 µg/ml in distilled water, (Poly-L-lysine hydrobromide, 50m/ml)) for 30 minutes. Plates were washed at least 3 times with distilled water. Cells were trypsinized (around 300 µl of TRIPLEX) briefly, plated in a 15 cm dish (30 ml/well) and then incubated for 16-20 hours at 37 °C with 5% CO². Cells were transfected by calcium phosphate with the appropriated constructs and incubated at 37 °C with 5% CO² for 6-12h. Then the transfection mix was removed and cells washed once with a serum free medium (293 SFM II). Complete serum free medium (293 SFM II, 2 mM glutamine, 10 mM HEPES) was added (20 ml/15 cm dish) and cells were incubated at 37°C, 5 % CO². After 48h, the supernatants were harvested. The proteins were either extracted by methanol/chloroform precipitation (expression level checking) or directly purified from 0.22µm or 0.45µm filtered cell supernatants by affinity chromatography using an anti-HA column.

Out-source production:

As a high amount of purified proteins were required for our experiments. The in house produced plasmids containing the constructs of interest were further amplified by a local company (Fasteris SA, Geneva, Switzerland). The plasmid DNA coding for each generated construct was then provided to the EPFL protein expression core facility managed by Dr. David Hacker for high scale protein production [177].

Affinity chromatography purification

All antigens were purified using an anti-HA affinity matrix (Clone 3F10, Roche). Briefly, the affinity matrix was washed with wash buffer (20 mM Tris pH 7.5, 0.1 M NaCl, 0.1 mM EDTA, 0.05% of Tween 20 (Applichem)), centrifuged 4 min at 2000 rpm and loaded into a column (0.5-1.0 ml final volume). Then 10 column bed volumes of equilibration buffer were added (20 mM Tris pH 7.5, 0.1 M NaCl, 0.1 mM EDTA). The previously prepared protein supernatants (0.22 or 0.45 µm filtered) were loaded into the affinity matrix column. The matrix was washed with a minimum of 20 column bed-volumes of wash buffer at +15 to +25°C to remove nonspecifically bound protein. Affinity matrix column elution was performed by adding 3 times 1 bed-volume of Elution buffer (1mg/ml of HA peptide in equilibration buffer) and incubating it for 15 min at 37°C.

Immunoblotting

Protein expression levels and purification yields were checked by Western blotting. Briefly, proteins were mixed with either non-reducing or reducing (100 mM Dithiothreitol) SDS-PAGE sample buffer (31.1mM Tris-HCl pH 6.8, 10% glycerol, 1% sodium dodecyl sulphate, 2.5 %) and loaded into 7.5% or 12% polyacrylamide gels respectively, followed by either Coomassie blue staining or transfer of the proteins onto a nitrocellulose membrane (Whatman®). All proteins were detected with anti-HA (3F10) or anti-FLAG (M2) primary antibodies followed by polyclonal anti-rat or anti-mouse horseradish peroxidase (HRP) conjugated, respectively. Proteins were revealed by further incubation with HRP LiteAblot® chemiluminescent substrate (Euroclone) and transferred on an X-ray film.

Thrombin cleavage of the HA-tag

After affinity matrix purification the HA-tagged constructs were buffer exchanged by overnight (O/N) dialysis to thrombin cleavage buffer (20 mM Tris-HCl pH 8.4, 150mM NaCl, 2.5 mM CaCl₂). Thrombin-agarose (Novagen®), 3 units/mg of protein, was added to the buffer exchanged protein and incubated O/N at RT (23-25°) under mild shaking. The thrombin-agarose was then removed by centrifugation using a spin column (Novagen®) provided by the manufacturer.

Assessing the aldehyde tag reactivity

The aldehyde-tagged protein was reacted with 300µM aminoxy-biotin for 2h at RT in 100 µM Mes (pH 5.5) [132]. Protein loading was determined by Coomassie blue staining. Western blots were probed with streptavidin-HRP (1:1000 dilution; Millipore). Proteins were revealed by further incubation with HRP LiteAblot® chemiluminescent substrate (Euroclone) and transferred on an X-ray film.

Conjugation via reactive thiol residues

Conjugation of MACVΔGP1 onto the nanoparticles was carried by reducing the protein with TCEP beads in a 5:1 ratio (v/v) at 37°C for 1h in 50 mM HEPES, 50mM NaCl pH 7.4. The reduced protein was purified and mixed immediately with pyridyl disulfide functionalized nanoparticles, and left to react for 2 hours at RT. Conjugated nanoparticles were purified by size exclusion chromatography using a Sepharose CL6B resin and 50 mM HEPES, 50 mM NaCl pH7.4 as eluent. The conjugation efficiency was analyzed by taking the area under the curve of an elution profile detected by fluorescamine. Protein in the particle fraction was confirmed by Western blotting using the anti-HA antibody.

Conjugation via reactive hydrazine or oxyamine

A solution of 500 μ L containing 35mg/ml of NPs holding NH₂ terminal groups in 0.1M sodium phosphate buffer, 50mM NaCl, pH 8.0 was mixed with 2mg of HyNIC reagent (Solulink™) in 50 μ L of DMF. After 16h, the HyNIC activated NPs were transferred into a dialysis membrane of 5KDa MW and dialyzed extensively against 0.1 sodium phosphate buffer pH 6.0. (conjugation buffer). Finally, NPs were mixed with a 500 μ L of solution of Ald-MACV-GP1 (1mg/ml) in conjugation buffer, and let to react during 2 days at 4°C. The protein-NPs conjugates were purified by size exclusion chromatography on a Sepharose CL6B resin using a solution of 0.9% NaCl as eluent. The conjugation efficiency was analyzed by taking the area under the curve of an elution profile detected by fluorescamine.

Receptor binding assay

MACV Δ GP1 binding to hTfr1 was verified by adding the protein at various concentrations to Chinese hamster ovary subclone K1 (CHO-K1) cells transiently transfected with hTfr1. Binding was measured by flow cytometry on a CyAn™ ADP Analyzer (Beckman Coulter). MACV Δ GP1 was detected by a polyclonal rabbit anti-FLAG antibody, followed by a secondary anti-rabbit antibody conjugated with Alexafluor 647. Only live (Live/Dead violet, Invitrogen), hTfr1+ (PE-anti hTfr1 clone M-A712) cells were analyzed by taking the normalized geometric mean of the FL8 channel, which reflects the AF647 fluorescence intensity. Analysis was done using FlowJo (version 7.5.5, Tree Star) software.

Humoral responses

Groups of five age- and sex-matched C57/Bl6 mice were immunized intradermally on their hind legs as described previously in the part 1 of project 2 results section. Blood draws were performed at defined time points. IgG antibody titers were measured by ELISA using purified MACV Δ GP1 immobilized in microtiter plates (Greiner bio-one) and IgG class specific secondary antibodies HRP coupled.

T cell responses

Six age- and sex-matched C57/Bl6 mice were vaccinated intradermally on their hind legs as described previously in the part 2 of project 2 results section. At day 21 mice were sacrificed and spleens collected. T cell responses were measure by detecting IFN- γ production by splenic epitope-specific CD8 T cells by ELISpot and intracellular staining followed by flow cytometry. In brief, 10⁵ splenocytes were plated in 96 well microplates and restimulated with

the corresponding peptide. The ELISpot was developed according to the manufacturer's instructions (ELISPOT READY-SET-GO!), eBioscience). For intracellular cytokine staining, splenocytes were restimulated *in vitro* with respective peptides for 6h and brefeldin A was added for the last 3h of incubation. Splenocytes were surface stained to identify CD8 T cells with CD3 ϵ and CD8 α , and intracellular stained for IFN- γ followed by analysis by flow cytometry. Controls were restimulated with PMA/ionomycin.

Neutralization assay

MACVGPC pseudotyped virus carrying the reporter gene luciferase were pre-incubated with experimental sera from mice for 45 min. and then added at 40x dilution to A549 cells for 48h. Luminescence was revealed by removing the cell medium and adding 100 μ l/well of Bright-GloTM (Promega). The luminescent signal was then measured with a TriStar LB 941 luminometer (Berthold). Luciferase luminescence was normalized to wells infected with pseudotyped virus only and wells which saw no virus.

CelluspotsTM

CelluspotsTM slides were blocked with PBS-Tween 0.02% containing and 5% milk for 1h, followed by 2h incubation at room temperature with mice sera (1/200 dilution in PBS-Tween 0.02% containing 5% milk). Slides were further washed 3 times 5 min. with PBS-Tween 0.02% and incubated with an anti-mouse HRP-conjugated antibody (diluted 1/2000 in PBS-Tween 0.02%, and 5% milk) for 1h. Finally slides were washed 3 times 5 min. with Tween 0.02% containing and 5% milk. The epitopes were revealed by further incubation with HRP LiteAblo[®] chemiluminescent substrate (Euroclone) and transferred on an X-ray film.

Detection of Abs binding to native MACVGP

Sera from selected mice from each vaccination group were incubated for 1 hour at 4°C at 1/50 dilution with MACGPC, DGE (dystroglycan HA-tagged, positive control) and pCAGGS (empty vector, negative control) transfected HEK 293 T cells. Cells were washed twice with PBS/1%FCS. Secondary antibody rabbit anti-mouse-phycoerythrin labeled was added for 45 min at 4 °C. Cells were washed twice again and responses were measured by flow cytometry.

REFERENCES

1. EPFL (2011) Laboratory of Lymphatic and Cancer Bioengineering LLCB, Biomaterials design for immunomodulation.
2. Burri DJ, Palma JR, Kunz S, Pasquato A (2012) Envelope Glycoprotein of Arenaviruses. *Viruses* 4: 2162-2181.
3. Kourtis IC, Hirosue S, de Titta A, Kontos S, Stegmann T, et al. (2013) Peripherally Administered Nanoparticles Target Monocytic Myeloid Cells, Secondary Lymphoid Organs and Tumors in Mice. *PLoS ONE* 8: e61646.
4. Moraz M-L, Kunz S (2011) Pathogenesis of arenavirus hemorrhagic fevers. *Expert Review of Anti-infective Therapy* 9: 49-59.
5. Reddy ST, van der Vlies AJ, Simeoni E, Angeli V, Randolph GJ, et al. (2007) Exploiting lymphatic transport and complement activation in nanoparticle vaccines. *Nat Biotechnol* 25: 1159-1164.
6. Buchmeier MJ, de la Torre JC, Peters CJ (2007) Arenaviridae: the viruses and their replication. In: Knipe DL, Howley PM, editors. *Fields Virology*. 4th ed. Philadelphia: Lippincott-Raven. pp. p. 1791-1828.
7. Zapata J, Salvato M (2013) Arenavirus Variations Due to Host-Specific Adaptation. *Viruses* 5: 241-278.
8. Emonet SF, de la Torre JC, Domingo E, Sevilla N (2009) Arenavirus genetic diversity and its biological implications. *Infection, Genetics and Evolution* 9: 417-429.
9. de la Torre JC (2009) Molecular and cell biology of the prototypic arenavirus LCMV: implications for understanding and combating hemorrhagic fever arenaviruses. *Ann N Y Acad Sci* 1171 Suppl 1: E57-64.
10. Rojek JM, Kunz S (2008) Cell entry by human pathogenic arenaviruses. *Cell Microbiol* 10: 828-835.
11. Cao W, Henry MD, Borrow P, Yamada H, Elder JH, et al. (1998) Identification of α -Dystroglycan as a Receptor for Lymphocytic Choriomeningitis Virus and Lassa Fever Virus. *Science* 282: 2079-2081.
12. Radoshitzky SR, Longobardi LE, Kuhn JH, Retterer C, Dong L, et al. (2011) Machupo Virus Glycoprotein Determinants for Human Transferrin Receptor 1 Binding and Cell Entry. *PLoS ONE* 6: e21398.
13. Shimojima M, Stroher U, Ebihara H, Feldmann H, Kawaoka Y (2012) Identification of cell surface molecules involved in dystroglycan-independent lassa virus cell entry. *J Virol* 86: 2067-2078.
14. Rojek JM, Sanchez AB, Nguyen NT, de la Torre JC, Kunz S (2008) Different mechanisms of cell entry by human-pathogenic Old World and New World arenaviruses. *J Virol* 82: 7677-7687.
15. Pasqual G, Rojek JM, Masin M, Chatton JY, Kunz S (2011) Old world arenaviruses enter the host cell via the multivesicular body and depend on the endosomal sorting complex required for transport. *PLoS Pathog* 7: e1002232.
16. Martinez MG, Cordo SM, Candurra NA (2007) Characterization of Junin arenavirus cell entry. *J Gen Virol* 88: 1776-1784.
17. Perez M, de la Torre JC (2003) Characterization of the genomic promoter of the prototypic arenavirus lymphocytic choriomeningitis virus. *J Virol* 77: 1184-1194.
18. Baird NL, York J, Nunberg JH (2012) Arenavirus infection induces discrete cytosolic structures for RNA replication. *J Virol* 86: 11301-11310.
19. Perez M, Craven RC, de la Torre JC (2003) The small RING finger protein Z drives arenavirus budding: implications for antiviral strategies. *Proc Natl Acad Sci U S A* 100: 12978-12983.

20. Strecker T, Eichler R, Meulen J, Weissenhorn W, Dieter Klenk H, et al. (2003) Lassa virus Z protein is a matrix protein and sufficient for the release of virus-like particles [corrected]. *J Virol* 77: 10700-10705.
21. Urata S, Noda T, Kawaoka Y, Yokosawa H, Yasuda J (2006) Cellular factors required for Lassa virus budding. *J Virol* 80: 4191-4195.
22. Capul AA, Perez M, Burke E, Kunz S, Buchmeier MJ, et al. (2007) Arenavirus Z-glycoprotein association requires Z myristoylation but not functional RING or late domains. *J Virol* 81: 9451-9460.
23. McCormick JB, Fisher-Hoch SP (2002) Lassa fever. *Curr Top Microbiol Immunol* 262: 75-109.
24. Peters CJ (2002) Human infection with arenaviruses in the Americas. *Current topics in microbiology and immunology* 262: 65-74.
25. McCormick JB, Webb PA, Krebs JW, Johnson KM, Smith ES (1987) A prospective study of the epidemiology and ecology of Lassa fever. *J Infect Dis* 155: 437-444.
26. Weissenbacher MC, Laguens RP, Coto CE (1987) Argentine hemorrhagic fever. *Curr Top Microbiol Immunol* 134: 79-116.
27. Yun NE, Walker DH (2012) Pathogenesis of Lassa Fever. *Viruses* 4: 2031-2048.
28. Grant A, Seregin A, Huang C, Kolokoltsova O, Brasier A, et al. (2012) Junín Virus Pathogenesis and Virus Replication. *Viruses* 4: 2317-2339.
29. Baize S, Kaplon J, Faure C, Pannetier D, Georges-Courbot M-C, et al. (2004) Lassa Virus Infection of Human Dendritic Cells and Macrophages Is Productive but Fails to Activate Cells. *The Journal of Immunology* 172: 2861-2869.
30. Hawiger D, Inaba K, Dorsett Y, Guo M, Mahnke K, et al. (2001) Dendritic Cells Induce Peripheral T Cell Unresponsiveness under Steady State Conditions in Vivo. *The Journal of Experimental Medicine* 194: 769-780.
31. Dhodapkar MV, Steinman RM, Krasovsky J, Munz C, Bhardwaj N (2001) Antigen-Specific Inhibition of Effector T Cell Function in Humans after Injection of Immature Dendritic Cells. *The Journal of Experimental Medicine* 193: 233-238.
32. Pannetier D, Reynard S, Russier M, Journeaux A, Tordo N, et al. (2011) Human Dendritic Cells Infected with the Nonpathogenic Mopeia Virus Induce Stronger T-Cell Responses than Those Infected with Lassa Virus. *J Virol* 85: 8293-8306.
33. Le Bon A, Tough DF (2002) Links between innate and adaptive immunity via type I interferon. *Current Opinion in Immunology* 14: 432-436.
34. Baize S, Marianneau P, Loth P, Reynard S, Journeaux A, et al. (2009) Early and strong immune responses are associated with control of viral replication and recovery in lassa virus-infected cynomolgus monkeys. *J Virol* 83: 5890-5903.
35. Walker DH, McCormick JB, Johnson KM, Webb PA, Komba-Kono G, et al. (1982) Pathologic and virologic study of fatal Lassa fever in man. *Am J Pathol* 107: 349-356.
36. Harrison LH, Halsey NA, McKee KT, Jr., Peters CJ, Barrera Oro JG, et al. (1999) Clinical case definitions for Argentine hemorrhagic fever. *Clin Infect Dis* 28: 1091-1094.
37. Geisbert TW, Jahrling PB (2004) Exotic emerging viral diseases: progress and challenges. *Nat Med* 10: S110-121.
38. Kunz S (2009) The role of the vascular endothelium in arenavirus haemorrhagic fevers. *Thromb Haemost* 102: 1024-1029.
39. Fischer SA, Graham MB, Kuehnert MJ, Kotton CN, Srinivasan A, et al. (2006) Transmission of lymphocytic choriomeningitis virus by organ transplantation. *N Engl J Med* 354: 2235-2249.
40. Palacios G, Druce J, Du L, Tran T, Birch C, et al. (2008) A new arenavirus in a cluster of fatal transplant-associated diseases. *N Engl J Med* 358: 991-998.

41. Johnson KM, McCormick JB, Webb PA, Smith ES, Elliott LH, et al. (1987) Clinical virology of Lassa fever in hospitalized patients. *J Infect Dis* 155: 456-464.
42. Russier M, Pannetier D, Baize S (2012) Immune Responses and Lassa Virus Infection. *Viruses* 4: 2766-2785.
43. Hayes M, Salvato M (2012) Arenavirus Evasion of Host Anti-Viral Responses. *Viruses* 4: 2182-2196.
44. Botten J, Sidney J, Mothé BR, Peters B, Sette A, et al. (2010) Coverage of Related Pathogenic Species by Multivalent and Cross-Protective Vaccine Design: Arenaviruses as a Model System. *Microbiology and Molecular Biology Reviews* 74: 157-170.
45. Baize S, Marianneau P, Loth P, Reynard S, Journeaux A, et al. (2009) Early and Strong Immune Responses Are Associated with Control of Viral Replication and Recovery in Lassa Virus-Infected Cynomolgus Monkeys. *Journal of Virology* 83: 5890-5903.
46. McCormick JB, King IJ, Webb PA, Scribner CL, Craven RB, et al. (1986) Lassa fever. Effective therapy with ribavirin. *N Engl J Med* 314: 20-26.
47. Jahrling PB (1983) Protection of Lassa virus-infected guinea pigs with Lassa-immune plasma of guinea pig, primate, and human origin. *J Med Virol* 12: 93-102.
48. Jahrling PB, Peters CJ (1984) Passive antibody therapy of Lassa fever in cynomolgus monkeys: importance of neutralizing antibody and Lassa virus strain. *Infect Immun* 44: 528-533.
49. Enria DA, Barrera Oro JG (2002) Junin virus vaccines. *Curr Top Microbiol Immunol* 263: 239-261.
50. Trombetta ES, Mellman I (2005) Cell biology of antigen processing in vitro and in vivo. *Annu Rev Immunol* 23: 975-1028.
51. Burgdorf S, Kurts C (2008) Endocytosis mechanisms and the cell biology of antigen presentation. *Curr Opin Immunol* 20: 89-95.
52. van Kooyk Y (2008) C-type lectins on dendritic cells: key modulators for the induction of immune responses. *Biochem Soc Trans* 36: 1478-1481.
53. van Kooyk Y, Geijtenbeek TB (2003) DC-SIGN: escape mechanism for pathogens. *Nat Rev Immunol* 3: 697-709.
54. Geijtenbeek TB, Kwon DS, Torensma R, van Vliet SJ, van Duijnhoven GC, et al. (2000) DC-SIGN, a dendritic cell-specific HIV-1-binding protein that enhances trans-infection of T cells. *Cell* 100: 587-597.
55. Kwon DS, Gregorio G, Bitton N, Hendrickson WA, Littman DR (2002) DC-SIGN-mediated internalization of HIV is required for trans-enhancement of T cell infection. *Immunity* 16: 135-144.
56. Alvarez CP, Lasala F, Carrillo J, Muniz O, Corbi AL, et al. (2002) C-type lectins DC-SIGN and L-SIGN mediate cellular entry by Ebola virus in cis and in trans. *J Virol* 76: 6841-6844.
57. Simmons G, Reeves JD, Grogan CC, Vandenberghe LH, Baribaud F, et al. (2003) DC-SIGN and DC-SIGNR bind ebola glycoproteins and enhance infection of macrophages and endothelial cells. *Virology* 305: 115-123.
58. Jeffers SA, Tusell SM, Gillim-Ross L, Hemmila EM, Achenbach JE, et al. (2004) CD209L (L-SIGN) is a receptor for severe acute respiratory syndrome coronavirus. *Proc Natl Acad Sci U S A* 101: 15748-15753.
59. Tassaneeritthep B, Burgess TH, Granelli-Piperno A, Trumpfheller C, Finke J, et al. (2003) DC-SIGN (CD209) mediates dengue virus infection of human dendritic cells. *J Exp Med* 197: 823-829.
60. Navarro-Sanchez E, Altmeyer R, Amara A, Schwartz O, Fieschi F, et al. (2003) Dendritic-cell-specific ICAM3-grabbing non-integrin is essential for the productive infection of

- human dendritic cells by mosquito-cell-derived dengue viruses. *EMBO Rep* 4: 723-728.
61. Davis CW, Nguyen HY, Hanna SL, Sanchez MD, Doms RW, et al. (2006) West Nile virus discriminates between DC-SIGN and DC-SIGNR for cellular attachment and infection. *J Virol* 80: 1290-1301.
 62. Lozach PY, Kuhbacher A, Meier R, Mancini R, Bitto D, et al. (2011) DC-SIGN as a receptor for phleboviruses. *Cell Host Microbe* 10: 75-88.
 63. Parker WB (2005) Metabolism and antiviral activity of ribavirin. *Virus Res* 107: 165-171.
 64. Kilgore PE, Peters CJ, Mills JN, Rollin PE, Armstrong L, et al. (1995) Prospects for the control of Bolivian hemorrhagic fever. *Emerg Infect Dis* 1: 97-100.
 65. Andrei G, De Clercq E (1993) Molecular approaches for the treatment of hemorrhagic fever virus infections. *Antiviral Res* 22: 45-75.
 66. Andrei G, De Clercq E (1990) Inhibitory effect of selected antiviral compounds on arenavirus replication in vitro. *Antiviral Res* 14: 287-299.
 67. Candurra NA, Maskin L, Damonte EB (1996) Inhibition of arenavirus multiplication in vitro by phenothiazines. *Antiviral Res* 31: 149-158.
 68. Wachsman MB, Lopez EM, Ramirez JA, Galagovsky LR, Coto CE (2000) Antiviral effect of brassinosteroids against herpes virus and arenaviruses. *Antivir Chem Chemother* 11: 71-77.
 69. Cordo SM, Candurra NA, Damonte EB (1999) Myristic acid analogs are inhibitors of Junin virus replication. *Microbes Infect* 1: 609-614.
 70. Garcia CC, Candurra NA, Damonte EB (2000) Antiviral and virucidal activities against arenaviruses of zinc-finger active compounds. *Antivir Chem Chemother* 11: 231-237.
 71. Garcia CC, Djavani M, Topisirovic I, Borden KL, Salvato MS, et al. (2006) Arenavirus Z protein as an antiviral target: virus inactivation and protein oligomerization by zinc finger-reactive compounds. *J Gen Virol* 87: 1217-1228.
 72. Garcia CC, Topisirovic I, Djavani M, Borden KL, Damonte EB, et al. (2010) An antiviral disulfide compound blocks interaction between arenavirus Z protein and cellular promyelocytic leukemia protein. *Biochem Biophys Res Commun* 393: 625-630.
 73. Lee AM, Rojek JM, Gundersen A, Stroher U, Juteau JM, et al. (2008) Inhibition of cellular entry of lymphocytic choriomeningitis virus by amphipathic DNA polymers. *Virology* 372: 107-117.
 74. Bolken TC, Laquerre S, Zhang Y, Bailey TR, Pevear DC, et al. (2006) Identification and characterization of potent small molecule inhibitor of hemorrhagic fever New World arenaviruses. *Antiviral Res* 69: 86-97. Epub 2005 Nov 2028.
 75. Lee AM, Rojek JM, Spiropoulou CF, Gundersen AT, Jin W, et al. (2008) Unique small molecule entry inhibitors of hemorrhagic fever arenaviruses. *J Biol Chem* 283: 18734-18742.
 76. Larson RA, Dai D, Hosack VT, Tan Y, Bolken TC, et al. (2008) Identification of a broad-spectrum arenavirus entry inhibitor. *J Virol* 82: 10768-10775.
 77. Lenz O, ter Meulen J, Klenk HD, Seidah NG, Garten W (2001) The Lassa virus glycoprotein precursor GP-C is proteolytically processed by subtilase SKI-1/S1P. *Proc Natl Acad Sci U S A* 98: 12701-12705.
 78. Rojek JM, Lee AM, Nguyen N, Spiropoulou CF, Kunz S (2008) Site 1 protease is required for proteolytic processing of the glycoproteins of the South American hemorrhagic fever viruses Junin, Machupo, and Guanarito. *J Virol* 82: 6045-6051.
 79. Beyer WR, Popplau D, Garten W, von Laer D, Lenz O (2003) Endoproteolytic processing of the lymphocytic choriomeningitis virus glycoprotein by the subtilase SKI-1/S1P. *J Virol* 77: 2866-2872.

80. Kunz S, Edelmann KH, de la Torre JC, Gorney R, Oldstone MB (2003) Mechanisms for lymphocytic choriomeningitis virus glycoprotein cleavage, transport, and incorporation into virions. *Virology* 314: 168-178.
81. Rojek JM, Pasqual G, Sanchez AB, Nguyen NT, de la Torre JC, et al. (2010) Targeting the proteolytic processing of the viral glycoprotein precursor is a promising novel antiviral strategy against arenaviruses. *J Virol* 84: 573-584.
82. Maisa A, Stroher U, Klenk HD, Garten W, Strecker T (2009) Inhibition of Lassa Virus Glycoprotein Cleavage and Multicycle Replication by Site 1 Protease-Adapted alpha(1)-Antitrypsin Variants. *PLoS Negl Trop Dis* 3: e446.
83. Pasquato A, Rochat C, Burri DJ, Pasqual G, de la Torre JC, et al. (2012) Evaluation of the anti-arenaviral activity of the subtilisin kexin isozyme-1/site-1 protease inhibitor PF-429242. *Virology* 423: 14-22.
84. Urata S, Yun N, Pasquato A, Paessler S, Kunz S, et al. (2011) Antiviral activity of a small-molecule inhibitor of arenavirus glycoprotein processing by the cellular site 1 protease. *J Virol* 85: 795-803.
85. Lukashevich I (2012) Advanced Vaccine Candidates for Lassa Fever. *Viruses* 4: 2514-2557.
86. Botten J, Whitton JL, Barrowman P, Sidney J, Whitmire JK, et al. (2010) A Multivalent Vaccination Strategy for the Prevention of Old World Arenavirus Infection in Humans. *Journal of Virology* 84: 9947-9956.
87. McCormick JB, Mitchell SW, Kiley MP, Ruo S, Fisher-Hoch SP (1992) Inactivated Lassa virus elicits a non protective immune response in rhesus monkeys. *Journal of Medical Virology* 37: 1-7.
88. Fisher-Hoch SP, Hutwagner L, Brown B, McCormick JB (2000) Effective Vaccine for Lassa Fever. *Journal of Virology* 74: 6777-6783.
89. Morrison HG, Bauer SP, Lange JV, Esposito JI, McCormick JB, et al. (1989) Protection of guinea pigs from lassa fever by vaccinia virus recombinants expressing the nucleoprotein or the envelope glycoproteins of lassa virus. *Virology* 171: 179-188.
90. Geisbert TW, Jones S, Fritz EA, Shurtleff AC, Geisbert JB, et al. (2005) Development of a New Vaccine for the Prevention of Lassa Fever. *PLoS Med* 2: e183.
91. Jiang X, Dalebout TJ, Bredenbeek PJ, Carrion Jr R, Brasky K, et al. (2011) Yellow fever 17D-vectored vaccines expressing Lassa virus GP1 and GP2 glycoproteins provide protection against fatal disease in guinea pigs. *Vaccine* 29: 1248-1257.
92. Bredenbeek PJ, Molenkamp R, Spaan WJM, Deubel V, Marianneau P, et al. (2006) A recombinant Yellow Fever 17D vaccine expressing Lassa virus glycoproteins. *Virology* 345: 299-304.
93. Lukashevich IS, Patterson J, Carrion R, Moshkoff D, Ticer A, et al. (2005) A Live Attenuated Vaccine for Lassa Fever Made by Reassortment of Lassa and Mopeia Viruses. *Journal of Virology* 79: 13934-13942.
94. Carrion Jr R, Patterson JL, Johnson C, Gonzales M, Moreira CR, et al. (2007) A ML29 reassortant virus protects guinea pigs against a distantly related Nigerian strain of Lassa virus and can provide sterilizing immunity. *Vaccine* 25: 4093-4102.
95. Lukashevich IS, Carrion Jr R, Salvato MS, Mansfield K, Brasky K, et al. (2008) Safety, immunogenicity, and efficacy of the ML29 reassortant vaccine for Lassa fever in small non-human primates. *Vaccine* 26: 5246-5254.
96. Pushko P, Geisbert J, Parker M, Jahrling P, Smith J (2001) Individual and Bivalent Vaccines Based on Alphavirus Replicons Protect Guinea Pigs against Infection with Lassa and Ebola Viruses. *Journal of Virology* 75: 11677-11685.

97. Branco L, Grove J, Geske F, Boisen M, Muncy I, et al. (2010) Lassa virus-like particles displaying all major immunological determinants as a vaccine candidate for Lassa hemorrhagic fever. *Virology Journal* 7: 279.
98. Rodriguez-Carreno MP, Nelson MS, Botten J, Smith-Nixon K, Buchmeier MJ, et al. (2005) Evaluating the immunogenicity and protective efficacy of a DNA vaccine encoding Lassa virus nucleoprotein. *Virology* 335: 87-98.
99. Djavani M, Yin C, Xia L, Lukashevich IS, Pauza CD, et al. (2000) Murine immune responses to mucosally delivered Salmonella expressing Lassa fever virus nucleoprotein. *Vaccine* 18: 1543-1554.
100. Guy B, Guirakhoo F, Barban V, Higgs S, Monath TP, et al. (2010) Preclinical and clinical development of YFV 17D-based chimeric vaccines against dengue, West Nile and Japanese encephalitis viruses. *Vaccine* 28: 632-649.
101. Maiztegui JI, McKee KT, Oro JGB, Harrison LH, Gibbs PH, et al. (1998) Protective Efficacy of a Live Attenuated Vaccine against Argentine Hemorrhagic Fever. *Journal of Infectious Diseases* 177: 277-283.
102. Rehor A, Schmoekel H, Tirelli N, Hubbell JA (2008) Functionalization of polysulfide nanoparticles and their performance as circulating carriers. *Biomaterials* 29: 1958-1966.
103. Reddy ST, Rehor A, Schmoekel HG, Hubbell JA, Swartz MA (2006) In vivo targeting of dendritic cells in lymph nodes with poly(propylene sulfide) nanoparticles. *J Control Release* 112: 26-34.
104. Hirosue S, Kourtis IC, van der Vlies AJ, Hubbell JA, Swartz MA (2010) Antigen delivery to dendritic cells by poly(propylene sulfide) nanoparticles with disulfide conjugated peptides: Cross-presentation and T cell activation. *Vaccine* 28: 7897-7906.
105. Hajishengallis G, Lambris JD (2010) Crosstalk pathways between Toll-like receptors and the complement system. *Trends Immunol* 31: 154-163.
106. Thomas SN, van der Vlies AJ, O'Neil CP, Reddy ST, Yu SS, et al. (2011) Engineering complement activation on polypropylene sulfide vaccine nanoparticles. *Biomaterials* 32: 2194-2203.
107. Carroll MC (2004) The complement system in regulation of adaptive immunity. *Nat Immunol* 5: 981-986.
108. Carroll MC (2004) The complement system in B cell regulation. *Mol Immunol* 41: 141-146.
109. Stano A, van der Vlies AJ, Martino MM, Swartz MA, Hubbell JA, et al. (2011) PPS nanoparticles as versatile delivery system to induce systemic and broad mucosal immunity after intranasal administration. *Vaccine* 29: 804-812.
110. Ballester M, Nembrini C, Dhar N, de Titta A, de Piano C, et al. (2011) Nanoparticle conjugation and pulmonary delivery enhance the protective efficacy of Ag85B and CpG against tuberculosis. *Vaccine* 29: 6959-6966.
111. Mintern JD, Bedoui S, Davey GM, Moffat JM, Doherty PC, et al. (2009) Transience of MHC Class I-restricted antigen presentation after influenza A virus infection. *Proceedings of the National Academy of Sciences of the United States of America* 106: 6724-6729.
112. Lukashevich IS (2012) Advanced vaccine candidates for Lassa fever. *Viruses* 4: 2514-2557.
113. Parren PW, Burton DR (2001) The antiviral activity of antibodies in vitro and in vivo. *Adv Immunol* 77: 195-262.
114. Burton DR, Saphire EO, Parren PW (2001) A model for neutralization of viruses based on antibody coating of the virion surface. *Curr Top Microbiol Immunol* 260: 109-143.

115. Leifer E, Gocke DJ, Bourne H (1970) Lassa fever, a new virus disease of man from West Africa. II. Report of a laboratory-acquired infection treated with plasma from a person recently recovered from the disease. *Am J Trop Med Hyg* 19: 677-679.
116. Monath TP, Maher M, Casals J, Kissling RE, Cacciapuoti A (1974) Lassa fever in the Eastern Province of Sierra Leone, 1970-1972. II. Clinical observations and virological studies on selected hospital cases. *Am J Trop Med Hyg* 23: 1140-1149.
117. Whitton JL (2002) Designing arenaviral vaccines. *Curr Top Microbiol Immunol* 263: 221-238.
118. Peters CJ (2002) Human infection with arenaviruses in the Americas. *Curr Top Microbiol Immunol* 262: 65-74.
119. Enria DA, Briggiler AM, Sanchez Z (2008) Treatment of Argentine hemorrhagic fever. *Antiviral Res* 78: 132-139.
120. Fisher-Hoch SP, McCormick JB (2004) Lassa fever vaccine. *Expert Rev Vaccines* 3: 189-197.
121. Parren PW, Burton DR (2001) The antiviral activity of antibodies in vitro and in vivo. *Advances in immunology* 77: 195-262.
122. Karlsson Hedestam GB, Fouchier RA, Phogat S, Burton DR, Sodroski J, et al. (2008) The challenges of eliciting neutralizing antibodies to HIV-1 and to influenza virus. *Nature reviews Microbiology* 6: 143-155.
123. Igonet S, Vaney MC, Vohnrein C, Bricogne G, Stura EA, et al. (2011) X-ray structure of the arenavirus glycoprotein GP2 in its postfusion hairpin conformation. *Proc Natl Acad Sci U S A* 108: 19967-19972.
124. Bowden TA, Crispin M, Graham SC, Harvey DJ, Grimes JM, et al. (2009) Unusual molecular architecture of the machupo virus attachment glycoprotein. *J Virol* 83: 8259-8265.
125. Abraham J, Corbett KD, Farzan M, Choe H, Harrison SC (2010) Structural basis for receptor recognition by New World hemorrhagic fever arenaviruses. *Nat Struct Mol Biol* 17: 438-444.
126. Sanchez A, Pifat DY, Kenyon RH, Peters CJ, McCormick JB, et al. (1989) Junin virus monoclonal antibodies: characterization and cross-reactivity with other arenaviruses. *J Gen Virol* 70: 1125-1132.
127. Borrow P, Oldstone MB (1992) Characterization of lymphocytic choriomeningitis virus-binding protein(s): a candidate cellular receptor for the virus. *J Virol* 66: 7270-7281.
128. Cresta B, Padula P, de Martinez Segovia M (1980) Biological properties of Junin virus proteins. I. Identification of the immunogenic glycoprotein. *Intervirology* 13: 284-288.
129. van der Vlies AJ, O'Neil CP, Hasegawa U, Hammond N, Hubbell JA (2010) Synthesis of pyridyl disulfide-functionalized nanoparticles for conjugating thiol-containing small molecules, peptides, and proteins. *Bioconjug Chem* 21: 653-662.
130. Abraham J, Corbett KD, Farzan M, Choe H, Harrison SC (2010) Structural basis for receptor recognition by New World hemorrhagic fever arenaviruses. *Nat Struct Mol Biol* 17: 438-444.
131. Rojek JM, Spiropoulou CF, Kunz S (2006) Characterization of the cellular receptors for the South American hemorrhagic fever viruses Junin, Guanarito, and Machupo. *Virology* 349: 476-491. Epub 2006 Mar 2030.
132. Wu P, Shui W, Carlson BL, Hu N, Rabuka D, et al. (2009) Site-specific chemical modification of recombinant proteins produced in mammalian cells by using the genetically encoded aldehyde tag. *Proceedings of the National Academy of Sciences* 106: 3000-3005.

133. Rabuka D, Rush JS, deHart GW, Wu P, Bertozzi CR (2012) Site-specific chemical protein conjugation using genetically encoded aldehyde tags. *Nat Protocols* 7: 1052-1067.
134. Hangartner L, Zinkernagel RM, Hengartner H (2006) Antiviral antibody responses: the two extremes of a wide spectrum. *Nat Rev Immunol* 6: 231-243.
135. Zinkernagel RM (2002) Lymphocytic choriomeningitis virus and immunology. *Curr Top Microbiol Immunol* 263: 1-5.
136. Liou LY, Walsh KB, Vartanian AR, Beltran-Valero de Bernabe D, Welch M, et al. (2010) Functional glycosylation of dystroglycan is crucial for thymocyte development in the mouse. *PLoS one* 5: e9915.
137. Cambi A, de Lange F, van Maarseveen NM, Nijhuis M, Joosten B, et al. (2004) Microdomains of the C-type lectin DC-SIGN are portals for virus entry into dendritic cells. *J Cell Biol* 164: 145-155.
138. Quirin K, Eschli B, Scheu I, Poort L, Kartenbeck J, et al. (2008) Lymphocytic choriomeningitis virus uses a novel endocytic pathway for infectious entry via late endosomes. *Virology* 378: 21-33.
139. Scutera S, Fraone T, Musso T, Cappello P, Rossi S, et al. (2009) Survival and migration of human dendritic cells are regulated by an IFN- α -inducible Axl/Gas6 pathway. *J Immunol* 183: 3004-3013.
140. Rojek JM, Spiropoulou CF, Campbell KP, Kunz S (2007) Old World and clade C New World arenaviruses mimic the molecular mechanism of receptor recognition used by alpha-dystroglycan's host-derived ligands. *J Virol* 81: 5685-5695.
141. Kanagawa M, Toda T (2006) The genetic and molecular basis of muscular dystrophy: roles of cell-matrix linkage in the pathogenesis. *J Hum Genet* 13: 13.
142. Barresi R, Campbell KP (2006) Dystroglycan: from biosynthesis to pathogenesis of human disease. *J Cell Sci* 119: 199-207.
143. Kanagawa M, Saito F, Kunz S, Yoshida-Moriguchi T, Barresi R, et al. (2004) Molecular recognition by LARGE is essential for expression of functional dystroglycan. *Cell* 117: 953-964.
144. Imperiali M, Thoma C, Pavoni E, Brancaccio A, Callewaert N, et al. (2005) O Mannosylation of alpha-dystroglycan is essential for lymphocytic choriomeningitis virus receptor function. *J Virol* 79: 14297-14308.
145. Kunz S, Rojek JM, Kanagawa M, Spiropoulou CF, Barresi R, et al. (2005) Posttranslational modification of alpha-dystroglycan, the cellular receptor for arenaviruses, by the glycosyltransferase LARGE is critical for virus binding. *J Virol* 79: 14282-14296.
146. Michele DE, Barresi R, Kanagawa M, Saito F, Cohn RD, et al. (2002) Post-translational disruption of dystroglycan-ligand interactions in congenital muscular dystrophies. *Nature* 418: 417-422.
147. Barresi R, Michele DE, Kanagawa M, Harper HA, Dovicio SA, et al. (2004) LARGE can functionally bypass alpha-dystroglycan glycosylation defects in distinct congenital muscular dystrophy. *Nat Med* 10: 696-703.
148. Manya H, Chiba A, Yoshida A, Wang X, Chiba Y, et al. (2004) Demonstration of mammalian protein O-mannosyltransferase activity: Coexpression of POMT1 and POMT2 required for enzymatic activity. *Proceedings of the National Academy of Sciences of the United States of America* 101: 500-505.
149. Yoshida A, Kobayashi K, Manya H, Taniguchi K, Kano H, et al. (2001) Muscular Dystrophy and Neuronal Migration Disorder Caused by Mutations in a Glycosyltransferase, POMGnT1. *Developmental Cell* 1: 717-724.

150. Barresi R, Campbell KP (2006) Dystroglycan: from biosynthesis to pathogenesis of human disease. *Journal of Cell Science* 119: 199-207.
151. Macal M, Lewis Gavin M, Kunz S, Flavell R, Harker James A, et al. (2012) Plasmacytoid Dendritic Cells Are Productively Infected and Activated through TLR-7 Early after Arenavirus Infection. *Cell Host & Microbe* 11: 617-630.
152. Dunn WA, Hubbard AL, Aronson NN, Jr. (1980) Low temperature selectively inhibits fusion between pinocytotic vesicles and lysosomes during heterophagy of 125I-asialofetuin by the perfused rat liver. *J Biol Chem* 255: 5971-5978.
153. Doherty GJ, McMahon HT (2009) Mechanisms of endocytosis. *Annu Rev Biochem* 78: 857-902.
154. Mayor S, Pagano RE (2007) Pathways of clathrin-independent endocytosis. *Nat Rev Mol Cell Biol* 8: 603-612.
155. Wang X, Huang L (2008) Identifying dynamic interactors of protein complexes by quantitative mass spectrometry. *Mol Cell Proteomics* 7: 46-57.
156. Puig-Kroger A, Serrano-Gomez D, Caparros E, Dominguez-Soto A, Relloso M, et al. (2004) Regulated expression of the pathogen receptor dendritic cell-specific intercellular adhesion molecule 3 (ICAM-3)-grabbing nonintegrin in THP-1 human leukemic cells, monocytes, and macrophages. *The Journal of biological chemistry* 279: 25680-25688.
157. Radoshitzky SR, Abraham J, Spiropoulou CF, Kuhn JH, Nguyen D, et al. (2007) Transferrin receptor 1 is a cellular receptor for New World haemorrhagic fever arenaviruses. *Nature* 446: 92-96. Epub 2007 Feb 2007.
158. Negrete OA, Levroney EL, Aguilar HC, Bertolotti-Ciarlet A, Nazarian R, et al. (2005) EphrinB2 is the entry receptor for Nipah virus, an emergent deadly paramyxovirus. *Nature* 436: 401-405.
159. Frei AP, Jeon OY, Kilcher S, Moest H, Henning LM, et al. (2012) Direct identification of ligand-receptor interactions on living cells and tissues. *Nat Biotechnol*.
160. Ballester M, Nembrini C, Dhar N, de Titta A, de Piano C, et al. (2011) Nanoparticle conjugation and pulmonary delivery enhance the protective efficacy of Ag85B and CpG against tuberculosis. *Vaccine* 29: 6959-6966.
161. Eddy GA, Wagner FS, Scott SK, Mahlandt BJ (1975) Protection of monkeys against Machupo virus by the passive administration of Bolivian haemorrhagic fever immunoglobulin (human origin). *Bull World Health Organ* 52: 723-727.
162. Walker LM, Burton DR (2010) Rational antibody-based HIV-1 vaccine design: current approaches and future directions. *Current opinion in immunology* 22: 358-366.
163. Kenyon RH, McKee KT, Jr., Zack PM, Rippey MK, Vogel AP, et al. (1992) Aerosol infection of rhesus macaques with Junin virus. *Intervirology* 33: 23-31.
164. Choe H, Jemielity S, Abraham J, Radoshitzky SR, Farzan M (2011) Transferrin receptor 1 in the zoonosis and pathogenesis of New World hemorrhagic fever arenaviruses. *Curr Opin Microbiol* 14: 476-482.
165. Radoshitzky SR, Kuhn JH, Spiropoulou CF, Albarino CG, Nguyen DP, et al. (2008) Receptor determinants of zoonotic transmission of New World hemorrhagic fever arenaviruses. *Proc Natl Acad Sci U S A* 105: 2664-2669.
166. Weissenbacher MC, Coto CE, Calello MA (1975) Cross-protection between Tacaribe complex viruses. Presence of neutralizing antibodies against Junin virus (Argentine hemorrhagic fever) in guinea pigs infected with Tacaribe virus. *Intervirology* 6: 42-49.
167. Birmingham K, Kenyon G (2001) Lassa fever is unheralded problem in West Africa. *Nat Med* 7: 878.
168. Richmond JK, Baglolle DJ (2003) Lassa fever: epidemiology, clinical features, and social consequences. *BMJ* 327: 1271-1275.

169. Jahrling PB, Peters CJ, Stephen EL (1984) Enhanced treatment of Lassa fever by immune plasma combined with ribavirin in cynomolgus monkeys. *J Infect Dis* 149: 420-427.
170. Eichler R, Lenz O, Garten W, Strecker T (2006) The role of single N-glycans in proteolytic processing and cell surface transport of the Lassa virus glycoprotein GP-C. *Virology* 3: 41.
171. Yoshida-Moriguchi T, Yu L, Stalnaker SH, Davis S, Kunz S, et al. (2010) O-mannosyl phosphorylation of alpha-dystroglycan is required for laminin binding. *Science* 327: 88-92.
172. Oehen S, Junt T, Lopez-Macias C, Kramps TA (2000) Antiviral protection after DNA vaccination is short lived and not enhanced by CpG DNA. *Immunology* 99: 163-169.
173. An LL, Rodriguez F, Harkins S, Zhang J, Whitton JL (2000) Quantitative and qualitative analyses of the immune responses induced by a multivalent minigene DNA vaccine. *Vaccine* 18: 2132-2141.
174. Yokoyama M, Zhang J, Whitton JL (1995) DNA immunization confers protection against lethal lymphocytic choriomeningitis virus infection. *Journal of virology* 69: 2684-2688.
175. Hassett DE, Slifka MK, Zhang J, Whitton JL (2000) Direct ex vivo kinetic and phenotypic analyses of CD8(+) T-cell responses induced by DNA immunization. *Journal of virology* 74: 8286-8291.
176. Shedlock DJ, Talbott KT, Cress C, Ferraro B, Tuyishme S, et al. (2011) A highly optimized DNA vaccine confers complete protective immunity against high-dose lethal lymphocytic choriomeningitis virus challenge. *Vaccine*.
177. EPFL (2011) Protein Expression Core Facility PECF.

APPENDIX

ORIGINAL MANUSCRIPT:**“Characterization of the cell entry of Lassa virus via the TAM receptor Axl”**

Marie-Laurence Moraz, **Ana-Rita Goncalves**, Antonella Pasquato, and Stefan Kunz*

Institute of Microbiology, Lausanne University Hospital and University of Lausanne, Lausanne, Switzerland.

* Corresponding author. Mailing address: Institute of Microbiology, University Hospital Center and University of Lausanne, Lausanne CH-1011, Switzerland. Phone: +41-21 314 7743, Fax: +41-21 314 4060, E-mail: Stefan.Kunz@chuv.ch

Manuscript in preparation

AUTHORS' CONTRIBUTION:

*Conceived and designed the experiments: Marie-Laurence Moraz, Antonella Pasquato, Stefan Kunz

*Performed the experiments: Marie-Laurence Moraz, **Ana-Rita Goncalves**

*Analyzed the data: Marie-Laurence Moraz, **Ana-Rita Goncalves**, Stefan Kunz

*Wrote the paper: Marie-Laurence Moraz, Stefan Kunz

ABSTRACT

The Old World arenavirus Lassa (LASV) is the causative agent of a severe hemorrhagic fever in humans causing several hundred thousand infections per year in Western Africa. The first cellular receptor discovered for LASV is dystroglycan (DG) a versatile receptor for proteins of the extracellular matrix (ECM). Recognition of DG by LASV critically depends on functional glycosylation of DG involving the glycosyltransferase LARGE, which occurs in a tissue-specific manner. Recent studies identified the TAM-family receptor tyrosine kinases Axl and Dtk as alternative cellular receptors for LASV in cells lacking functional DG. Here we further characterized Axl-mediated cell entry of LASV in the context of productive arenavirus infection using a chimera of the prototypic arenavirus lymphocytic choriomeningitis virus (LCMV) expressing the LASV envelope glycoprotein (rLCMV-LASVGP). In line with previous studies, we found that cell entry of rLCMV-LASVGP via Axl was less efficient when compared to functional DG. However, Axl-mediated productive infection with rLCMV-LASVGP showed kinetics similar to DG-dependent entry. Axl-mediated cell entry of LASV involved a clathrin-independent pathway that critically depended on actin and dynamin, was sensitive to EIPA, but not to PAK inhibitors.

INTRODUCTION

The Old World arenavirus Lassa (LASV) is the causative agent of a severe hemorrhagic fever with high mortality in humans (29). LASV is endemic in Western Africa from Senegal to Cameroon and causes several hundred thousand infections per year with thousands of deaths. Considering the number of people affected, the current lack of a licensed vaccine and the limited therapeutic options at hand, LASV represents a serious public health problem. LASV is an enveloped negative strand RNA virus with a non-lytic life cycle (5). The genome of LASV consists of two single-stranded RNA species, a large segment encoding the virus polymerase (L) and a small zinc finger motif protein (Z), and a small segment encoding the virus nucleoprotein (NP) and glycoprotein precursor (GPC). GPC is processed into GP1, implicated in receptor binding, and the transmembrane GP2, which contains the viral fusion machinery, allowing fusion of the viral and the cellular membrane during viral entry (37).

The first cellular receptor discovered for LASV and the prototypic Old World Arenavirus arenavirus lymphocytic choriomeningitis virus (LCMV) is dystroglycan (DG) an ubiquitously expressed receptor for extracellular matrix (ECM) proteins (9, 41). Binding of LASV and LCMV to DG critically depends on the functional glycosylation of the α -DG subunit that critically depends on the glycosyltransferase LARGE (19). Upon binding to DG, LASV and LCMV enter the host cell via an endocytotic pathway that is independent of clathrin, caveolin, dynamin, and actin (47, 51, 52). Upon internalization, the virus is delivered to acidified endosomes via a pathway that is independent of the small GTPases Rab5 and Rab7, suggesting an unusual route of incoming vesicular trafficking (Fig. 2). Recent studies revealed that LASV passes through the multivesicular body (MVB), where it undergoes sorting into intraluminal vesicles (ILV) by hijacking the host cell's endosomal sorting complex required for transport (ESCRT) machinery (42). Upon sorting into ILV, the virus is delivered to late endosomes, where fusion occurs at an unusually low pH (18). Using an expression cloning approach, Shimojima and colleagues identified the C-type lectins DC-SIGN and LSECtin, as well as the Tyro3/Axl/Mer (TAM) receptor tyrosine kinases Axl and Tyro3(Dtk) as alternative LASV receptors (57). The data at hand convincingly show that Axl and Tyro-3 enhance LASV binding to DG-deficient cells and were able to mediate infection in a DG-independent manner.

Tyro-3, Axl, and Mer compose the TAM family of receptor tyrosine kinases (RTKs), whose extracellular domain is comprised of tandems of two immunoglobulin (Ig) domains and two fibronectin type II domains. Tyro-3, Axl and Mer are expressed in a wide variety of

cell types, with overlapping but unique patterns. Among the TAM receptors implicated in LASV cell entry, Axl shows the widest expression pattern (38) and is found on epithelial cells, platelets, endothelial cells, in the heart, liver, kidney, skeletal muscle, testis (1, 13, 36), and the brain (3). Tyro-3 is primarily expressed in the nervous system and is also detected in lung, kidney, retina and sexual organs, as well as hematopoietic cells (1, 21, 25, 26, 44). TAM receptors undergo interactions with serum protein S, and growth-arrest-specific protein 6 (Gas6), and proteins of the tubby family (7, 23, 24). Gas6 serves as ligand for all three TAM receptors, albeit with different affinity: Axl > Tyro3/Dtk >> Mer. Ligand binding induces homo- or hetero-dimerization of TAM receptors with consequent activation of their cytoplasmic tyrosine kinase domain. TAM-receptors are involved in many cellular functions, including chemotaxis (12), cell survival (22), the modulation of innate immunity (24, 55), and clearance of apoptotic debris (23). Apoptotic cells display the phospholipid phosphatidylserine (PS) that is recognized by Gas6 and ProS via their N-terminal gamma-carboxylated glutamic acid (GLA) domain. Subsequent engagement of TAM receptors by the C-terminal domains of Gas6 and ProS results in the endocytosis of apoptotic cell debris.

In the co-evolution with their hosts, viruses developed several strategies to hijack and manipulate cellular functions. Recent studies revealed that viruses are able to hijack the host's apoptotic clearance machinery for cell entry (31, 32, 35). Enveloped viruses display PS at their surface, which can act as an "eat me" signal triggering endocytosis. This strategy of "apoptotic mimicry" to gain access to the host cell was initially described for vaccinia virus (32). Subsequent studies demonstrated that a variety of enveloped viruses expose PS and can hijack the Gas6/TAM system to enter the host cell (35), providing an entry mechanism that is not dependent on specific interaction between viral envelope proteins and cellular receptors, thus enlarging the tropisms of viruses. TAM kinases have been implicated in cell entry of the filoviruses Ebola and Marburg virus (58), as well as Dengue virus (30). Axl was shown to enhance uptake of Ebola virus via macropinocytosis (15) and cell entry via Axl did not involve a direct interaction with the viral glycoprotein (4). Mutagenesis of Axl highlighted the importance of a functional ligand-binding domain and signal transduction for Ebola virus entry (56), however, the exact underlying mechanism remains unclear.

In the present study, we sought to characterize the unknown endocytotic pathway involved in Axl-mediated cell entry of LASV.

MATERIALS AND METHODS

Cell lines and viruses

HT-1080, HEK293H and A549 cells were cultured in DMEM, 10 % (vol/vol) FBS, supplemented with penicillin/streptomycin. The recombinant virus rLCMV-LASVGP and rLCMV-VSVG have been described (43, 52). Viruses were produced and titers determined as previously described (10). Recombinant vaccinia virus expressing GFP (VV-GFP) was kindly provided by Jason Mercer and produced as described (32). A recombinant Moloney murine leukemia virus expressing an Amphotropic envelope was generated as reported (54). Recombinant adenoviral vector (AdV)-Ad5-LARGE-enhanced green fluorescent protein (EGFP) and (AdV)-Ad5-EGFP have been described and were produced and titered as previously defined (2).

Virus infection

For virus infection, 5×10^4 HT-1080 cells per well were seeded in 96-well microtiter plates and cultured overnight. For infection of cells with rLCMV-LASVGP and rLCMV-VSVG, seed stocks were diluted to the indicated MOI and added to cells for 1 hour at 37°C. After 1 hour of incubation, the inoculum was removed; cells were washed once with serum-free medium and replaced with normal medium. To prevent secondary infection, 20 mM ammonium chloride (NH₄Cl) was added to the cells 4 hours post-infection. Cells were fixed at 16 hours post-infection and infected cells quantified by immunofluorescence assay (IFA) for LCMV NP using mAb 113 combined with fluorescence-labeled secondary antibodies (20).

Antibodies and reagents

Monoclonal antibody (mAb) 113 (anti-LCMVNP) and mAb clone 83.6 (anti-LCMVGP) have been previously described (6, 61). The mAb IIH6 anti- α -DG was used to detect functional DG (11). To detect the DG core protein, the mouse mAb anti- β -DG clone 56 from BD Biosciences was used (NJ, USA). TAM kinases were detected using the polyclonal goat anti-Axl Ab, anti-Dtk and anti-Mer PE-conjugated mouse mAbs from R&D Systems® (AF154, FAB859P, FAB8912P, MN, USA). DC-SIGN was detected using the mAb DCN46 anti-CD209 (DC-SIGN)-PE purchased from BD Pharmingen. Mouse mAb anti- α -tubulin was purchased from Sigma-Aldrich (MO, USA). The rabbit polyclonal anti-Adenovirus Type 5 was purchased from Abcam® (ab6982, UK) and directed against all capsid proteins. To detect Vaccinia virus (VV), an anti-A27L viral protein rabbit polyclonal antibody was used from LifeSpan BioSciences (Cat. No. LS-C19415, WA, USA). Horseradish peroxidase (HRP)

conjugated polyclonal rabbit secondary antibodies anti-goat and anti-mouse IgG were purchased from Dako (P0449, P0260, (Glostrup, Denmark). The HRP-conjugated polyclonal goat anti-mouse IgM antibody was purchased from Thermo Scientific (PA1-85999). Rhodamine Red-X-AffiniPure goat anti-mouse IgG from Jackson ImmunoResearch (EU) and Alexa Fluor 488 goat anti-mouse IgG2b were from Molecular Probes (A11017, Eugene, OR). Streptavidin HRP-conjugated secondary antibody was used to detect biotinylated annexin-V (ANX5) purchased from Thermo Fisher Scientific Inc. Dharmacon (Lafayette, CO).

Cytochalasin B, jasplakinoline, latrunculin A, Phalloidin-FITC, chlorpromazine hydrochloride, dynasore hydrate, p21-activated kinase (PAK)-1 inhibitor 2,2'-dihydroxy-1, 1'-dinaphthylsulfide (IPA-3) and 5-(N-Ethyl-N-isopropyl) amiloride (EIPA) were purchased from Sigma-Aldrich. LIVE/DEAD® fixable dead cell stain kit was from Molecular probes® Invitrogen. The annexin-V-Biotin conjugated from Roche-applied-science (Cat. No. 11 828 690 001) was used to detect the phosphatidylserine on purified viral particles. HT-1080 cells transduced with lentiviral vectors were then selected using the Puromycin antibiotic from Calbiochem® (Merck Millipore, MA, USA). For all experiments, HT-1080 cells were plated in poly-L-lysine-coated wells purchased from Sigma-Aldrich® (P8920).

Lentivirus shRNA production and transduction of HT-1080 cells

To deplete DG core protein in HT-1080 cells, lentiviral vectors expressing validated shRNA targeting human DG (sh-DG) (ID clone: TRCN0000056191, Thermo Scientific RHS3979-9623375) or a scrambled control shRNA (sh-sc) were generated following the manufacturers recommendations. Briefly, 3×10^6 HEK293T cells were cultured in 10-cm-diameter dishes in serum-free 293 SFM II medium (Gibco™, Cat. No. 11686-029). At 24 hours post-seeding, fresh medium was added to cells 4 hours before the transfection. CaCl_2 (250 mM CaCl_2 , ultrapure H_2O) and HBS (50 mM Hepes, 1.5 mM Na_2HPO_4 , 140 mM NaCl, ultrapure H_2O) solutions were used to co-transfect the four required plasmids: pLP1 helper (gag/ pol), pLP2 helper (rev), pCAGGS/ VSVG, with sh-DG 56191 (human pLKO.1) or with sh-sc (human pLKO.1) shRNA control. Transfected cells were incubated for 16 hours at 37°C, 5% CO_2 . After 16 hours, the transfection medium was replaced by fresh serum-free 293 SFM II medium and cells incubated for circa 24 hours more at 37°C, 5% CO_2 . Circa 40 hours post-transfection, cell supernatants were collected and centrifuged for 5 min at 500 g to remove cellular debris. Each lentivirus was concentrated using the Amicon® Ultra-15 Centrifugal Filter Devices by ultra-centrifugation according to the manufacturer's instructions (Millipore, Ultracel® 100KREF. UFC910024). Then, 5×10^5 HT-1080 cells/well were seeded

in 6-well plate format and cultured for 24 hours at 37°C, 5% CO₂. The day after, cell medium was replaced by classical medium supplemented with [6 µg/ml] Polybrene® in which 100 µl of each crude lentivirus stock was added. The cells were spinoculated at 2600 rpm for 3 hours at 23°C. Cells were then washed twice with supplemented classical medium to remove Polybrene®. The transduced cells were then incubated for 72 hours at 37°C, 5% CO₂. After 72 hours, cells were washed once with 1 x PBS and [2 µg/ml] puromycin selective medium added. After 48 hours, cell death was checked and the selective medium replaced each two days by fresh one during all the selective process. Depletion of DG was verified by Western-blot detecting the β-DG core protein.

Immunoblotting

Proteins were separated by gel electrophoresis using 6% or 8% polyacrylamide gels and transferred to nitrocellulose. After blocking in 3% (wt/vol) skim milk in PBS, membranes were incubated with primary Abs used at 5-10 µg/ml in 3% (wt/vol) skim milk in PBS for 1 hour at room temperature. After several washes in PBS, 0.1 % (wt/vol) Tween, secondary Abs coupled to HRP were applied 1:6000 in PBS, 0.1 % (wt/vol) Tween for 1 hour at room temperature. Blots were developed by enhanced chemiluminescence (ECL) using Super Signal West Pico ECL Substrate or TrueBlot® detection system (Pierce).

Rescue of functional DG in HT-1080 cells

Functional DG was rescued in HT-1080 cells by over-expression of LARGE using recombinant adenoviral vector (AdV)-Ad5-LARGE-EGFP and (AdV)-Ad5-EGFP as control (2). Briefly, 3 x 10⁵ HT-1080 and A549 cells per well were seeded in poly-L lysine-coated 6-well plate format and incubated for 24 hours at 37°C, 5% CO₂. At 24 hours post-seeding, AdV-LARGE and AdV-EGFP vectors were added to cells at indicated MOI and incubated for 4 hours at 37°C, 5% CO₂. 4 hours post-transduction, inoculums were removed, cells washed with fresh normal medium and incubated overnight at 37°C, 5% CO₂. Twenty-four hours post-transduction, transduced cells were re-seeded in 96-well plate format at 5x10⁴ cells/well. At 48 hours post-transduction, cells were either infected with rLCMV-LASVGP at MOI = 1 and infection quantified by detection of LCMV NP in IFA, or lysed to extract functional DG using Jacalin affinity purification as described (53). Lectin-bound proteins were then subjected to SDS-PAGE and Western-blotting using mAb IIH6 to functionally glycosylated α-DG (17) and mAb anti-β-DG clone 56 to β-DG core protein.

Flow cytometry analysis

For extracellular staining with enzyme-free cell dissociation solution, resuspended in FACS buffer (1% (vol/vol) FCS, 0.1% (wt/vol) sodium azide, PBS), and plated in conical 96-well plates, followed by one hour on ice with FACS buffer diluted with corresponding primary antibody. Cells were then washed twice in FACS buffer and labeled with secondary antibodies (as needed) for 1 hour on ice in the dark. After two wash-steps in 1% (vol/vol) FBS in PBS, cells were fixed with 1:10 CellFix® solution for 10 minutes at room temperature. Cells were washed twice with PBS, and fluorescence intensity assessed using a FACS Calibur flow cytometer (Becton Dickinson) using the CellQuest Pro® acquisition and analysis software. Intracellular FACS staining of LCMV NP antigen was performed as described (49).

RNA interference (RNAi)

RNA interference (RNAi) was performed using validated small interfering RNAs (siRNAs) ON-TARGETplus SMARTpool for Axl (L-003104-00-0005) and scrambled siRNA (D-001820-10-05) as control from Thermo Scientific Dharmacon (Lafayette, CO). Briefly, 3×10^6 HT-1080 cells were reverse transfected with 0.72 μ M siRNA using a 10-cm-diameter dish and Lipofectamine RNAiMAX (Invitrogen, Paisley, United Kingdom) according to the manufacturer's recommendation. Twenty-four hours after transfection, cells were replated in 96-well plate format, and 48 hours post-transfection, cells were infected with rLCMV-LASVGP (MOI = 0.1) and rLCMV-VSVG (MOI = 0.02) or mock infected or lysed to confirm by Western-blotting Axl knock-down using specific antibodies. To prevent secondary infection, 20 mM ammonium chloride (NH_4Cl) was added to the cells 4 hours post-infection. Cells were fixed 16 hours post-infection and infected cells quantified by immunofluorescence assay (IFA) detection of LCMV NP using mAb 113 (anti- LCMVNP) and combined with fluorescence-labeled secondary antibody.

Inhibitor studies in HT-1080 cells

HT-1080 cells were seeded in round bottom 96-well plates (Costar) pretreated for 2 hours in the presence of chlorpromazine, or for 30 minutes in presence of the actin inhibitors cytochalasin B, latrunculin A, and jasplakinoline, dynasore, EIPA, and IPA-3 at the indicated concentrations at 37°C. Cells were then infected in the presence of inhibitors for 1 hour with rLCMV-LASVGP at 37°C. At 4 hours post-infection, 20 mM NH_4Cl was added to prevent secondary infection. Infection was detected 16 hours post-infection by IFA as mentioned

above. The viability of drug-treated cells was determined by staining of single-cell preparations with Live and dead staining.

Entry kinetics of rLCMV-LASVGP in HT-1080 cells

The kinetics of rLCMV-LASVGP cell entry by NH_4Cl treatment was performed as described (52). Briefly, 3×10^5 HEK293 and HT-1080 cells per well were seeded in 24-well plate format coated with poly-L-lysine and incubated for 24 hours. The day after, seeded cells were incubated on ice for 30 min and fresh ice cold medium containing rLCMV-LASVGP (MOI 3; 10) was added and cells incubated on ice for 1 hour to allow virus attachment. Unbound virus was removed by washing with cold medium. Pre-warmed complete medium was added and cells rapidly shifted to 37°C at 5% CO_2 . 20 mM NH_4Cl was added at 0, 10, 20, 30, 40, 50, 60, 75, 90, 120 and 240 min. After 16 hours, rLCMV-LASVGP infection was quantified by intracellular staining of the viral proteins by flow cytometry as described above.

RESULTS

Axl mediates cell entry of rLCMV-LASVGP independently of DG

LASV is a BSL4 pathogen and work with the live virus requires high containment laboratories. To circumvent the biosafety restrictions associated with live LASV, we used a recombinant LCMV expressing the LASV envelope GP (rLCMV-LASVGP) (52). Based on the close structural and genetic relationship between LASV and LCMV and the fact that receptor binding and entry of arenaviruses are mediated exclusively by the viral envelope, rLCMV-LASVGP represents a suitable BSL2 surrogate for studies on LASV cell entry in the context of productive arenavirus infection (42, 50, 52).

Previous studies had shown that Axl can function as a cellular receptor for lentiviral pseudotypes of LASV in the human fibrosarcoma cell line HT-1080 (57). Consistent with earlier studies (57, 58), Western blot analysis revealed abundant Axl, but only low amounts of functionally glycosylated α -DG in HT-1080 cells, whereas HEK293-H cells expressed high amounts of functional DG, but lacked Axl (Fig. 1A, B). To exclude a possible contribution of residual functional DG to rLCMV-LASVGP entry into HT-1080 cells, we depleted the DG core protein by RNA interference (RNAi). For this purpose, HT-1080 cells were stably transduced with a lentival vector expressing a small hairpin (sh)RNA targeting DG or a scrambled control siRNA. Selected cells stable transfected with DG shRNA showed a reduction in DG expression of > 95%, as assessed in Western blot (Fig. 1C). DG-depleted and control HT-1080 were infected with rLCMV-LASVGP at low multiplicity (0.01). At 16 hours post infection, cells were fixed and infection detected by immunofluorescence assay (IFA). As shown in Fig. 1D, depletion of DG in HT-1080 cells did not affect infection of rLCMV-LASVGP (Fig. 1B), indicating a negligible role for residual functional DG.

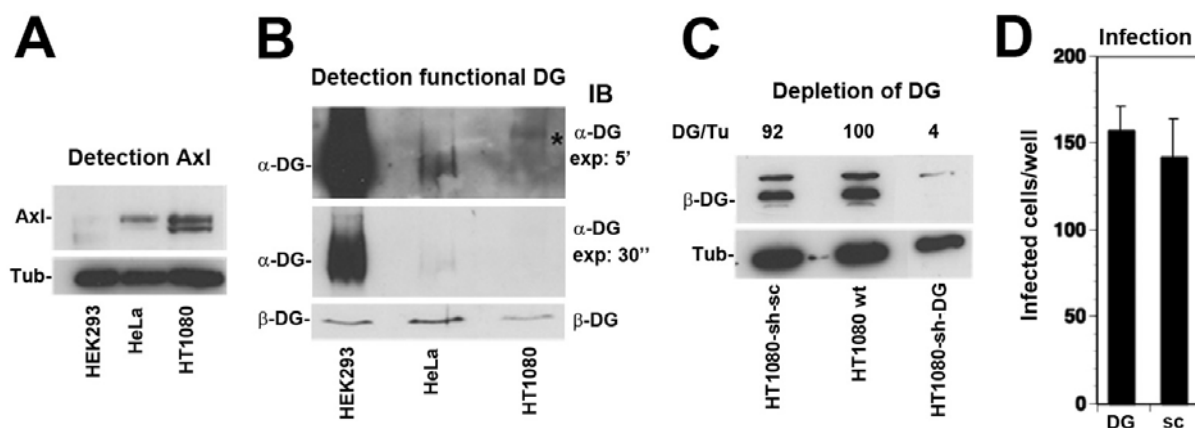


Figure 1. DG is dispensable for infection of rLCMV-LASVGP in HT-1080 cells. (A) Detection of Axl in HT-1080 cells. HT-1080, HeLa, and HEK293-H cells were lysed, total proteins separated by SDS-PAGE, and blotted to nitrocellulose. Blots were probed with a polyclonal rabbit antibody to Axl and an HRP-conjugated secondary antibody using enhanced chemiluminescence (ECL) for development. As a loading control, α -tubulin was detected. The positions of Axl and α -tubulin (Tub) are indicated. (B) Detection of functional DG. HT-1080, HeLa, and HEK293-H cells (5×10^6 cells) were lysed and subjected to jacalin affinity purification as described (53). Lectin-bound proteins were eluted by boiling in reducing SDS-PAGE sample buffer and analyzed in Western blot (IB) using mAb IIH6 to functionally glycosylated α -DG (17) and mAb 8D5 to β -DG. Prolonged exposure time (exp) of blots for glycosylated α -DG revealed a weak, but specific band for HT-1080 cells (asterisk) indicating the presence of residual functional DG. The positions of glycosylated α -DG in HeLa and HEK293-H, as well as β -DG are indicated. (C) Depletion of DG core protein by RNAi. HT-1080 cells were transduced with a lentiviral vector expressing a shRNA targeting human DG (sh-DG) or a scrambled control shRNA that does not target any known human gene (sh-sc). After 48 hours of transfection, transduced cells were subjected to antibiotic selection with puromycin for a total of ten days. Resistant colonies were isolated and expanded. Depletion of DG by RNAi was validated by Western blot for β -DG. Shown are selected clones for HT-1080 cells expressing DG-specific shRNA (HT-1080-sh-DG), scrambled shRNA (HT-1080-sh-sc), and wild-type HT-1080 cells. Beta-DG and α -tubulin (loading control) were detected as in (B). Prolonged exposure of β -DG blots lead to the detection of an unspecific band of circa 50-55 kDa (*). The positions of β -DG and α -tubulin are indicated. The efficiency of DG depletion was quantified by normalization of the β -DG signals with α -tubulin in densitometry. The rate of β -DG/ α -tubulin (DG/Tu) in parental HT-1080 cells was set as 100. (D) Infection of DG-depleted HT-1080 cells with rLCMV-LASVGP. HT-1080-sh-DG cells (DG) and HT-1080-sh-sc cells (Sc) were infected with rLCMV-LASVGP at multiplicity of 0.01. After 4 hours, 20 mM ammonium chloride was added to prevent secondary infection. At 16 hours post infection, cells were fixed and infection detected by intracellular staining of LCMV NP using mAb 113 combined with a Rhodamine-conjugated secondary antibody as described (42). Data are total numbers of infected foci per well (means \pm DG, n = 3).

In line with published data, HT-1080 cells expressed only Axl, but lacked the candidate LASV receptors Dtk, DC-SIGN (Fig. 2A and B), and LSECtin (data not shown). Two consecutive transfections of HT-1080 cells with Axl-specific siRNA resulted in depletion of > 95% of the protein after 72 hours (Fig. 2C). Axl-depleted and control cells treated with scrambled siRNA were infected with rLCMV-LASVGP and a recombinant LCMV expressing the G protein of vesicular stomatitis virus (rLCMV-VSVG) (43), which mediates infection in an Axl-independent manner (35). As expected, depletion of Axl markedly reduced infection with rLCMV-LASVGP, but not rLCMV-VSVG, confirming a crucial role of Axl in LASV entry into HT-1080 cells (Fig. 2D). To address the relative efficiency of Axl

and DG as cellular receptors for LASV, functional DG was rescued in HT-1080 cells by overexpression of LARGE (Fig. 2E). Expression of functional DG greatly enhanced infection with rLCMV-LASVGP (Fig. 2F), confirming that DG acts as preferred receptor (57).

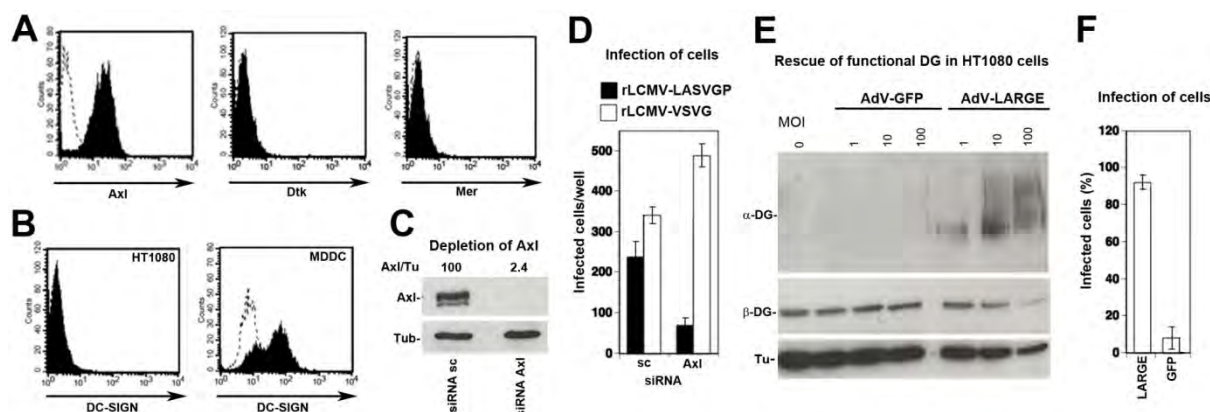


Figure 2. Infection of HT-1080 cells with rLCMV-LASVGP is mediated by Axl. (A) Detection of the TAM receptors Axl, Mer, and Dtk in HT-1080 cells. Live non-permeabilized HT-1080 cells were stained with a polyclonal rabbit antibody to Axl, combined with a PE-conjugated secondary antibody in the cold. Dtk and Mer were detected with PE-conjugated mAb to Dtk and mAb to Mer, respectively. Cells were fixed and analyzed by flow cytometry in a FACSCalibur flow cytometer (Becton Dickinson) using the CellQuest Pro® acquisition and analysis software. Empty peaks: secondary antibody only, shaded peaks: primary and secondary antibody. (B) Detection of DC-SIGN in HT-1080 cells. Live non-permeabilized HT-1080 cells and human monocyte-derived dendritic cells (MDDC) were stained with mAb 120507 to DC-SIGN and a PE-conjugated secondary antibody. Cells were fixed and analyzed by flow cytometry as in (A). Empty peaks: secondary antibody only, shaded peaks: primary and secondary antibody. (C) Depletion of Axl by RNAi. HT-1080 cells were transfected with Axl-specific siRNA (siRNA Axl) and a scrambled control RNA (siRNA sc) by reverse transfection as described (42). After 24 hours, cells were subjected to a second round of transfection with the same siRNAs (forward transfection). At 72 hours after the first transfection, cells were lysed and Axl detected by Western blot as in 1A, using α -tubulin for normalization. The efficiency of Axl depletion was assessed by normalization of the Axl signals with α -tubulin in densitometry and the rate of Axl/ α -tubulin (Axl/Tu) in HT-1080 cells transfected with scrambled RNA set at 100. (D) Infection of Axl-depleted cells with rLCMV-LASVGP. HT-1080 cells transfected with siRNA to Axl (Axl) or scrambled siRNA (sc) were infected with rLCMV-LASVGP and rLCMV-VSVG at multiplicity of 0.01 and infection detected after 16 hours as in 1D. Data represent total numbers of infected foci per well (means \pm DG, n = 3). (E) Rescue of functional DG in HT-1080 cells. HT-1080 cells were infected with adenoviral vectors expressing GFP (AdV-GFP) or LARGE (AdV-LARGE) at the indicated multiplicities of infection (MOI). After 48 hours, DG was extracted by jacalin affinity purification as in (B). Functionally glycosylated α -DG and β -DG were detected as in 1B. The broad band in cells transfected with AdV-LARGE at MOI = 100 corresponds to glycosylated α -DG. (F) Infection with rLCMV-LASVGP. HT-1080 cells were infected with AdV-LARGE and AdV-GFP at MOI = 100 as in (E). After 48 hours, cells were infected with rLCMV-LASVGP at multiplicity of 1 and infection detected after 16 hours as in (D). Shown are percentages of infected cells (means \pm DG, n = 3).

Axl-mediated cell entry of rLCMV-LASVGP occurs rapidly

In a next step, we compared the entry kinetics of rLCMV-LASVGP via Axl and DG. To assess how fast receptor-bound rLCMV-LASVGP trafficked to late endosomes, we assessed the time required for the viruses to become resistant to ammonium chloride a lysosomotropic agent that raises the endosomal pH rapidly and prevents low pH-dependent membrane fusion without causing overall cytotoxicity (39, 40). The virus was bound to HEK293H cells that express functional DG, but lack Axl, and HT-1080 cells in the cold, allowing receptor attachment without internalization. Unbound virus was removed and cells rapidly shifted to 37°C to restore membrane mobility. Ammonium chloride was added at different time points post infection and kept throughout the experiment. Cells were fixed and infection assessed by IFA. In line with published data, DG-mediated infection allowed rLCMV-LASVGP to escape from late endosomes after circa 20 minutes (Fig. 3) (52). The kinetics of the infection of HT-1080 cells mediated by Axl followed a similar kinetics with escape from the late endosome after only 15-20 minutes. In sum, the data confirm and extend published results by showing that Axl can serve as a cellular receptor in DG-deficient cells. While Axl seems significantly less efficient in mediating LASV cell entry when compared to DG, the two receptors mediate productive infection with similar kinetics.

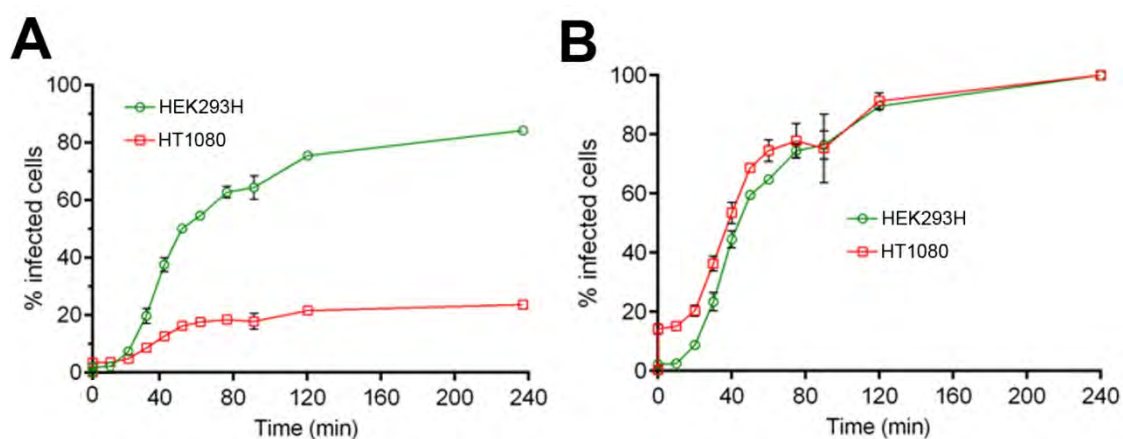


Figure 3. Entry kinetics of rLCMV-LASVGP in HEK293H and HT-1080 cells. (A) Cells were incubated with rLCMV-LASVGP at multiplicity of 3 for one hour in the cold. Unbound virus was removed and cells shifted to 37 °C. At the indicated time points, 20 mM ammonium chloride was added and left throughout the experiment. After 16 hours cells were fixed and infection detected by IFA as in Fig. 1. The percentage of infected cells was plotted against time. Data are triplicates means \pm SEM. (B) Data from (A) normalized with the 240 minutes time point set as 100%.

Axl-dependent cell entry of rLCMV-LASVGP resembles macropinocytosis

Next, we sought to characterize the Axl-mediated entry pathway for LASV using our rLCMV-LASVGP chimera in HT-1080 cells. To characterize the Axl-dependent LASV entry

pathway, we first perturbed clathrin-mediated endocytosis (CME) using chlorpromazine (CPZ), which prevents assembly of clathrin-coated pits at the plasma membrane. As control, we used a recombinant LCMV expressing the glycoprotein of vesicular stomatitis virus (VSV) that enters cells via CME (16). Treatment of HT-1080 cells with up to 8 μ M CPZ did not significantly affect infection with rLCMV-LASVGP, but diminished infection with rLCMV-VSVG in a dose-dependent manner (Fig. 4A). Next, we addressed the role of dynamin employing the dynamin inhibitor dynasore. As shown in Fig. 4B, infection of rLCMV-LASVGP in HT-1080 was blocked by dynasore in a dose-dependent manner, similar to rLCMV-VSVG, which depends on dynamin for cell entry (16). In contrast, infection of rLCMV-LASVGP in HEK293 cells was not inhibited by dynasore, suggesting a specific role of dynamin in LASV entry via Axl, but not DG.

To address a possible role of actin in Axl-mediated LASV cell entry, HT-1080 and HEK293H cells were treated with cytochalasin B or latrunculin A, which disrupt actin fibers, as well as jasplakinolide, an actin-polymer stabilizing drug that blocks the dynamics of actin filaments. Staining of actin fibers in drug-treated HT-1080 cells with fluorescence-labeled phalloidin revealed the characteristic disruption of F-actin by cytochalasin B or latrunculin A, whereas jasplakinolide reduced phalloidin staining, as expected (Fig. 4C). Drug treatment did not affect cell viability as assessed by Cell titer Glo® assay (Fig. 4D). Perturbation of actin by all three inhibitors significantly reduced infection of rLCMV-LASVGP in HT-1080 cells, whereas DG-mediated infection in HEK293-H cells was unaffected.

The marked actin- and dynamin-dependence of Axl-mediated LASV provided first hints towards a possible role of macropinocytosis. To address this possibility, HT-1080 cells were treated with ethylisopropyl amiloride (EIPA), an inhibitor of Na^+/H^+ exchangers (33). Pre-treatment with EIPA reduced infection with rLCMV-LASVGP, but did not affect infection with a recombinant Murine Mooney leukemia virus (MMLV) pseudotypes bearing an amphotropic envelope that mediated fusion at the cell membrane (Fig. 4F). Using the inhibitor IPA-3, we blocked PAK1, which plays a central role in macropinocytosis of some viruses (32). As shown in Fig. 4G, IPA-3 had no significant effects on infection with rLCMV-LASVGP, but significantly reduced infection with vaccinia virus, in line with published data (32). Although by no means comprehensive, our first characterization of Axl-dependent rLCMV-LASVGP entry revealed the involvement of a pathway that shares some characteristics of macropinocytosis (33, 34) and is strikingly different from DG-mediated entry (52).

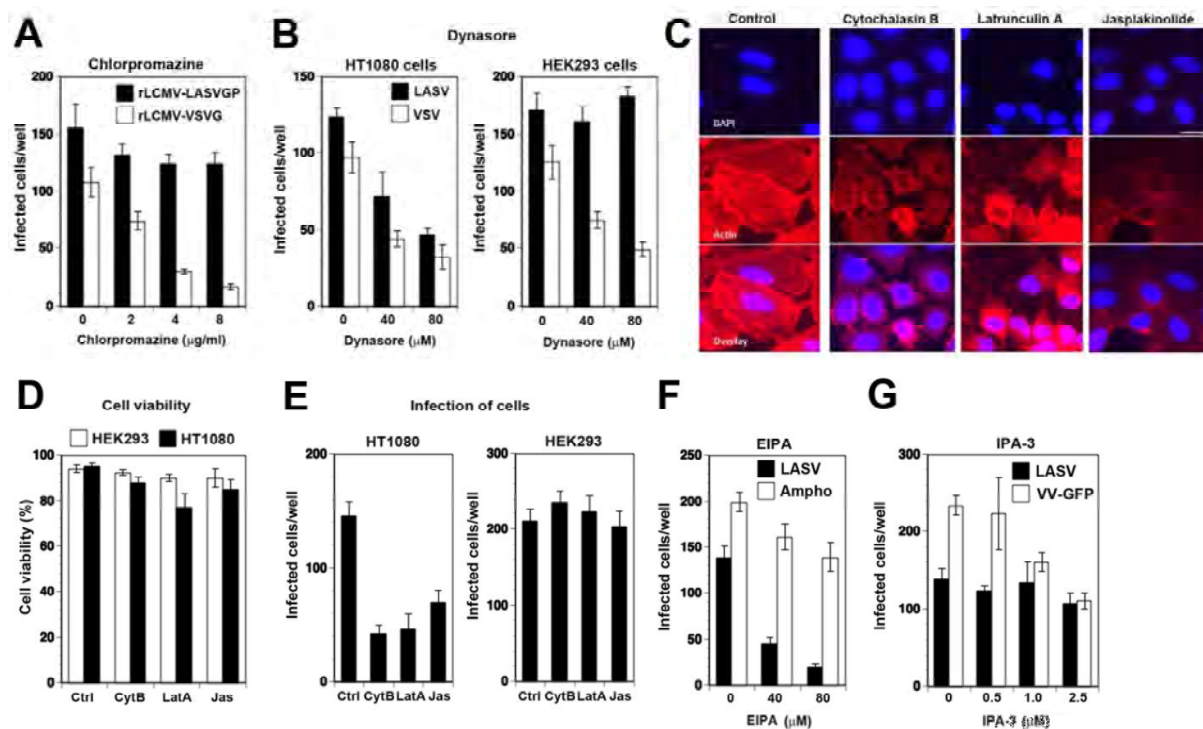


Figure 4. Characterization of the Axl-associated cell entry pathway of rLCMV-LASVGP in HT-1080 cells.

(A) Effect of CPZ on the infection of rLCMV-LASVGP. HT-1080 cells were treated with the indicated concentrations of CPZ or PBS only (0) for one hour, followed by infection with rLCMV-LASVGP or rLCMV-VSVG at a multiplicity of 0.01. After 4 hours, 20 mM ammonium chloride were added to prevent secondary infection, and infected cells detected after 16 hours by IFA as in 1D (means \pm SEM, $n = 3$). (B) Blocking of infection of rLCMV-LASVGP with dynasore. HT-1080 and HEK293H cells were pre-treated with the indicated concentrations of dynasore or vehicle control (0), followed by infection with rLCMV-LASVGP (LASV) or rLCMV-VSVG (VSV). Infection was detected after 16 hours as in (A) (means \pm SEM, $n = 3$). (C) Treatment of HT-1080 cells with actin inhibitors. HT-1080 cells were treated with cytochalasin B (20 μ M), latrunculin A (5 μ M), and jasplakinolide (1 μ M) for 30 minutes. Cells were fixed and permeabilized. F-actin was stained with Rhodamine-conjugated phalloidin (red) and nuclei counter-stained with DAPI (blue) Please note the reduced phalloidin staining in cells treated with jasplakinolide due to a competition of the drug for the phalloidin binding site. Bar = 20 μ m. (D) Cytotoxicity of actin inhibitors. HT-1080 cells were treated with 20 μ M cytochalasin D (Cyto), 5 μ M latrunculin A (Lat), and 1 μ M jasplakinolide (Jas), or solvent control (Ctrl) for 4 hours, followed by a wash out and incubation for a total of 16 hours. Cell viability was assessed by Cell Titer Glo[®] assay according to the manufacturer's recommendations. Data are triplicates \pm SD. (E) Axl-mediated infection of rLCMV-LASVGP in HT-1080 cells is actin-dependent. HT-1080 and HEK293-H cells were treated with 20 μ M cytochalasin D (Cyto), 5 μ M latrunculin A (Lat), and 1 μ M jasplakinolide (Jas), or solvent control (Ctrl) for 30 minutes, followed by infection with rLCMV-LASVGP. After 4 hours, drugs were washed out and fresh medium containing 20 mM ammonium chloride added. Infection was detected after a total of 16 hours post infection as in (A) (means \pm SEM, $n = 3$). (F) Inhibition of rLCMV-LASVGP infection in HT-1080 cells by EIPA. HT-1080 cells were pre-treated with the indicated concentrations of EIPA or vehicle control (0) for 30 minutes, prior to infection with rLCMV-LASVGP as in (A) (means \pm SEM, $n = 3$). As a control, we employed a recombinant Moloney murine leukemia virus expressing an Amphotropic (Ampho) envelope and a GFP reporter in its genome generated in the Retro-X[™] Universal Packaging System (Clontech) as described (54). Infection by the Ampho retrovirus was detected by direct fluorescence at 24 hours post infection. (G) Effect of the PAK1 inhibitor IPA-3 on infection of rLCMV-LASVGP. HT-1080 cells were pre-treated with the indicated concentration of IPA-3 or vehicle control (0) for 30 minutes, followed by infection with rLCMV-LASVGP (LASV) or recombinant vaccinia virus expression GFP (VV) (32). Infection with rLCMV-LASVGP was assessed as in (A) and infection with VV by detection of the GFP reporter in direct fluorescence microscopy at 12 hours post infection (means \pm SEM, $n = 3$).

DISCUSSION

In line with previous studies (57), our results confirmed the TAM receptor Axl as an entry receptor for LASV in absence of DG. However, the molecular mechanisms of Axl recognition by LASV are largely unknown. Recently, a general model for cell entry of enveloped viruses *via* TAM receptors has been proposed based on the concept of “apoptotic mimicry”. According to this model, viral entry via Axl critically depends on phosphatidylserine (PS) of the viral envelope, which is bound by the serum proteins Gas6 or protein S that provide a bridge to cellular TAM receptors (35). Previous studies detected PS in the envelope of the Clade A New World arenavirus Pichinde (59), and studies in our laboratory revealed that virions of LCMV and rLCMV-LASVGP also display PS at their surface (Moraz et al., unpublished results). Current efforts in our laboratory investigate the exact role of virus-derived PS, Gas6, and protein S in Axl mediated cell entry of LASV and Old World arenaviruses in general. Alternatively, LASV GP may be able to directly bind to cellular Axl, a possibility we are likewise testing.

Previous work on cell entry of the Old World arenaviruses, revealed that these viruses use an unusual pathway to invade the host cell. Upon DG binding, LASV is internalized via a cholesterol-dependent endocytic pathway that seems independent of classical regulatory proteins like clathrin, caveolin, and dynamin and apparently bypasses the classical Rab5-dependent incoming pathways of vesicular trafficking, suggesting an unusual way of delivery to late endosomes (47, 51, 52, 60). Here we performed an initial characterization of the LASV entry pathway linked to Axl. We found that Axl-mediated cell entry of rLCMV-LASVGP was clathrin-independent, but critically depended on actin and dynamin. Combined with the exquisite sensitivity to EIPA, these initial findings suggest the involvement of a macropinocytosis-like pathway that has recently been implicated in cell entry of several viruses, including poxviruses and filoviruses (33, 34). Comparison of the entry kinetics of rLCMV-LASVGP via DG or Axl revealed similar rapid escape of the virus from the late endosome after less than 20 minutes. Rescue of functional DG in HT-1080 cells revealed much higher efficiency of cell entry of rLCMV-LASVGP when compared to Axl. This suggests that in cells co-expressing the two receptors, like e.g. epithelial or endothelial cells, LASV cell entry occurs predominantly via DG.

A hallmark of LASV infection in most cell types is the inability of the infected host cell to induce a type I interferon (IFN) response. One reason for this is the ability of the arenavirus NP to counteract the activation of the IFN regulatory factor (IRF)-3 (27, 28) and

NF- κ B (48). The NP contains a 3'-5' exonuclease activity that is linked to its immunosuppressive activity (14, 46) and targets the non-canonical interferon regulatory factor-activating kinase IKK ϵ (45). Since the viral NP act as an IFN antagonist in the cytoplasm, the suppression of IFN production by NP depends on productive viral infection with expression of sufficiently high levels of NP. During viral entry, the virus is located in extracellular space where NP cannot act as an IFN antagonist. It is thus possible that incoming arenaviruses could be detected by pathogen recognition receptors (PRRs) located in endosomal compartments, e.g. Toll-like receptors (TLRs). Upon DG binding, Old World arenaviruses are internalized via a pathway of endocytosis that bypasses the early endosome where PRRs like TLRs localize (52), possibly allowing the virus to evade innate detection. It will be of interest to investigate if LASV entry *via* Axl likewise allows the virus to evade innate detection of its entry *via* Axl results in innate detection with the consequent induction of IRF3 and NF- κ B or not.

ACKNOWLEDGEMENTS

This research was supported by Swiss National Science Foundation grant FN 310030_132844 (S.K.) and the Marie Curie International Reintegration Grant Nr. 224780 of the European Community (S.K.). We thank Kevin P. Campbell (Howard Hughes Medical Institute, University of Iowa) for the mAb IIIH6 and the adenoviral vector expressing LARGE.

REFERENCES

1. **Angelillo-Scherrer, A., P. de Frutos, C. Aparicio, E. Melis, P. Savi, F. Lupu, J. Arnout, M. Dewerchin, M. Hoylaerts, J. Herbert, D. Collen, B. Dahlback, and P. Carmeliet.** 2001. Deficiency or inhibition of Gas6 causes platelet dysfunction and protects mice against thrombosis. *Nat Med* **7**:215-21.
2. **Barresi, R., D. E. Michele, M. Kanagawa, H. A. Harper, S. A. Dovico, J. S. Satz, S. A. Moore, W. Zhang, H. Schachter, J. P. Dumanski, R. D. Cohn, I. Nishino, and K. P. Campbell.** 2004. LARGE can functionally bypass alpha-dystroglycan glycosylation defects in distinct congenital muscular dystrophies. *Nat Med* **10**:696-703.
3. **Bellosta, P., M. Costa, D. A. Lin, and C. Basilico.** 1995. The receptor tyrosine kinase ARK mediates cell aggregation by homophilic binding. *Mol Cell Biol* **15**:614-25.
4. **Brindley, M. A., C. L. Hunt, A. S. Kondratowicz, J. Bowman, P. L. Sinn, P. B. McCray, Jr., K. Quinn, M. L. Weller, J. A. Chiorini, and W. Maury.** 2011. Tyrosine kinase receptor Axl enhances entry of Zaire ebolavirus without direct interactions with the viral glycoprotein. *Virology* **415**:83-94.
5. **Buchmeier, M. J., J. C. de la Torre, and C. J. Peters.** 2007. Arenaviridae: the viruses and their replication, p. p. 1791-1828. *In* D. L. Knipe and P. M. Howley (ed.), *Fields Virology*, 4th ed. Lippincott-Raven, Philadelphia.
6. **Buchmeier, M. J., H. A. Lewicki, O. Tomori, and M. B. Oldstone.** 1981. Monoclonal antibodies to lymphocytic choriomeningitis and pichinde viruses: generation, characterization, and cross-reactivity with other arenaviruses. *Virology* **113**:73-85.
7. **Caberoy, N. B., Y. Zhou, and W. Li.** 2010. Tubby and tubby-like protein 1 are new MerTK ligands for phagocytosis. *The EMBO journal* **29**:3898-910.
8. **Callahan, M. K., P. M. Popernack, S. Tsutsui, L. Truong, R. A. Schlegel, and A. J. Henderson.** 2003. Phosphatidylserine on HIV envelope is a cofactor for infection of monocytic cells. *J Immunol* **170**:4840-5.
9. **Cao, W., M. D. Henry, P. Borrow, H. Yamada, J. H. Elder, E. V. Ravkov, S. T. Nichol, R. W. Compans, K. P. Campbell, and M. B. Oldstone.** 1998. Identification of alpha-dystroglycan as a receptor for lymphocytic choriomeningitis virus and Lassa fever virus [see comments]. *Science* **282**:2079-81.
10. **Dutko, F. J., and M. B. Oldstone.** 1983. Genomic and biological variation among commonly used lymphocytic choriomeningitis virus strains. *J Gen Virol* **64**:1689-98.
11. **Ervasti, J. M., and K. P. Campbell.** 1991. Membrane organization of the dystrophin-glycoprotein complex. *Cell* **66**:1121-31.
12. **Fridell, Y. W., J. Villa, Jr., E. C. Attar, and E. T. Liu.** 1998. GAS6 induces Axl-mediated chemotaxis of vascular smooth muscle cells. *J Biol Chem* **273**:7123-6.
13. **Graham, D. K., G. W. Bowman, T. L. Dawson, W. L. Stanford, H. S. Earp, and H. R. Snodgrass.** 1995. Cloning and developmental expression analysis of the murine c-mer tyrosine kinase. *Oncogene* **10**:2349-59.
14. **Hastie, K. M., C. R. Kimberlin, M. A. Zandonatti, I. J. MacRae, and E. O. Saphire.** 2011. Structure of the Lassa virus nucleoprotein reveals a dsRNA-specific 3' to 5' exonuclease activity essential for immune suppression. *Proceedings of the National Academy of Sciences of the United States of America* **108**:2396-401.
15. **Hunt, C. L., A. A. Kolokoltsov, R. A. Davey, and W. Maury.** 2011. The Tyro3 receptor kinase Axl enhances macropinocytosis of Zaire ebolavirus. *J Virol* **85**:334-47.
16. **Johannsdottir, H. K., R. Mancini, J. Kartenbeck, L. Amato, and A. Helenius.** 2009. Host cell factors and functions involved in vesicular stomatitis virus entry. *J Virol* **83**:440-53.
17. **Kanagawa, M., F. Saito, S. Kunz, T. Yoshida-Moriguchi, R. Barresi, Y. M. Kobayashi, J. Muschler, J. P. Dumanski, D. E. Michele, M. B. Oldstone, and K. P. Campbell.** 2004. Molecular recognition by LARGE is essential for expression of functional dystroglycan. *Cell* **117**:953-64.
18. **Klewitz, C., H. D. Klenk, and J. ter Meulen.** 2007. Amino acids from both N-terminal hydrophobic regions of the Lassa virus envelope glycoprotein GP-2 are critical for pH-dependent membrane fusion and infectivity. *J Gen Virol* **88**:2320-8.

19. **Kunz, S., J. M. Rojek, M. Kanagawa, C. F. Spiropoulou, R. Barresi, K. P. Campbell, and M. B. Oldstone.** 2005. Posttranslational modification of alpha-dystroglycan, the cellular receptor for arenaviruses, by the glycosyltransferase LARGE is critical for virus binding. *J Virol* **79**:14282-96.
20. **Kunz, S., N. Sevilla, J. M. Rojek, and M. B. Oldstone.** 2004. Use of alternative receptors different than alpha-dystroglycan by selected isolates of lymphocytic choriomeningitis virus. *Virology* **325**:432-45.
21. **Lai, C., M. Gore, and G. Lemke.** 1994. Structure, expression, and activity of Tyro 3, a neural adhesion-related receptor tyrosine kinase. *Oncogene* **9**:2567-78.
22. **Lee, W. P., Y. Liao, D. Robinson, H. J. Kung, E. T. Liu, and M. C. Hung.** 1999. Axl-gas6 interaction counteracts E1A-mediated cell growth suppression and proapoptotic activity. *Mol Cell Biol* **19**:8075-82.
23. **Lemke, G., and T. Burstyn-Cohen.** 2010. TAM receptors and the clearance of apoptotic cells. *Ann N Y Acad Sci* **1209**:23-9.
24. **Lemke, G., and C. V. Rothlin.** 2008. Immunobiology of the TAM receptors. *Nat Rev Immunol* **8**:327-36.
25. **Lu, Q., and G. Lemke.** 2001. Homeostatic regulation of the immune system by receptor tyrosine kinases of the Tyro 3 family. *Science* **293**:306-11.
26. **Mark, M. R., D. T. Scadden, Z. Wang, Q. Gu, A. Goddard, and P. J. Godowski.** 1994. rse, a novel receptor-type tyrosine kinase with homology to Axl/Ufo, is expressed at high levels in the brain. *J Biol Chem* **269**:10720-8.
27. **Martinez-Sobrido, L., S. Emonet, P. Giannakas, B. Cubitt, A. Garcia-Sastre, and J. C. de la Torre.** 2009. Identification of amino acid residues critical for the anti-interferon activity of the nucleoprotein of the prototypic arenavirus lymphocytic choriomeningitis virus. *J Virol* **83**:11330-40.
28. **Martinez-Sobrido, L., E. I. Zuniga, D. Rosario, A. Garcia-Sastre, and J. C. de la Torre.** 2006. Inhibition of the type I interferon response by the nucleoprotein of the prototypic arenavirus lymphocytic choriomeningitis virus. *J Virol* **80**:9192-9.
29. **McCormick, J. B., and S. P. Fisher-Hoch.** 2002. Lassa fever. *Curr Top Microbiol Immunol* **262**:75-109.
30. **Meertens, L., X. Carnec, M. P. Lecoin, R. Ramdasi, F. Guivel-Benhassine, E. Lew, G. Lemke, O. Schwartz, and A. Amara.** 2012. The TIM and TAM Families of Phosphatidylserine Receptors Mediate Dengue Virus Entry. *Cell Host Microbe* **12**:544-57.
31. **Mercer, J., and A. Helenius.** 2010. Apoptotic mimicry: phosphatidylserine-mediated macropinocytosis of vaccinia virus. *Ann N Y Acad Sci* **1209**:49-55.
32. **Mercer, J., and A. Helenius.** 2008. Vaccinia virus uses macropinocytosis and apoptotic mimicry to enter host cells. *Science* **320**:531-5.
33. **Mercer, J., and A. Helenius.** 2009. Virus entry by macropinocytosis. *Nat Cell Biol* **11**:510-20.
34. **Mercer, J., M. Schelhaas, and A. Helenius.** 2010. Virus entry by endocytosis. *Annu Rev Biochem* **79**:803-33.
35. **Morizono, K., Y. Xie, T. Olafsen, B. Lee, A. Dasgupta, A. M. Wu, and I. S. Chen.** 2011. The soluble serum protein Gas6 bridges virion envelope phosphatidylserine to the TAM receptor tyrosine kinase Axl to mediate viral entry. *Cell Host Microbe* **9**:286-98.
36. **Neubauer, A., A. Fiebeler, D. K. Graham, J. P. O'Bryan, C. A. Schmidt, P. Barckow, S. Serke, W. Siegert, H. R. Snodgrass, D. Huhn, and et al.** 1994. Expression of axl, a transforming receptor tyrosine kinase, in normal and malignant hematopoiesis. *Blood* **84**:1931-41.
37. **Nunberg, J. H., and J. York.** 2012. The curious case of arenavirus entry, and its inhibition. *Viruses* **4**:83-101.
38. **O'Bryan, J. P., R. A. Frye, P. C. Cogswell, A. Neubauer, B. Kitch, C. Prokop, R. Espinosa, 3rd, M. M. Le Beau, H. S. Earp, and E. T. Liu.** 1991. axl, a transforming gene isolated from primary human myeloid leukemia cells, encodes a novel receptor tyrosine kinase. *Mol Cell Biol* **11**:5016-31.

39. **Ohkuma, S., and B. Poole.** 1981. Cytoplasmic vacuolation of mouse peritoneal macrophages and the uptake into lysosomes of weakly basic substances. *J Cell Biol* **90**:656-64.
40. **Ohkuma, S., and B. Poole.** 1978. Fluorescence probe measurement of the intralysosomal pH in living cells and the perturbation of pH by various agents. *Proc Natl Acad Sci U S A* **75**:3327-31.
41. **Oldstone, M. B., and K. P. Campbell.** 2011. Decoding arenavirus pathogenesis: essential roles for alpha-dystroglycan-virus interactions and the immune response. *Virology* **411**:170-9.
42. **Pasqual, G., J. M. Rojek, M. Masin, J. Y. Chatton, and S. Kunz.** 2011. Old world arenaviruses enter the host cell via the multivesicular body and depend on the endosomal sorting complex required for transport. *PLoS Pathog* **7**:e1002232.
43. **Pinschewer, D. D., M. Perez, A. B. Sanchez, and J. C. de la Torre.** 2003. Recombinant lymphocytic choriomeningitis virus expressing vesicular stomatitis virus glycoprotein. *Proc Natl Acad Sci U S A* **100**:7895-900.
44. **Prasad, D., C. V. Rothlin, P. Burrola, T. Burstyn-Cohen, Q. Lu, P. Garcia de Frutos, and G. Lemke.** 2006. TAM receptor function in the retinal pigment epithelium. *Mol Cell Neurosci* **33**:96-108.
45. **Pythoud, C., W. W. Rodrigo, G. Pasqual, S. Rothenberger, L. Martinez-Sobrido, J. C. de la Torre, and S. Kunz.** 2012. Arenavirus nucleoprotein targets interferon regulatory factor-activating kinase IKK{varepsilon}. *J Virol*.
46. **Qi, X., S. Lan, W. Wang, L. M. Schelde, H. Dong, G. D. Wallat, H. Ly, Y. Liang, and C. Dong.** 2010. Cap binding and immune evasion revealed by Lassa nucleoprotein structure. *Nature* **468**:779-83.
47. **Quirin, K., B. Eschli, I. Scheu, L. Poort, J. Kartenbeck, and A. Helenius.** 2008. Lymphocytic choriomeningitis virus uses a novel endocytic pathway for infectious entry via late endosomes. *Virology* **378**:21-33.
48. **Rodrigo, W. W., E. Ortiz-Riano, C. Pythoud, S. Kunz, J. C. de la Torre, and L. Martinez-Sobrido.** 2012. Arenavirus nucleoproteins prevent activation of nuclear factor kappa B. *J Virol* **86**:8185-97.
49. **Rojek, J. M., K. P. Campbell, M. B. Oldstone, and S. Kunz.** 2007. Old World Arenavirus Infection Interferes with the Expression of Functional {alpha}-Dystroglycan in the Host Cell. *Mol Biol Cell* **29**:29.
50. **Rojek, J. M., M. L. Moraz, C. Pythoud, S. Rothenberger, F. G. Van der Goot, K. P. Campbell, and S. Kunz.** 2012. Binding of Lassa virus perturbs extracellular matrix-induced signal transduction via dystroglycan. *Cell Microbiol* **14**:1122-34.
51. **Rojek, J. M., M. Perez, and S. Kunz.** 2008. Cellular entry of lymphocytic choriomeningitis virus. *J Virol* **82**:1505-17.
52. **Rojek, J. M., A. B. Sanchez, N. T. Nguyen, J. C. de la Torre, and S. Kunz.** 2008. Different mechanisms of cell entry by human-pathogenic Old World and New World arenaviruses. *J Virol* **82**:7677-87.
53. **Rojek, J. M., C. F. Spiropoulou, K. P. Campbell, and S. Kunz.** 2007. Old World and clade C New World arenaviruses mimic the molecular mechanism of receptor recognition used by alpha-dystroglycan's host-derived ligands. *J Virol* **81**:5685-95.
54. **Rojek, J. M., C. F. Spiropoulou, and S. Kunz.** 2006. Characterization of the cellular receptors for the South American hemorrhagic fever viruses Junin, Guanarito, and Machupo. *Virology* **349**:476-91.
55. **Rothlin, C. V., and G. Lemke.** 2010. TAM receptor signaling and autoimmune disease. *Curr Opin Immunol* **22**:740-6.
56. **Shimajima, M., Y. Ikeda, and Y. Kawaoka.** 2007. The mechanism of Axl-mediated Ebola virus infection. *J Infect Dis* **196 Suppl 2**:S259-63.
57. **Shimajima, M., U. Stroher, H. Ebihara, H. Feldmann, and Y. Kawaoka.** 2012. Identification of cell surface molecules involved in dystroglycan-independent lassa virus cell entry. *J Virol* **86**:2067-78.
58. **Shimajima, M., A. Takada, H. Ebihara, G. Neumann, K. Fujioka, T. Irimura, S. Jones, H. Feldmann, and Y. Kawaoka.** 2006. Tyro3 family-mediated cell entry of Ebola and Marburg viruses. *J Virol* **80**:10109-16.

59. **Soares, M. M., S. W. King, and P. E. Thorpe.** 2008. Targeting inside-out phosphatidylserine as a therapeutic strategy for viral diseases. *Nat Med* **14**:1357-62.
60. **Vela, E. M., L. Zhang, T. M. Colpitts, R. A. Davey, and J. F. Aronson.** 2007. Arenavirus entry occurs through a cholesterol-dependent, non-caveolar, clathrin-mediated endocytic mechanism. *Virology* **369**:1-11.
61. **Weber, E. L., and M. J. Buchmeier.** 1988. Fine mapping of a peptide sequence containing an antigenic site conserved among arenaviruses. *Virology* **164**:30-8.